Title
Cell Interactions within Biomimetic Apatite Microenvironments

Author
Tsang, Eric

Publication Date
2014

Peer reviewed|Thesis/dissertation

UNIVERSITY OF CALIFORNIA

Los Angeles

Cell Interactions within Biomimetic Apatite Microenvironments

A dissertation submitted in partial satisfaction of the

requirements for the degree Doctor of Philosophy

in Biomedical Engineering

by

Eric Joseph Tsang

2014

ABSTRACT OF THE DISSERTATION

Cell Interactions within Biomimetic Apatite Microenvironments

by

Eric Joseph Tsang

Doctor of Philosophy in Biomedical Engineering

University of California, Los Angeles, 2014

Professor Benjamin Wu, Co-Chair

Professor Patricia Zuk, Co-Chair

Bioactive ceramics, such as calcium phosphate-based materials, have been studied extensively for the regeneration of bone tissue. Accelerated apatite coatings prepared from biomimetic methods is one approach that has had a history of success in both *in vitro* and *in vivo* studies for bone regeneration [1]–[4]. However, how cells interact within the apatite microenvironment remains largely unclear, despite the vast literature available today. In response, this thesis evaluates the *in vitro* interactions of a well-characterized osteoblast cell line with the apatite microenvironment. For this, the cellular response to several aspects of the apatite microenvironment was separately examined in order to piece together a more simplified picture of a complex and dynamic system: (1) the influence of accelerated apatite on local calcium and phosphate concentration, (2) the role of protein adsorption onto apatite surfaces, and (3) apatite surface charge. Furthermore, the immunopotentiating properties of apatite were also

characterized by examining monocyte response to 2D and 3D apatite-coated model culture systems *in vitro*.

A rapid "pull-down" of extracellular Ca^{2+} and PO_4^{3-} ions onto the apatite surface could be measured upon the incubation of apatites in cell culture medium, suggesting that cells may be subject to changing levels of Ca^{2+} and PO_4^{3-} within their microenvironment. Changing levels of Ca^{2+} and PO_4^{3-} are likely to have large implications for the biological response to apatites as increasing concentrations above a certain threshold were confirmed to be cytotoxic. Proteins were found to be critical in the mediation of cell-apatite interactions, as adherence of MC3T3-E1 cells to apatite surfaces without protein coatings resulted in significant levels of cell death within 24 hours in serum-free media. In the absence of protein-apatite interaction, cell viability could be restored upon treatment of the cells with inhibitors to PO_4^{3-} transport, suggesting that PO_4^{3-} uptake may play a role in viability. In contrast, rescue was not observed upon treatment with calcium channel inhibitors. The apatite surface charge could be modulated by treating the apatite surface with biomolecular coatings (proteins, polyamino acids), or with non-biological coatings of carbon or gold. In general, surface treatments that resulted in a more negatively-charged apatite surface, relative to that of bare apatite, promoted cell survival in a dose-dependent manner. A potential immunomodulatory role for apatite may contribute to its overall pro-osteogenic capacity, as apatite coatings could enhance monocyte adhesion in the absence of activation factors. Moreover, the presence of monocytes or monocyte conditioned media was shown to promote osteoblastic differentiation on apatite-coated substrates *in vitro*. Taken together, this investigation provides an initial understanding of the cellular response to various elements within the apatite microenvironment, and may provide the foundation for furthering the development of apatite materials for bone tissue engineering.

The dissertation of Eric Joseph Tsang is approved.

Anahid Jewett

Min Lee

Ichiro Nishimura

Benjamin Wu, Committee Co-Chair

Patricia Zuk, Committee Co-Chair

University of California, Los Angeles

2014

TABLE OF CONTENTS

LIST OF FIGURES

LIST OF TABLES

ACKNOWLEDGMENTS

First and foremost, I would like to express my greatest appreciation to my mentors, Professor Benjamin Wu and Professor Patricia Zuk, for their patience, guidance, and support throughout my graduate career. I would also like to thank my dissertation committee members, Prof. Anahid Jewett, Prof. Min Lee, and Prof. Ichiro Nishimura, for their invaluable suggestions and comments which have helped make this a more complete thesis.

I am grateful for the many hours that my undergraduate research assistants put in the lab performing experiments and collecting data. Christopher Arakawa, my first undergrad assistant, set the bar high, and contributed immensely from the very beginning as the identity of my project was starting to develop. I also would like to thank Kayvon for his work on the ASC project, Jojo for his work characterizing apatite nanoparticles, Shirin for having a hand in a little bit of everything (especially the monocyte project), and Aaron and Samantha for their help collecting a vast amount of data in short period of time towards the end of my dissertation. I am also grateful to Rishi for all of his work and enthusiasm in the monocyte project despite being here for just one short summer. I know all of you will be extremely successful in your future endeavors.

Thank you to my labmates: Helena Chia, Arnold Suwarnasarn, Abigail Parks, Chase Linsley, Yulong Zhang, Cheng-Han Chen, Stephanie Reed, Chris Walthers, as well as all past members that have made their way through the Wu and/or Zuk labs. Your input on everything from technical advice to grad life in general has been indispensable in helping me survive grad school.

Special thanks are also deserved to other members of the UCLA community who have helped make this thesis possible: Dr. Sergey Prikhodko for his extensive knowledge and training on the SEM, Dr. Armando Durazo for help with the ICP-OES, Dr. Marianne Cilluffo and Dr. Sirus Kohan for allowing me to use their carbon coater, the Weintraub Center staff for their help with microCT, the TPCL Core for help with histology, and the UCLA Genotyping & Sequencing Core for running the many RT-PCR plates I've sent their way.

My deepest appreciation goes to my family: Mom, Dad, and Caroline & Eric & baby Hunter—Thank you for your constant love, support, and devotion in supporting me as I pursued my Ph.D.

And last but not least, I would like to especially thank Laurie Jane Leyden for her unmitigated love, devotion, and friendship. Her presence in my life has been an immeasurable blessing in helping me endure the demands of this journey. Thank you for your endless patience and understanding. ILYWAMHMBAS.

VITA

2005	B.S. Bioengineering University of California, Berkeley
2005-2006	Research Assistant Center for Cerebrovascular Research (CCR) Cardiovascular Research Institute (CVRI) University of California, San Francisco
2007-2013	Graduate Student Researcher Bioengineering University of California, Los Angeles
2007-2008	Teaching Assistant Bioengineering University of California, Los Angeles

CHAPTER 1

1.1 INTRODUCTION AND SIGNIFICANCE

Human bone is a dynamic and highly vascularized connective tissue that can be viewed as a natural, composite biomaterial composed of a biopolymer and bioceramic. The biopolymer component is an organic matrix that consists primarily of Type I collagen, while the bioceramic component is hydroxyapatite, a mineralized phase made up of predominantly calcium and phosphate ions. Together, these components give bone the rigidity and strength needed to provide structural support for the body and protection of its vital internal organs. In addition to structural support, bone provides an important function in normal homeostasis, serving as a mineral reservoir to maintain and regulate calcium and phosphate ion levels [5], and to house marrow which is central to the development of blood and immune cells. Adult bone is maintained continuously, undergoing a remodeling process where the removal (resorption) and replacement (formation) of bone occurs equally. The main cellular players in the bone remodeling process include osteoblasts (responsible for the formation of bone matrix), and osteoclasts (responsible for bone resorption). Cross-talk between both cell types helps to regulate each other's activity to orchestrate a well-organized bone remodeling process.

Because of its high vascularization and ability to maintain itself through remodeling, bone is known to have self-healing properties when damaged due to trauma or disease. However, bone's ability to heal itself is limited when the defect reaches a critical size. Beyond this critical defect size, medical intervention is often needed, usually in the form of bone grafts. There is a growing need for bone graft substitutes to replace damaged or lost bone tissue due to both traumatic and non-traumatic injury. These include acute fractures, fracture non-unions, and

defects due to musculoskeletal disorders including osteoporosis, osteonecrosis, and bone cancer. Of the more than 3 million musculoskeletal procedures performed each year in the U.S., approximately half require bone grafting procedures at a cost of $2.5 billion annually [6]. Approximately 90% of these bone graft procedures involve the use of autograft or allograft bone tissue. As the gold standard of treatment, autografts (bone grafts taken from another part of the patient's body) are ideal for their lack of immune rejection, but a host of limitations—supply, requirement of a second surgery for tissue harvest, donor site morbidity, and increased risk of infection—restrict its unencumbered use [7]. Most of these concerns can be mitigated through the use of allografts that are harvested from donors, but supply issues and the potential for disease transmission does exist [8].

Because of the limitations associated with autografts and allografts, more attention has turned toward synthetic bone graft substitutes. A popular choice for load-bearing bone replacement is metallic graft implants, which have been used to restore mechanical support at the defect site. However, implant failure is often a problem since metallic grafts show poor integration with the native bone tissue due to mechanical fatigue, metal ion leaching, corrosion or wear debris leading to inflammation [9]. Ceramic materials have also garnered traction as bone graft substitutes, being more resistant to corrosion as well as exhibiting better bioactivity, which improves its ability to bond to host bone and enhance bone tissue formation. Ceramics are limited, however, to non-load bearing applications because of their brittleness and other shortcomings in mechanical properties. As a compromise, the mechanical strength of metal implants and the osteoconductive properties of ceramics have been combined by coating a metal implant with a layer of hydroxyapatite. However, due to the implants permanency, problems such as foreign body reaction could persist. Ideally, a biodegradable implant would be employed

that could match its degradation to the formation or in-growth of new tissue. For this reason, biodegradable polymers have been extensively researched for bone tissue engineering applications, but polymers alone do not integrate well with native bone. Again, a likely successful bone graft substitute will be a composite that harnesses the aforementioned advantages and eliminates the limitations, ultimately producing a material that is osteoconductive, osteoinductive, and supports good osteointegration within the native tissue.

Calcium phosphate (or apatite) based materials are still an attractive approach for bone regeneration for its osteoconductivity, biocompatibility, and versatility. Many *in vitro* studies have demonstrated their good cellular compatibility with a range of cells including osteoblasts and mesenchymal stem cells [10]–[12]. Furthermore, implants made from or coated with apatite did not induce significant inflammatory response and also demonstrated the ability to facilitate bone regeneration in the surrounding tissue [13]–[15]. As such, apatite materials to this day continue to be an active area of research as a bone substitute material for many orthopaedic and dental applications. The following sections will provide an overview on the history of apatite materials (especially in regard to biomimetic apatite coatings—the focus of this dissertation), briefly reviewing its physicochemical properties, methods of fabrication, and the corresponding biological response.

1.2 REVIEW OF LITERATURE

1.2.1 Hydroxyapatite and biological apatites

Bone formation is a complex physiological process conducted by osteoblast cells to produce a mineralized extracellular matrix (ECM). As previously mentioned, this matrix comprises two primary phases: the organic phase (~30% of bone by weight)—composed of Type I collagen and other non-collagenous proteins such as proteoglycans/glycoproteins—and the mineral phase (~70% of bone by weight), which is primarily made up of hydroxyapatite [$Ca_{10(}PO_4)_6(OH)_2$]. The general mechanism of bone mineralization involves a two-step process: (1) heterogeneous nucleation, where ions are deposited onto the organic matrix to form amorphous calcium phosphate clusters (2) propagation and crystal growth, which involves phase transformation of the calcium phosphate clusters into a more crystalline structure [16], [17].

Stoichiometric hydroxyapatite, which has a Ca/P molar ratio of 1.67, is characterized by calcium and phosphate ions arranged around columns of hydroxyl ions in a hexagonal crystal structure with a space group of $P6_3/m$ and unit cell dimensions of a = b = 9.431 Å, c = 6.881 Å [18]. Biological apatites (such as enamel, dentin, and bone) typically contain ionic impurities, causing it to differ somewhat in their composition, crystal size, structure and physicochemical properties relative to stoichiometric hydroxyapatite. X-ray diffraction (XRD) analysis of various apatites shows that pure hydroxyapatite produces sharp and well-defined diffraction peaks suggesting the larger crystal size in contrast to several biological apatites, which produce broad, poorly-defined diffraction peaks [19]. Biological apatites also differ from stoichiometric hydroxyapatite in Ca/P molar ratio, which can range from well-below or above 1.6, depending on age, species, and type of bone [20]. For example the Ca/P ratio of enamel, dentin, and bone

are 1.63, 1.61, and 1.71, respectively [19]. Chemical analysis of bone apatites demonstrate the presence of minor ionic impurities consisting of carbonate, magnesium, sodium, fluoride, and acid phosphate, as well as trace amounts of elements including strontium and lead [21].

As a result of these ionic substitutions, the crystal structure of biological apatite tends to be less stable, which in turn increases its solubility. Altering the dissolution properties of apatite can have large implications for its use in bone repair. For example, an increase in solubility would lead to an increase in the local calcium and phosphate ion concentrations at the site of implantation. When supersaturated levels are reached, re-precipitation around both the implant and the native bone tissue may occur, thus enhancing the potential for better bone bonding and bone formation. However, the dissolution rate of apatite materials should be carefully regulated; above a certain threshold, calcium and phosphate concentration can reach harmful levels [22]. In addition to composition, pH and temperature are other parameters in the preparation of synthetic apatites that can be tuned appropriately in order to achieve desired apatite characteristics. A better understanding of how the fabrication parameters influence the resulting structure and stability can be used to optimize the efficacy of synthetic apatite materials. A review of the various forms of synthetic apatite materials that are available is presented below.

1.2.2 Synthetic apatite materials for bone tissue engineering

As mentioned in the previous section, apatite materials with varying physicochemical properties can be obtained depending on the apatite preparation conditions, which may include ionic composition, processing temperature and pH. Theoretically, highly controlled fabrication parameters and conditions will allow researchers to produce apatite materials with desired or predictable properties. This includes phase composition, crystallinity, crystal size, Ca/P ratio,

solubility, surface area and surface charge, which in turn can govern apatite features such as dissolution behavior and bioactivity. Ideally, synthetic apatites should be crystallographically and chemically analogous to natural biological apatites. The more common apatite phases that exist include octacalcium phosphate (OCP, $Ca_8H_2(PO_4)_6$, Ca/P = 1.3), β-tricalcium phosphate (β-TCP, $Ca_3(PO_4)$, Ca/P = 1.5), and dicalcium phosphate (DCP, $Ca_2P_2O_7$, Ca/P = 1). Compared to pure hydroxyapatite, which is the most thermodynamically stable, these apatite phases tend to be more soluble due to calcium deficiencies [23]–[25].

Bioceramics for bone repair, regeneration, or replacement are available in a variety of form factors, including bulk scaffolds, cements, and coatings. Bulk apatite materials have been created as either dense blocks or porous scaffolds with uniquely designed shapes and sizes. One approach has been to densely press calcium phosphate particles or granules into the desired shape (such as that of the bone defect). The composition and particle size of the bioceramic material has been shown to have influence over the amount of new bone formation. For example, a study investigating various ratios of hydroxyapatite/β-TCP (biphasic calcium phosphate) on new bone formation demonstrated that a 20:80 HA: β-TCP scaffold was more efficient than either apatite phase alone or higher hydroxyapatite/ β-TCP ratios [26]. It was also shown in another study that biphasic calcium phosphate particles near 0.2-0.25 mm in size had better bone formation relative to scaffolds formed from smaller or larger particles [27]. In general, among the various types of calcium phosphate phases, hydroxyapatite and β-TCP are most commonly used due to their osteoconductivity and bioactivity, as well as the ability to control their degradation properties.

One of the earliest concepts of calcium phosphate cements (CPC) was introduced by LeGeros, *et al.* where a powder calcium phosphate component was combined with calcium hydroxide and a dilute liquid phosphoric acid component [28]. At relatively low physiological temperatures, a semi-solid paste is obtained that subsequently hardens via hydrolysis reaction [29]. Since then, other formulations have been prepared with varying composition, powder/liquid ratios, and setting times. CPCs have obtained various degrees of success for use clinically in applications for restorative dentistry and orthopaedics, including treatment of bone cancer, fractures, bone graft fillers and vehicles for drug delivery [29]–[32]. Use of CPCs with stems cells have also been investigated, showing that incorporating human bone marrow-derived mesenchymal stem cells (hMSC) with CPC could increase ALP expression and mineral deposition of the cells [33].

Although calcium phosphate-based scaffolds and cements have proven osteoconductivity and bioactivity, they are mechanically weak and therefore limited for use in weight-bearing applications. Instead, high mechanical strength materials like titanium and its alloys are typically used, but normally lack the osteoconductivity and bone bonding properties of bioceramics. In response, calcium phosphate coating methods have been developed and have greatly enhanced the bioactivity and bone-bonding performance of non-bioactive materials, thus allowing researchers to combine the desirable advantages of each material [34], [35].

For non-load-bearing bone regeneration, the use of apatite-coated biodegradable polymers has advanced significantly in recent years. The ease of preparation and the availability of diverse fabrication methods like electrospinning, solvent casting/porogen leaching, and solid-free form fabrication make polymers attractive scaffold/implant materials for tissue engineering

[36]–[38]. Furthermore, polymers are appealing for their controllable properties including degradation, porosity, shape, biocompatibility, and the ability to add functionalization. For bone tissue engineering applications specifically, polymer scaffolds can be fabricated to mimic the organic component of bone, serving as a template or matrix for osteoprogenitor cell in-growth and mineralization. Poly(lactide-co-glycolide) (PLGA) is one such biodegradable polymer that is commonly chosen for tissue engineering because of its versatility and biocompatibility. However, by itself PLGA is limited for bone repair due to a lack of osteoconductive properties and poor integration with native bone—again, qualities that can be enhanced when a calcium phosphate coating is present on its surface [2], [39].

1.2.3 Methods for deposition of apatite coatings

Different strategies have been employed to deposit a layer of calcium phosphate onto the surface of implants and scaffolds. A long list of options are available, including plasma spraying [40], [41], ion sputtering [42], pulsed laser ablation [43], [44], electrophoretic deposition [45], [46], and biomimetic methods [1], [47]. Many of the methods listed above have limitations such as uneven coating thickness, non-uniform coverage due to line-of-sight restriction, and harsh processing conditions. Because of these limitations, the quality of the coating and ultimately the efficacy for bone repair will be deficient. For example, plasma spraying is commonly used for commercial implants, but due to the aforementioned disadvantages, this method often exhibits coating delamination, leading to increased wear and implant loosening. A more detailed discussion of the various apatite coating methods can be viewed in Sun *et al*. [40] and Yang, *et al*. [48]. Biomimetic coating methods, which is the focus of this dissertation, will be explored in more detail below.

1.2.4 Apatite coating via biomimetic methods—Immersion in simulated body fluids

Biomimetic methods have several significant advantages over the other apatite deposition methods described in the previous section. The biomimetic coating approach utilizes solutions prepared and processed under mild conditions (i.e. at or near physiological pH and temperature). Most of the aforementioned coating methods require high temperatures that are not ideal for heat-sensitive materials like polymers. Furthermore, the mild processing conditions of the biomimetic approach allow for the incorporation of bioactive factors that would otherwise denature or become inactive using other harsher methods. Implants to be coated are immersed in apatite solutions known as simulated body fluid (SBF), which has the added benefit of eliminating line-of-sight coating issues. As a result, more uniform and consistent coatings can be created on complex implant form factors, such as those with irregular shape or high degree of interconnected pores. SBF solutions contain ionic concentrations that mimic those found in human blood plasma, and can be prepared relatively inexpensively using routinely-found laboratory reagents. The resulting bone-like apatite that forms from spontaneous precipitation is considered biocompatible and thus has become an attractive approach for coating implants and scaffolds for bone tissue regeneration.

1.2.5 Conventional biomimetic apatite coatings

Originally developed by Kokubo, *et al*. in the early 1990s, conventional biomimetic apatite coating via SBF immersion was used as an *in vitro* apatite formation test to predict the *in vivo* bioactivity, or bone-bonding ability, of bone graft implants [49]–[51]. It was observed that when glass-ceramic A-W or Bioglass were immersed in SBF, a SiO_2-rich layer and calcium phosphate film would form on the surface, similar to that formed after *in vivo* implantation.

Crystallographic and chemical analysis confirmed that the formed calcium phosphate layer was nanocrystalline carbonated apatite, similar to bone mineral in composition and structure. Consequently, it was proposed that for a material to bond to native bone, a bonelike apatite layer must form on its surface upon implantation *in vivo*, and furthermore, formation of this apatite layer could be replicated with immersion in SBF solutions.

Apatite formation using Kokubo's original SBF involves a 2-step mineralization process that takes up to 10-21 days. The mechanism for apatite formation is initiated by a nucleation step at certain sites present on the substrate surface. The formation of nucleation sites can vary depending on the substrate material type [52]. For example, glass-ceramic substrates, when immersed in SBF, were shown to undergo surface changes where calcium and/or phosphate ions were released from the glasses. A hydrated silica layer formed on the surface as a result of calcium ion exchange for H_3O^+ ions in the SBF; these exposed silanol groups (Si-OH) were found to be responsible for apatite nucleation. Similarly, on titanium metal substrates, Ti-OH groups that formed on the surface acted as apatite nucleation sites upon SBF immersion. For organic polymer substrates, the presence $CaO\text{-}SiO_2$ glass particles were needed in solution to create nucleation sites, which formed as a result of silicate ion release from the glass and subsequent adsorption onto the polymer surface. When immersed in conventional SBF, the Si-OH groups again served as the catalyst for apatite nucleation. For all the above materials, precipitation and deposition of apatite nuclei continues until a uniform layer is created on the substrate surface during this initial SBF incubation period.

Following the formation of this preliminary apatite layer, the coated substrates are transferred to a 1.5x concentrated SBF solution (supersaturated with respect to the apatite) for 7-

14 days to allow for phase transformation of the initially amorphous apatite nuclei into crystalline apatites. In this 1.5x SBF, the apatite nuclei spontaneously grow by consuming excess calcium and phosphate ions from the surrounding solution, ultimately forming a dense and uniform crystalline apatite layer. The growth of the apatite layer reaches a steady state, with the coating thickness increasing in proportion to the immersion time in the second solution [52].

1.2.6 Accelerated biomimetic apatite coatings

Kokubo's original formulation for SBF has since been modified in several studies in order to more closely mimic the ionic composition of human blood plasma (i.e. "corrected SBF (c-SBF) [53]", "revised SBF (r-SBF)" [47], "newly improved SBF (n-SBF)" [54]). For example, c-SBF, which is now considered conventional SBF, was modified from the original SBF to include the SO_4^{2-} that is also present in blood plasma. The concentration of SBF has also been modified in order to accelerate the coating process from the original 10-21 days that is a result of using the conventional 1x and 1.5x SBF solutions. By using a 5x concentrated SBF solution, Barrere *et al*. demonstrated that the biomimetic mineralization process could occur within one day [55]. Furthermore, through a series of systematic investigations, Barrere also explored the influence of ionic strength, ionic composition, and pH on the final apatite structure and composition. For example, by adjusting the carbonate and magnesium content of the SBF, the precipitation kinetics and crystal growth rate could be accelerated [55], [56].

The accelerated biomimetic mineralization process could be enhanced further by segregating the nucleation and crystal growth steps into two distinct phases [57], [58]. An initial 5x SBF solution containing HCO_3^- and Mg^{2+} is used to initiate seeding of calcium phosphate nuclei on the substrate (heterogeneous nucleation). The release of CO_2 over time results in

increasing pH which favors mineralization and leads to formation of an amorphous layer of calcium phosphate. Growth of the apatite layer occurs in a second 5x SBF solution devoid of crystal growth inhibitors HCO_3^- and Mg^{2+}. This allows for phase transformation of the initial amorphous layer into crystalline apatite. A thick, dense, and crystalline apatite layer is needed for successful osteointegration, in contrast to amorphous calcium phosphate coatings, which are often to thin and dissolve too quickly to facilitate osteointegration of the implant [58].

1.2.7 Biological response to accelerated biomimetic apatite coatings

Early *in vivo* studies investigating apatite-coated metal implants have demonstrated higher bone-bonding ability and bone in-growth relative to non-coated controls [59]. The apatite in these studies was well-bonded to the metal surface and did not delaminate during implantation. The presence of the coating reduced fibrous tissue formation between the implant and bone, resulting in better bone apposition. Similarly, apatite-coated polymer bone implants exhibited improved osteoconductivity and demonstrated abundant bone formation *in vivo* by 4 weeks [60].

Accelerated biomimetic apatite coatings have also been applied to tissue engineering approaches that involve the use of porous biodegradable polymers. As described earlier, the mild conditions of the biomimetic approach provide a favorable mineralization environment for thermally-sensitive polymer scaffolds that would otherwise be incompatible with classical calcium phosphate coating methods (e.g. plasma spraying). Many *in vitro* and *in vivo* studies have investigated the influence of these coatings on the osteogenic potential of combined cellular/ polymer constructs for bone tissue engineering applications. For example, Chou *et al.* investigated the *in vitro* effect of accelerated apatite structure on cellular response [1], [2]. It was

found that amorphous accelerated apatite induced significant cell death, while a more favorable cellular response was observed on small polycrystalline (SmA) and large single crystal apatites (LgA). Furthermore, LgA coatings induced greater expression of mature osteogenic markers osteocalcin (OCN) and bone sialoprotein (BSP) in MC3T3-E1 murine pre-osteoblasts in both 2D and 3D apatite-coated systems [2], [3]. When implanted *in vivo*, accelerated apatite-coated 3D PLGA scaffolds seeded with osteoprogenitor cells were able to heal critical size mouse calvarial defects, without the need for osteogenic growth factors nor genetic manipulation of the cells [4].

1.2.8 Conclusion

A review of the vast calcium phosphate materials literature clearly demonstrates the advantages of the accelerated biomimetic apatite approach. Briefly, this method has the ability to create a uniform bone-like apatite coating in reduced growing time by using a 2-step process that optimizes both apatite nucleation and crystal growth. Moreover, it has the flexibility to coat a variety of materials (including metals, ceramics, and polymers) having unique and complex form factors. By adding a uniform coating of apatite, non-bioactive bone implants become significantly more osteoconductive, exhibiting better bone contact and bone in-growth. Tissue engineering approaches to bone regeneration using biodegradable polymer scaffolds demonstrate that accelerated apatite coatings provide a pro-osteogenic microenvironment both *in vitro* and *in vivo*.

Despite the growing list of studies reporting the efficacy of accelerated apatite coatings in promoting osteoblastic differentiation *in vitro* and new bone formation *in vivo*, the exact reasons remain unknown. By investigating the mechanisms or properties of accelerated apatite that influence particular cellular or biological behavior, researchers can leverage this information to

manipulate the appropriate elements in order to produce a desired response. Achieving a high-level of understanding with respect to the various components of the apatite microenvironment will thus allow researchers to create more effective tissue engineering constructs.

1.3 HYPOTHESIS AND SPECIFIC AIMS

The cellular response to the apatite microenvironment is likely to be governed, either directly or indirectly, by the physicochemical properties of the coating material. Osteoblast function is known to be sensitive to scaffold characteristics including surface topography, surface energy or charge, porosity and mechanical stiffness [61]–[64]. Osteoblasts and other osteoprogenitor cells are also expected to be exposed to the chemical constituents of apatite, namely calcium and phosphate, due to the leaching or dissolution characteristics of the material [65]–[68]. For this thesis, various elements of accelerated biomimetic apatite coatings (and how they influence the local microenvironment) will be explored. Moreover, the cellular interaction between these various elements will be investigated to help elucidate what role they may have in regulating biological response.

The core hypothesis of this thesis is that certain properties of the accelerated apatite microenvironment (calcium and phosphate ions, adsorbed proteins, and surface charge) play a central role in the regulation of cell function.

To test this hypothesis, the following specific aims were investigated:

1. Characterize the ability of accelerated apatite coatings to alter the concentration of calcium and phosphate in the microenvironment and determine the role of these ions in regulating osteoblast cell function.
2. Determine the role of adsorbed proteins in mediating the cell-apatite interaction
3. Characterize the surface zeta potential of accelerated coatings and evaluate the osteoblastic response to the exhibited surface charge.

4. Evaluate the *in vitro* inflammatory cell (monocyte) response to 2D and 3D accelerated apatite coating systems.

CHAPTER 2

ROLE OF Ca^{2+} / PO_4^{3-} IONSAND ADSORBED PROTEINS IN THE ACCELERATED APATITE MICROENVIRONMENT

2.1 Introduction

Accelerated biomimetic apatite coatings have a history of success in both *in vitro* [2], [3] and *in vivo* [4] studies for bone tissue engineering. Chou *et al.*[1] previously showed that the coating of two-dimensional surfaces with accelerated apatite could support cell attachment, spreading, viability, and proliferation in standard *in vitro* culture conditions. The osteoinductive properties of the apatite coatings were made evident by the upregulation of several bone-specific markers such as osteopontin (OPN), osteocalcin (OCN) and bone sialoprotein (BSP) in MC3T3-E1 cells cultured on apatite compared to cells cultured on standard uncoated TCPS. Furthermore, it was observed that the apatite surfaces could induce the MC3T3-E1 cells to express these osteogenic markers in the absence of commonly used osteogenic factors such as ascorbic acid and beta-glycerophosphate. On a three-dimensional substrate, MC3T3-E1 cells cultured on apatite-coated PLGA scaffolds *in vitro* also showed significant upregulation of OPN expression at day 3, while OCN and BSP expression was upregulated at 4 weeks relative to cells on non-coated PLGA scaffold controls [3]. These apatite-coated PLGA scaffolds have also shown potential in improving bone formation *in vivo*, demonstrating the ability to regenerate bone in critical-size mouse calvarial defects in conjunction with adipose-derived adult stromal cells [4]. Despite this success of using apatite coatings for bone tissue regeneration, little is known on the exact mechanism that induces the positive biological response of the apatite microenvironment. As a first step in elucidating the relationship between apatite surfaces and

the cellular response, MC3T3-E1 pre-osteoblast cells were cultured, in this study, on apatite-coated TCPS in the presence and absence of proteins, and the effect on adhesion and viability were assessed.

2.2 Materials and methods

2.2.1 Preparation of apatite-coated surfaces

Biomimetic apatite coated surfaces were prepared using an accelerated approach using Simulated Body Fluid solutions (5x SBF1 and 5x SBF2) as previously published [1]. Tissue culture polystyrene (TCPS) wells were coated through an initial incubation with 5x SBF1 for 24h at 37°C, followed by a 48h incubation (at 37°C) with 5X SBF2. Each well was then rinsed gently with sterile distilled deionized water and dried in a laminar flow hood over night.

2.2.2 Apatite morphology

Surface morphology and elemental composition (Ca and P) of the apatite coatings were analyzed with a FEI NovaSEM 230 scanning electron microscope with attached EDS detector (FEI Co., Hillsboro, OR). Sections of apatite-coated TCPS were analyzed with SEM under low-vacuum mode with an accelerating voltage of 10 kV. Energy dispersive X-ray analysis (EDS) was performed on the samples to obtain Ca and P content of the apatite coatings [2].

2.2.3 MC3T3-E1 cell culture and viability on apatite surfaces

MC3T3-E1 cells were purchased from ATCC (CRL-2594). The cells were expanded under standard tissue culture conditions in MC3T3-E1 Expansion Medium (EM) containing α-MEM, 10% FBS and 1% penicillin/streptomycin. For experiments performed on bare apatite surfaces, monolayers of MC3T3-E1 cells were prepared for serum-free conditions by incubating

in EM containing 5% FBS for 6h, followed by 12h in serum-free EM. The cells were then harvested using 0.25% tryspin/2.21mM EDTA, and resuspended at a desired density in serum-free EM. The apatite surfaces were seeded by incubating with the cell suspension overnight in a 37°C, 5% CO_2 incubator. All tissue culture reagents were purchased from Mediatech CellGro (Manassas, VA).

To assess the effect of adhesion to the apatite surface on cell viability, MC3T3-E1 cells were seeded onto apatite surfaces at 10,000 cells/cm^2, and viability determined at select time points up to 24 hrs using either a Live/Dead kit (Invitrogen, Carlsbad, CA) or an Alamar Blue assay (AbD Serotec, Oxford, UK). For the Live/Dead assay, cells were incubated at the desired time points with a solution of Calcein AM and Ethidium homodimer-1 (EthD-1) as outlined by the manufacturer to determine living (green) and dead (red) cells, respectively. For cell quantitation, Alamar Blue reagent, which is metabolically processed by the cells, was added directly to the MC3T3-E1 EM at select time points and the cells incubated for 1 hour at 37C. The EM containing the metabolized Alamar Blue was then removed and measured at 535/590 nm (excitation/emission). Cell number was determined based on these absorbances according to the manufacturer. Viability assays were repeated three times (n=3) and expressed as the average number of viable cells ±SD.

2.2.4 Protein adsorption on apatite surfaces

To assess the effect of adsorbed proteins on viability, either FBS or BSA was absorbed to the apatite-coated surfaces. Since FBS contains a variety of proteins including albumin, BSA was also chosen in this study to eliminate possible confounding effects that multiple protein adsorption from FBS may have on influencing cell behavior or function.

For BSA-coated apatite, a 1% (w/v) stock solution was made by dissolving BSA protein (#A9418, Sigma, St. Louis, MO) in PBS ($Ca^{2+}$and Mg^{2+}free, Mediatech CellGro, Manassas, VA). The BSA stock solution was sterile filtered and further diluted with sterile 1XPBS to make 0.1%, 0.01%, and 0.001% BSA solutions. FBS solutions were created by the dilution of FBS (Omega Scientific, Tarzana, CA) in sterile 1XPBS to make concentrations of 10%, 1%, 0.1%, and 0.01% FBS. Apatite-coated 12-well TCPS plates were then incubated with the BSA and FBS solutions for 12 hours in a 37°C incubator. For all wells, the apatite surface area to protein solution volume ratio was 3.9 cm^2/ml. Each well was then rinsed gently three times with 1XPBS and the amount of protein adsorbed to the apatite surfaces was quantified using BCA assay (Pierce BCA Protein Assay, Thermo, Waltham, MA).

2.2.5 Determination of caspase signaling activity by immunofluorescence

To study apoptosis, caspase-3 activity was assessed in MC3T3-E1 cells cultured on apatite surfaces. Cells were cultured at a cell seeding density of 10,000 cells/cm^2 in serum-free EM for 24h on bare apatite, 1% BSA-coated apatite, or bare apatite surfaces in the presence of 1mM phosphonoformic acid (PFA). The cells were then fixed and probed with antibodies specific for activated caspase-3, washed 3 times with 1XPBS for 5 minutes/wash, and then incubated with FITC-conjugated goat anti-rabbit secondary antibodies. Cell nuclei were counterstained with DAPI mount (Southern Biotech, Birmingham, AL). As a positive control, MC3T3-E1 cells were cultured on TCPS in the presence of 1uM doxorubicin (Sigma) a DNA intercalator that induces apoptosis through the caspase cascade. Staining for caspase activity was observed under fluorescence microscopy (Leica DM IRB, Wetzlar, Germany).

2.2.6 Effect of caspase inhibition on MC3T3-E1 cell viability upon culture on apatite surfaces

To further assess the role of apoptosis in cell death on apatite surfaces, MC3T3-E1 cells were cultured on bare apatite in serum-free EM in the presence of the general caspase inhibitor zVAD-fmk [69]. MC3T3-E1 cells were prepared for serum-free conditions as described above, and treated with various concentrations of zVAD-fmk (0, 10uM, 50uM, 100uM) prior to seeding onto apatite. The cells were then seeded at density of 10,000 cell/cm^2 onto apatite-coated TCPS, and again treated following seeding with zVAD-fmk at the concentrations listed above for 24h. Cells cultured on 1% BSA-coated apatite were used as a control. After 24h, cell viability was assessed with Live/Dead staining and Alamar Blue as before.

2.2.7 The effect of extracellular calcium (Ca^{2+}) and phosphate (PO_4^{3-}) on MC3T3-E1 viability

The effect of Ca^{2+} and PO_4^{3-} uptake on cell viability was performed by supplementing EM with known amounts of Ca^{2+} and PO_4^{3-}. For this, 10 mM stock solutions of $CaCl_2$ (EMD) and NaH_2PO_4 (Sigma) were prepared separately in EM. MC3T3-E1 cells were cultured on TCPS at 10,000 cells per cm^2 for 4h in unsupplemented EM to allow cell attachment. After 4h, the media from each well was replaced with EM supplemented with various concentrations of Ca^{2+} and PO_4^{3}, prepared from the 10 mM stock solutions of $CaCl_2$ and NaH_2PO_4. The cells were cultured in the Ca^{2+} /PO_4^{3}-supplemented media for 24 hrs and cell viability was assessed using Live/dead staining or Alamar Blue assay. The pH of the Ca^{2+} and PO_4^{3}-supplemented EM at each of the different concentrations was measured to verify that the pH had not altered significantly from physiological pH (data not shown).

To confirm the effect of Ca^{2+} and PO_4^{3-} uptake on cell death, MC3T3-E1 cells were incubated in EM containing cytotoxic levels of Ca^{2+} and PO_4^{3-} in the presence of Ca^{2+} blockers or PO_4^{3-} transporter inhibitor. Cells were seeded at 10,000 cells/cm^2 on either uncoated or apatite-

coated 12-well TCPS plates and immediately treated with EM for 24 hrs supplemented with ion transport inhibitor. To block Ca^{2+} uptake, the L-type Ca^{2+}-channel inhibitors, nifedipine (Sigma) or verapamil (Sigma), or the generalized Ca^{2+}-channel inhibitor lanthanum chloride (Sigma) were added to EM at a concentration ranging from 25uM to 100uM. To block uptake of PO_4^{3-}, the PO_4^{3-} transport inhibitor phosphonoformate (PFA, Sigma) [22] was added to the culture medium at concentrations ranging from 25uM to 1mM. The effect of these inhibitors on MC3T3-E1 viability was assessed by Live/Dead staining and Alamar Blue assay.

2.2.8 Inductively Coupled Plasma-Optical Emission Spectroscopy and radio-labeled calcium phosphate tracking

Analysis of extracellular Ca and P concentration in culture media was performed using inductively coupled plasma-optical emission spectroscopy (ICP-OES). For this, apatite-coated surfaces were incubated in the presence of serum-free α-MEM from 15 min to 24 hrs. Basal levels of Ca and P are reported by the manufacturer to be 1.8 mM and 1.0 mM, respectively. The medium from each apatite-coated well was then collected and digested with nitric acid for 2 hrs on a 90°C heating block. Each digested sample was diluted with glass distilled water until the final concentration of nitric acid reached 5% to match that of the calibration standards, which contained a known amount of Ca and P. The samples were then analyzed for elemental Ca and P with a TJA Radial Iris 1000 ICP-OES machine (Thermo, Waltham, MA).

To confirm that Ca^{2+} and PO_4^{3-} ions from culture medium were adsorbing to the apatite surface, α-MEM was supplemented with radioactive Ca-45 or P-32 isotopes (MP Biomedicals, Santa Ana, CA) at a concentration of 1uCi/ml, and incubated over apatite-coated surfaces up to 24h. The media was collected and radioactivity measured with a Beckman Coulter LS6500

multi-purpose scintillation counter (Beckman Coulter, Brea, CA). In addition, the apatite coatings were digested with 1mM HCl from the bottom of each well and their radioactivity also measured to determine the amount of radioactive Ca^{2+} and PO_4^{3-} adsorbed to the apatite.

2.3. Results

2.3.1 Apatite Morphology

Apatite surfaces prepared through an accelerated approach [1], [2] showed a plate-like structure, with plate length ranging from approximately 1-5um (Figure 1). EDS analysis confirmed that the apatite consisted primarily of Ca and P, in a Ca/P atomic ratio of 1.48, which is slightly below the reported 1.67 stoichiometric ratio of pure hydroxyapatite,[24] but is consistent with other apatite coatings prepared from this biomimetic approach [1].

2.3.2 Protein adsorption on apatite surfaces is required for cell viability

Previous studies have shown that adsorption of serum proteins onto biomaterial surfaces can mitigate cell death [70]. Consistent with this data, the bare apatite surfaces created in this study rapidly induced the death of MC3T3-E1 cells. Using a Live/Dead immunofluorescent (IF) assay, short-term adhesion to bare apatite (i.e. 1 hour) did not appear to affect MC3T3-E1 viability, with the majority of the adherent cells capable of metabolically cleaving the calcein-AM viability marker. However, adhesion of cells to bare apatite for only 3 hrs began to produce significant levels of cell death (Figure 2A). Increasing adhesion time to 24 hours resulted in a dramatic increase in cell death with the majority of cells incorporating EthD-1 as a fluorescent marker of dead cells. Quantitatively, a similar time course of increasing cell death was observed using an Alamar Blue assay – an assay that quantifies viable cells through metabolic processing

of the Alamar Blue reagent [71]. As with the Live/Dead assay, the Alamar Blue assay confirmed that the majority of MC3T3-E1 cells, after 1 hour adherence to bare apatite, were still metabolically active (i.e. viable). However, a significant drop in the number of viable cells (i.e. a 79.6% decrease in viability) was observed after 3 hours (Figure 2B). Unlike the Live/Dead IF assay, Alamar Blue failed to measure any further decrease in cell viability between 3 and 24 hours, whereas there was an obvious drop in viability using the Live/Dead assay. This discrepancy may be due to inherent differences in the sensitivity of these two assays. However, both assays confirm that cellular adhesion to bare apatite layers induces their death.

To mitigate cell death, apatite surfaces, prior to cell seeding, were pre-absorbed with increasing concentrations of BSA or FBS as a source of protein. A simple BCA protein assay confirmed the adsorption of these proteins to the apatite surface (Figure 3A). For FBS a linear relationship between adsorbed protein and FBS concentration was observed between the ranges of 0.1% to 10%. After 12 hours incubation with a 0.01% FBS solution, the surface coverage of FBS protein on apatite was measured to be approximately 1.1 ug/cm^2. Increasing the FBS concentration 100-fold to 1.0% FBS resulted in almost a 1.5-fold increase in adsorbed FBS protein (1.54 ug/cm^2), while a 1000-fold increase to 10% FBS resulted in almost a 1.75-fold increase (1.84 ug/cm^2). While not shown, there was no appreciable increase in protein absorption if the FBS concentration was increased beyond 10% (data not shown). Linearity in the adsorption of BSA to apatite surfaces was not as apparent. However, a moderate linear relationship was observed between the ranges of 0.1% and 0.001% BSA. For adsorbed BSA on apatite, incubation for 12 hours with a 0.001% BSA solution resulted in approximately 0.5 ug/cm^2 surface coverage. A 10-fold increase in the BSA concentration to 0.01% led to a 2-fold increase in adsorbed BSA at 1.1 ug/cm^2. Only a slight increase in BSA adsorption was observed

after increasing the BSA solution 100- and 1000-fold, with protein surface coverage of 1.22 ug/cm^2 and 1.28 ug/cm^2, being measured respectively.

Live/dead staining of MC3T3-E1 cells cultured in serum-free EM on protein-coated apatite surfaces showed that "rescuing" cell viability was related to the amount of pre-adsorbed protein on the apatite surface prior to cell seeding (Figure 3B). As shown in Figure 3B, the viability of cells maintained in serum-free media for 24 hours on apatite surfaces with increasing amounts of adsorbed BSA or FBS, increased in a qualitative manner. For example, approximately 50% of the seeded cells maintained on apatite surfaces pre-treated with a 0.1% FBS solution remained viable, while nearly all cells remained viable on apatite surfaces pre-treated with 10% FBS. Similarly, MC3T3-E1 cells cultured for 24 hours on apatite surfaces pre-exposed to 0.01% BSA (i.e. the approximate concentration of albumin found in 0.1% FBS) showed close to 50% viability, while protein pre-adsorption with a 1% BSA solution (i.e. the approximate content of albumin found in 10% FBS) rescued viability in nearly 100% of the adherent cells. Quantifying cell metabolic activity as a means of measuring viability confirmed the Live/Dead studies (Figure 3C). As with the protein adsorption studies of Figure 3A, a definitive dose-dependent relationship appeared to exist between FBS concentration and cell viability. In contrast, the effect of BSA on MC3T3-E1 viability was not as linear, but appeared to plateau out at 0.01% BSA. Increasing the concentration of BSA beyond 0.01% did not enhance viability in a statistically significant manner.

2.3.3 Apatite-induced cell death is not through caspase-mediated apoptosis

To determine whether apatite-induced cell death was mediated by an apoptotic mechanism, MC3T3-E1 cells were cultured on bare apatite surfaces at various time points and

probed for caspase-mediated activation of apoptosis using an antibody specific to cleaved caspase-3. As shown in the Live/Dead and Alamar Blue assays, MC3T3-E1 cells cultured on bare apatite for only one hour did not show any evidence of caspase-3 cleavage, consistent with the viable state of these cells at this juncture (Figure 4A). However, cleaved caspase-3 was still not observed when the culture time was increased to 3 or 24 hours – times in which MC3T3-E1 cell death has been detected (data not shown). In contrast to these results, strong immunofluorescence for cleaved caspase-3 was observed in positive controls in which cells were treated with 1 uM doxorubicin to induce apoptosis.

To determine if other effector caspases known to induce apoptosis (i.e. caspase-6, caspase-7) were mediating MC3T3-E1 cell death, cells were cultured on bare apatite surfaces in the presence of the general caspase inhibitor zVAD-fmk. Over the range of zVAD-fmk concentrations tested (0 uM, 10 uM, 50 uM, 100 uM), Live/Dead staining (Figure 4B) and Alamar Blue viability quantification (Figure 4C) showed that general inhibition of caspase activity was not sufficient for preventing MC3T3-E1 cell death when cultured on bare apatite. Adsorbed BSA on apatite, however, still demonstrated the ability to mitigate the cytotoxic effects of the apatite surface, with or without the presence of zVAD-fmk in the medium. Taken together, the lack of caspase-3 activation and the inability to rescue cell viability through the inhibition of caspase activity, suggest that the mechanism of apatite-induced cell death over 24 hours of culture is not due to caspase-mediated apoptosis.

2.3.4 Elevated levels of Ca^{2+} in combination with PO_4^{3-} can decrease MC3T3-E1 cell viability

Previous work by Adams *et al*. [22] has shown that extracellular Ca^{2+} and PO_4^{3-} can decrease the viability of human osteoblast-like cells and MC3T3-E1 murine pre-osteoblast cells

in a dose-dependent manner. Since biomimetic apatite surfaces are composed primarily of Ca^{2+} and PO_4^{3-}, it is possible that the release of these ions into the medium upon culture onto apatites could expose MC3T3-E1 cells to elevated levels of these ions. To confirm the effects of elevated extracellular Ca^{2+} and PO_4^{3-} on MC3T3-E1 viability, MC3T3-E1 cells were cultured on TCPS in basal EM, containing 1.8mM total Ca^{2+} and 1.0 mM total PO_4^{3-} and in EM supplemented with increasing concentrations of these two ions. Using Alamar Blue to quantify cell viability (Figure 5A), it was confirmed that exposure of cells to elevated extracellular Ca^{2+} and PO_4^{3-} resulted in a decrease in MC3T3-E1 viability. Cell death by Ca^{2+} and PO_4^{3-} ions was concentration-dependent and required the presence of both ions for maximal effect. For example, when the concentration of extracellular Ca^{2+} was held constant at its basal level of 1.8 mM, increasing extracellular PO_4^{3-} levels (e.g. 2.5mM to 10mM) did not significantly alter cell viability. Likewise, when cells were cultured at basal PO_4^{3-} levels (i.e. 1.0 mM), increasing extracellular Ca^{2+}concentrations (i.e. 2.5 mM to 10mM) had no significant effect on cell death. However, when both the concentrations of Ca^{2+} and PO_4^{3-} were increased, MC3T3-E1 cell death levels also increased. Increasing extracellular PO_4^{3-} to 5.0mM, combined with increasing Ca^{2+} levels to 5.0mM led to nearly a 33% decrease in the number of viable cells, while increasing Ca^{2+} further to 10mM decreased cell viability 98%. Similarly, when PO_4^{3-} levels were increased to their maximal level of 10mM, a Ca^{2+} concentration of 5.0mM resulted in a 50% drop in viable cells, while a Ca^{2+} concentration of 10mM decreased cell viability 95%. Taken together, the results confirmed previous studies showing that the ion-pairing of extracellular Ca^{2+} and PO_4^{3-} at specific concentrations can be cytotoxic to MC3T3-E1 cells. Moreover, the data indicates that at higher levels of PO_4^{3-} (i.e. 5mM, 10mM), elevating extracellular Ca^{2+} levels can dramatically decrease cell viability.

To further confirm the cytotoxic effects of Ca^{2+} and PO_4^{3-} on MC-3T3-E1 viability, cells, incubated on TCPS in the presence of cytotoxic levels of extracellular Ca^{2+} and PO_4^{3-}, were treated with the Na-Pi co-transporter inhibitor PFA, to block PO_4^{3-} entry into the cell, followed by an assessment of their viability. Results from the Alamar Blue assay confirmed previous studies [22] showing that administering PFA results in the "rescue" of MC3T3-E1 viability (Figure 5B). At the higher levels of extracellular PO_4^{3-} (i.e. 5mM, 10mM), which were shown to be cytotoxic in this study with a slight increase in extracellular Ca^{2+}, a delivered dose of 1mM PFA was sufficient to significantly reduce the amount of cell death that was observed above. In contrast, as has been shown previously [22], although the blockage of PO_4^{3-} transporters was sufficient to inhibit the Ca^{2+}/PO_4^{3-}-induced cell death, treatment of cells with L-type Ca^{2+} channel blockers (nifedipine or verapamil) and a general Ca^{2+} channel blocker (lanthanum chloride) did little to mitigate cell death in the presence of elevated extracellular Ca^{2+} and PO_4^{3-} (data not shown).

2.3.5 Apatite surfaces in culture medium induce the "pull-down" of extracellular Ca2+ and PO43-

As shown above, increasing levels of extracellular Ca^{2+} and PO_4^{3-} can be cytotoxic to adherent MC3T3-E1 cells. Since biomimetic apatite surfaces are composed primarily of Ca^{2+} and PO_4^{3-}, the observed cell death upon adherence of MC3T3-E1 cells to bare apatite may be the result of localized degradation of the apatite in culture conditions, thus elevating extracellular levels of these ions. Therefore, the stability of the apatite surface in culture was measured using ICP-OES. For this, acellular, bare apatite surfaces were incubated in serum-free α-MEM (as a component of EM) for up to 24 hours and extracellular levels of calcium and phosphorus (as a

component of phosphate) were measured by ICP-OES (Figure 6A). Consistent with reported values, basal levels of calcium and phosphorus within serum-free α-MEM was measured at 1.8mM and 1.0 mM, respectively. During the first 3 hours of incubation on apatite surfaces, the concentration of calcium and phosphorus within the α-MEM decreased to approximately 53±0.041% and 63±0.032% of their original concentrations, respectively, suggesting that the apatite layer may "pull-down" these ions from the overlying medium. After 12 hours, this calcium and phosphorus ion "pull-down" reached equilibrium, stabilizing at a concentration of approximately 0.58±0.14 mM Ca and 0.42±0.04 mM P (decreases of 32±0.072% and 44±.053% relative to basal levels), respectively. ICP-OES analysis of medium incubated over apatite surfaces for an additional 48 hours (i.e. 72 hours total) did not detect any further change in the levels of extracellular calcium and phosphorus. Taken together, the ICP-OES data suggests that the apatite surface does not significantly release Ca^{2+} and PO_4^{3-} ions into the extracellular environment but may induce a "pull-down" of these ions from the culture medium.

To confirm this data, apatite surfaces were cultured with serum-free α-MEM containing radioactive Ca-45 and P-32. After 3h incubation over apatite surfaces, the radioactivity of Ca-45 and P-32 in the serum-free α-MEM fell to levels nearly identical to that obtained from ICP-OES. (Figure 6B-C, dashed lines). The amount of radioactive Ca-45 and P-32 in the medium fell to 53±0.017% and 62±0.0067%, respectively. Similar to the results obtained by ICP-OES, the decrease in Ca-45 and P-32 in the medium began to level off after 12h incubation over apatite at approximately 36±0.017% of the starting Ca-45 levels and 49±0.011% of the P-32 initially added to the serum-free medium.

After removal of the Ca-45 and P-32-supplemented α-MEM from the apatite-coated wells at each time point, the apatite coatings were dissolved with dilute HCl and the amount of Ca-45 and P-32 that had deposited on the surfaces were measured. The radioactivity of deposited Ca-45 and P-32 onto the apatite surface correlated almost identically to the amount of radioactive material that had been depleted from the Ca-45 and P-32-supplemented medium collected at each time point (Figure 6B-C, solid lines). Along with the ICP-OES data, these results suggest that the apatite surfaces are capable of altering local extracellular ionic Ca^{2+} and PO_4^{3-} concentrations that are presented to the cultured MC3T3-E1 cells.

2.3.6 Inhibition of PO43- uptake can "rescue" MC3T3-E1 viability upon culture on apatite surfaces

The results from this study, as well as those obtained by others [22], suggest that the inhibition specifically of Na-Pi co-transporters can rescue viability of MC3T3-E1 cells cultured on TCPS in the presence of cytotoxic levels of Ca^{2+} and PO_4^{3-}. Therefore, the viability of MC3T3-E1 cells cultured on bare apatite was assessed in the presence of PFA. Consistent with our studies on TCPS, live-dead staining (Figure 7a) and Alamar Blue quantitation (Figure 7b) showed a concentration dependent effect of the ability of PFA to rescue MC3T3-E1 viability, with the minimum concentration required for significant rescue at 500uM. As expected, pre-coating apatite surfaces with 1% BSA negated the cytotoxic effect of the apatite surface. To assess if increasing levels of PFA could compound the toxicity of the apatite surface, cells were cultured on apatite surfaces coated with 1% BSA as a control and treated with increasing amounts of PFA. Viability levels were unchanged on these BSA-coated surfaces in the presence of increasing PFA, indicating a lack of toxicity by PFA. The observed rescue was specific to

PO_4^{3-} uptake as MC3T3-E1 cells cultured on apatite and treated with the Ca^{2+} channel inhibitors nifedipine, verapamil, or lanthanum chloride, showed similar levels of cell death when compared to samples cultured on apatite in the absence of these inhibitors (Figure 8). Viability levels were unchanged as concentrations of lanthanum chloride were increased on BSA-coated surfaces, indicating a lack of toxicity attributable to this inhibitor. However, a possible toxic effect was observed for nifedipine, with levels above 5uM decreasing the viability of cells cultured on BSA-coated apatite controls. However, even at subtoxic nifidepine levels (i.e. 1uM and 5uM), this inhibitor was still unable to rescue MC3T3-E1 viability on bare apatite surfaces. Based on these results, it is possible that the observed death of MC3T3-E1 cells cultured on bare apatite is due to the specific uptake of PO_4^{3-} ions into the cell.

2.4 Discussion

Despite the evidence suggesting that accelerated biomimetic apatite coatings are capable of mediating osteoblastic differentiation *in vitro* [2], [3] and new bone formation *in vivo* [4], the exact mechanisms by which cells interact with biomimetic apatite coatings to elicit these osteogenic responses remains largely unknown, and few studies in the literature have studied the direct cell-apatite relationship closely. As such, this study attempts to more closely examine the relationship between the apatite layer and the cellular response. In the in vivo environment, apatite materials are very biocompatible. However, performing the in vitro experiments in this study allows us to dissect the apatite microenvironment and evaluate the relative contribution of each component in this highly complex, dynamic system. To accomplish this, MC3T3-E1 pre-osteoblasts were cultured on apatite surfaces and the effect of this surface on the adhesion and viability of these cells was assessed.

As was previously shown [1], apatite coatings prepared from an accelerated biomimetic approach resulted in a uniform coating consisting of Ca^{2+} and PO_4^{3-} ions in a calcium/phosphorus atomic ratio of 1.48, which is below the stoichiometric ratio of 1.67 for hydroxyapatite. The coating consists of distinct plate-like apatite crystals around amorphous calcium phosphates. Electron diffraction of the calcium-deficient, plate-like apatite crystal revealed diffraction patterns at d_1=2.81 Å, d2=3.44 Å and d3=2.72 Å which correspond to (2 1 1), (0 0 2) and (1 1 2) planes of hydroxyapatite, respectively [1]. Although the direct effect of apatite crystal structure on cell viability remains largely undiscovered, it is known, however, that the crystalline phase of the apatite contributes to its stability and consequently its dissolution rate [72], [73]. It is known that both the amorphous and crystalline phases undergo continuous phase transformation, and fluctuations in Ca^{2+} and PO_3^{4-} levels may contribute significantly to changes in the overall microenvironment and subsequent in vitro cellular response.

Consistent with previous studies [74], MC3T3-E1 cells rapidly adhered to uncoated apatite materials (i.e. bare apatite). However, cell death began to appear within the first 3 hours post-seeding with increasing levels of cell death becoming apparent as culture time increased. The reason for this rapid cell death was found not to be due to canonical apoptotic mechanisms. Cells undergoing apoptosis, or "programmed cell death," typically commit to one of two distinct pathways (extrinsic or intrinsic) that converge upon one or more effector caspases (capase-3, -6, -7), whose activation results in cell death [75]. Our results, however, showed that the bare apatite surface did not induce activation of caspase-3 within adherent MC3T3-E1 cells, nor did inhibition of caspase activation by the general caspase inhibitor zVAD-fmk prevent cell death. Although our experiments preclude activation of the caspase cascade as the mechanism of death

in MC3T3-E1 cells cultured on bare apatite, it is still possible that cell death via apoptosis may be occurring through caspase-independent pathways [76].

Morphologically, apoptosis is generally marked by membrane blebbing, chromatin condensation, and DNA fragmentation [77], [78]. In this study, DAPI staining as well as Ethd-1 (dead) staining of cell nuclei clearly show that cells cultured on bare apatite exhibit significant alteration of nuclear morphology. However, instead of DNA condensation both DAPI and Ethd-1 show a very diffuse staining pattern, suggesting that DNA dispersion outside the nuclear envelope may be occurring when cells are cultured on bare apatite. This result may further suggest that when cultured on bare apatite surfaces, the mechanism of apatite-induced cell death over 24 hours of culture is not due to caspase-mediated apoptosis. A more likely scenario is death caused by necrosis, which is generally highlighted by nuclear swelling, early plasma membrane rupture and release of cellular contents [79]. Further morphological examination of MC3T3-E1 cells on apatite will be needed to determine whether the mechanism of apatite-induced cell death is through a necrotic process.

While bare apatite surfaces rapidly induced cell death, mitigation of cell death was observed upon pre-coating the apatite with either BSA or FBS. Previous studies have suggested that adsorbed protein layers mediate the interaction between cells and biomaterials, including biomimetic apatite coatings, promoting cell adhesion and survival [80]–[83]. A possible mechanism by which adsorbed proteins decrease cell death on apatite may be the activation of pro-survival intracellular signaling, initiated via membrane-bound integrin receptors and their transduction of the extracellular environment into intracellular signals that govern changes in cell function, including survival [84]. It has been shown in many cell types, including osteoblasts,

that survival signals are mediated through integrin-ECM interactions [85], [86]. For example, MC-3T3-E1 attachment to surfaces, modified with the ECM-integrin motif RGDS, can reduce apoptosis and promote their survival in the presence of various apoptogens [87]. Moreover, this attachment activates several signaling pathways thought to mediate cell survival, including FAK, Akt and PI3K. FAK and Akt activation and decreased osteoblast death has also been observed upon the adsorption of fibronectin and vitronectin to hydroxyapatite/PLLA composite scaffolds [70].

Alternatively, adsorbed protein layers may mitigate cell death via their alteration of the surface potential of the apatite coating or by modulation of the phase transformation rate of the apatite surface. Negatively charged surfaces of polarized hydroxyapatite ceramics are known to promote proliferation, while positively charged surfaces inhibit this response [88]. The interaction of acidic proteins, such as BSA, to cationic sites on the apatite surface is also known to cause the net surface charge to become more negative [89]. As such, the adsorption of BSA or FBS to the apatite layers in this study may alter surface charge sufficiently to improve cell adhesion and viability.

Adsorbed protein layers, alternatively, may increase the surface stability of the apatite through the modulation of phase transformation [90], [91]. Fibroblasts cultured on biphasic tricalcium phosphate-hydroxyapatite (TCP-HA) ceramics in the absence of proteins are thought to rupture due to adhesion to the unstable TCP-HA surface [74], while the addition of serum components to their culture media is capable of mitigating this response. The adsorption of serum protein to these TCP-HA surfaces and the increased stability of this surface are proposed

as the mechanism behind the increased survival of these fibroblasts. Additional studies on the surface charge and stability of the apatite surfaces created in this study are certainly warranted.

Previous *in vitro* work on MC3T3-E1 pre-osteoblasts has shown that elevated levels of *both* extracellular Ca^{2+} and PO_4^{3-} decrease cell viability, possibly through their complexing as an ion pair or cluster, thus triggering receptor-mediated induction of apoptosis, or endocytic activation of cell death [22], [92]. Consistent with these studies, we confirmed that MC3T3-E1 cells, cultured on TCPS showed increasing levels of cell death upon supplementation with *both* extracellular Ca^{2+} and PO_4^{3-}. Ca^{2+} uptake into osteoblasts is thought to be mediated through several types of calcium channels including conventional L- and T-type channels [93], [94] and G-protein coupled receptors termed "Ca^{2+} -sensing receptors" that respond to extracellular Ca^{2+} levels [95]. Phosphate uptake by these cells has been attributed to the type III Na-Pi transporters, Pit-1 and Pit-2 [96]. While both Ca^{2+} and PO_4^{3-} ions were needed to induce MC3T3-E1 cell death in this study, only specific inhibition of PO_4^{3-} uptake was able to mitigate this response, indicating that cell death is sensitive to PO_4^{3-} transport, and that this sensitivity has been shown to be Ca^{2+}-dependent [22]. In contrast, treatment with several Ca^{2+} channel blockers (i.e. nifedipine, verapamil, lanthanum chloride) was unable to change levels of cell death. Although the inhibition of the Ca^{2+} channels specific to the blockers used in this study failed to rescue cell viability, there may be other Ca^{2+} channels that play a more significant role in mediating cell viability and function, and efforts to determine intracellular Ca^{2+} levels will provide additional insight into this mechanism. Inhibition of extracellular PO_4^{3-} transport into human osteoblasts and MC3T3-E1 cells by the Pit-1 inhibitor phosphonoformate (PFA) has been shown to reduce Ca^{2+}/PO_4^{3-} -induced cell death through its ability to modulate the mitochondrial membrane permeability transition as well as caspase-mediated apoptosis [22], [97], [98]. The precise

reason for why both extracellular Ca^{2+} and PO_4^{3-} ions are needed to induce cell death in MC3T3-E1 cells, and why specifically inhibiting PO_4^{3-} uptake is able to rescue these cells remains unclear. In vascular smooth muscle cells, Pit-1 expression levels can be regulated by calcium concentration [99]. As such, it is possible that increasing extracellular Ca^{2+} levels may increase PO_4^{3-} uptake into MC3T3-E1 cells through its ability to regulate expression levels of the Pit-1 transporter. Further studies examining this possibility are certainly warranted.

As a rich source of Ca^{2+} and PO_4^{3-}, biomimetic apatite coatings may be able to induce cell death in a manner similar to extracellular Ca^{2+}/PO_4^{3-}. In vitro, slightly acidic conditions can induce the dissolution of calcium phosphate ceramic materials and the release of Ca^{2+} and PO_4^{3-} ions into the extracellular environment [100]. The release of these ions may create a microenvironment surrounding the cell in which the levels of Ca^{2+} and PO_4^{3-} are toxic. Subsequent PO_4^{3-} uptake by the adherent MC3T3-E1 cell would then lead to PO_4^{3-} -induced cell death. In support of this theory, the rescue of MC3T3-E1 viability on bare apatite was induced in the current study upon treatment of the cells with PFA, whereas blocking Ca^{2+} uptake had no effect. Furthermore, the presence of an adsorbed protein layer may be sufficient for mitigating PO_4^{3-} uptake by MC3T3-E1 cells in a similar manner as PFA. However, the ICP-OES analysis of our study confirmed that the culture conditions used did not cause a noticeable release of ions from the apatite into solution. Rather, levels of extracellular calcium and phosphorus (as a component of PO_4^{3-}) were found to *decrease* upon incubation of apatite surfaces with α-MEM, suggesting that the apatite surface may act to "pull-down" or "attract" Ca^{2+} and PO_4^{3-} ions from the overlying medium towards the apatite surface. Similar decreases in the concentrations of Ca^{2+} and PO_4^{3-} ions in culture medium have been reported with TCP-HA ceramics [101]. How this "pull-down" might relate to MC3T3-E1 death on bare apatite layers remains unknown but it

is tempting to speculate that an apatite-induced "flux" of PO_4^{3-} ions through the microenvironment of the adherent cell could result in increased uptake of these ions, thus resulting in the induction of cell death.

2.5 Conclusions

In the absence of an adsorbed protein layer, bare apatite surfaces induce cell death of MC3T3-E1 pre-osteoblasts in serum-free media. However, it was determined that the mechanism of cell death was not mediated by caspase-dependent activation of apoptosis. Cell death could be prevented by pre-coating apatite surfaces with BSA or FBS proteins, or by pre-treating the cells with PFA to inhibit Na-Pi transport into the cell. These results suggest that adsorbed proteins may be capable of altering the bare apatite microenvironment to make it less detrimental to cell viability, possibly through the modulation of phosphate-mediated cell death.

2.6 Figures

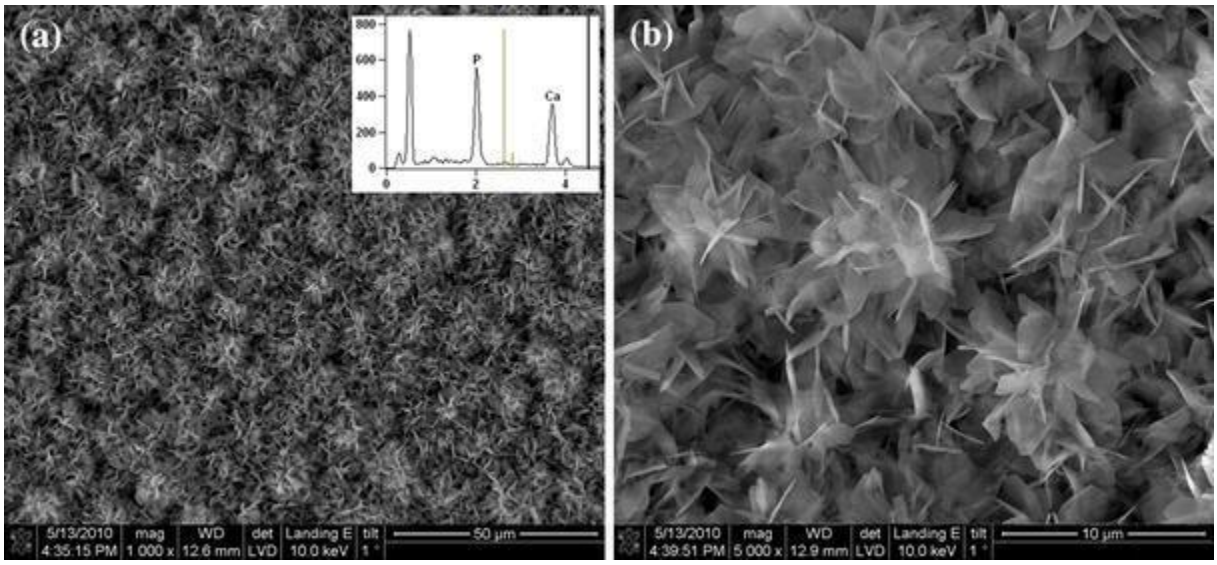

Figure 1: Plate-like morphology of biomimetically prepared apatite surfaces. Apatite surfaces were created in tissue culture polystyrene (TCPS) wells using an accelerated biomimetic approach. 1000x (A) and 5000x (B) scanning electron micrographs confirm the plate-like morphology of the resulting apatite surface. EDS analysis (A, inset) confirmed the content of calcium and phosphorus with a stoichiometric Ca/P ratio of 1.48.

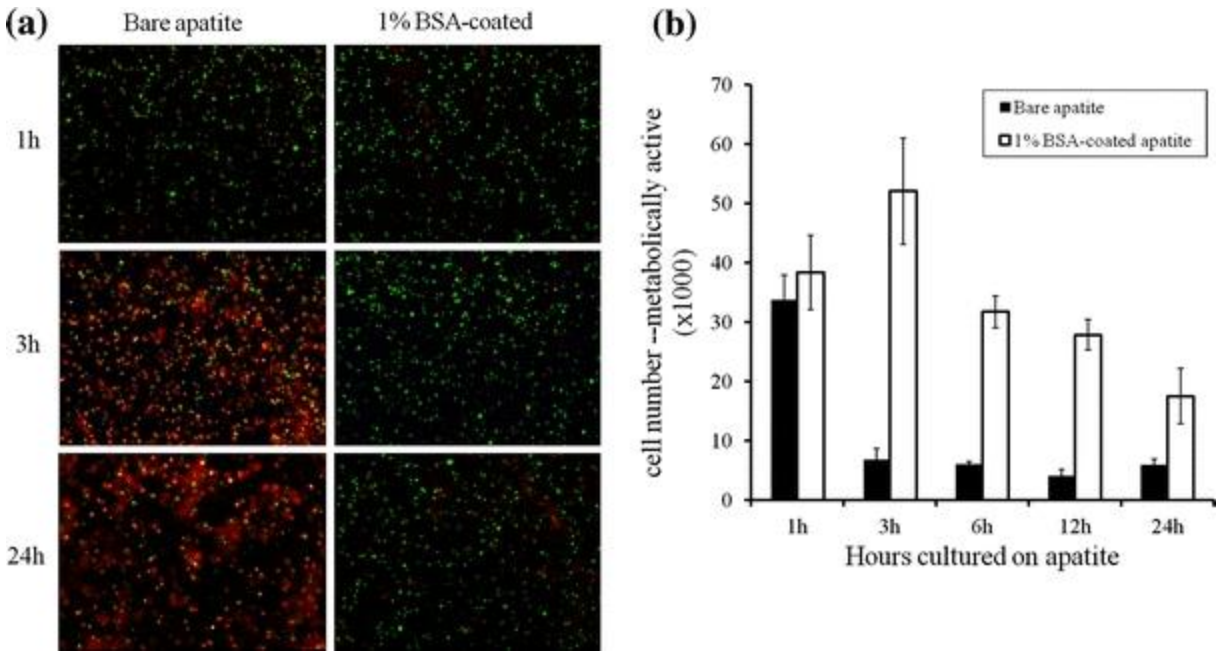

Figure 2: Bare apatite surfaces do not support cell viability. (A)MC3T3-E1 cells were seeded on uncoated apatite surfaces (i.e. Bare apatite) and viability assessed after 1 hour, 3 hours and 24 hours using a Live/dead stain. The majority of cells remain viable (green fluorescence) after 1 hour. However, increased cell death (red fluorescence) is observed between 3 and 24 hours. MC3T3-E1 cells cultured on 1% BSA-coated apatite surfaces retained viability at all time points assessed. (B) MC3T3-E1 viability was quantified over 24 hours culture on bare apatite at the indicated times using an Alamar Blue fluorometric assay. The total number of metabolically active (i.e. viable) cells on the apatite surface was determined (cell number – metabolically active (x1000)) and expressed with respect to time (Hours cultured on apatite).

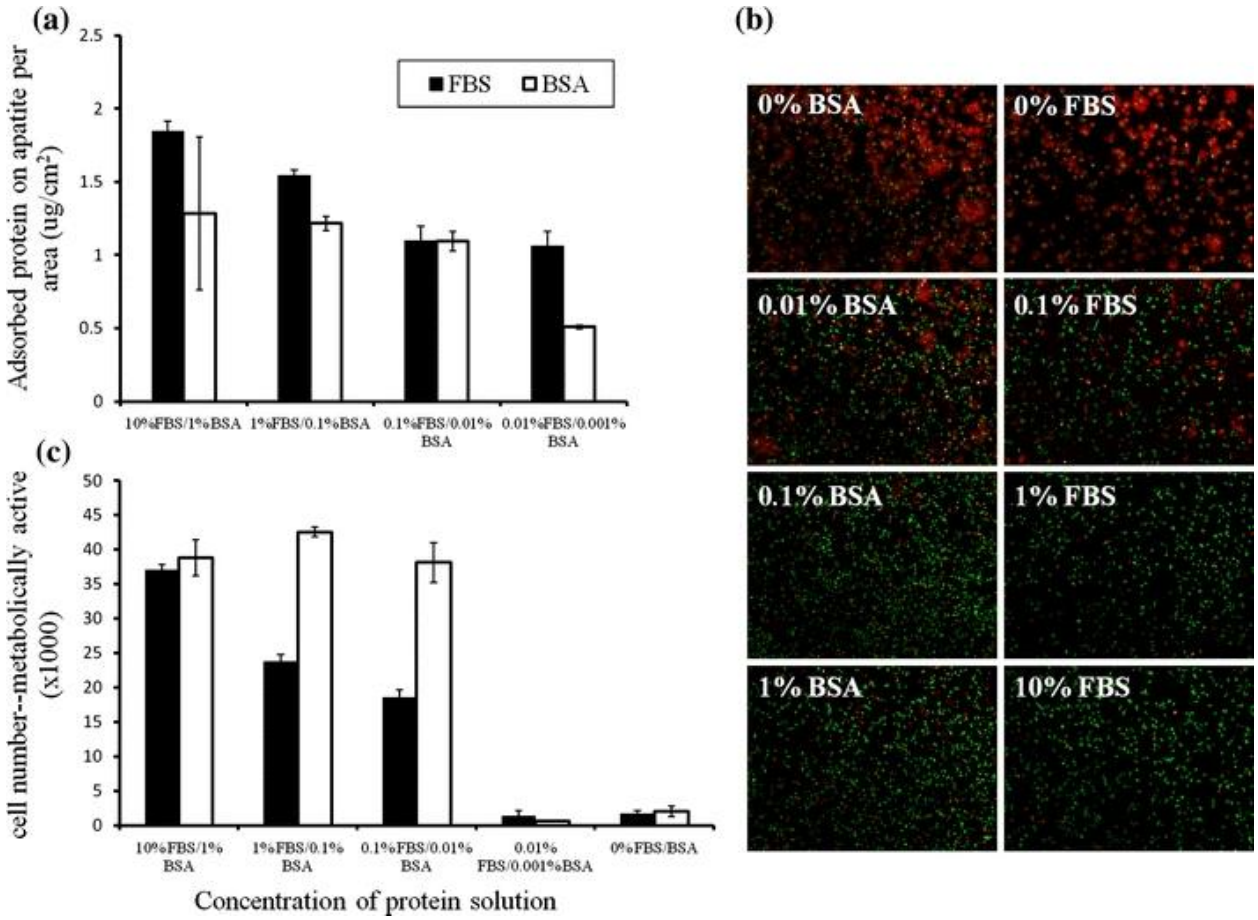

Figure 3: Protein adsorption to apatite surfaces can "rescue" MC3T3-E1 viability. (A) Increasing concentrations of either FBS (black bars) or BSA (white bars) were incubated with apatite surfaces for 12 hours to adsorb proteins onto their surface. Protein adsorption was confirmed using a conventional BCA protein assay. Protein adsorption (Adsorbed protein on apatite per area) was expressed as ug protein per cm^2 apatite surface. (B) MC3T3-E1 viability on bare apatite surfaces (0% BSA, 0% FBS) and on surfaces adsorbed to increasing concentration of FBS (right panel - 0.1% to 10%) or BSA (left panel - 0.01% to 1.0%) was assessed using Live/dead fluorescent staining. Cell viability shows a dose-dependent response with respect to the amount of protein pre-adsorbed onto the apatite coating prior to cell seeding, with an increasing number of live cells (green fluorescence) and a fewer number of dead cells (red fluorescence) being observed as protein concentration increases. (C) MC3T3-E1 viability on bare and protein-coated apatite surfaces was also quantified using a fluorescent Alamar Blue assay. Viable cells, measured through metabolic Alamar Blue reduction (cell number – metabolically active (x1000)), were expressed with respect to % protein adsorbed to the apatite surface (Concentration of protein solution). Increasing cell viability on apatite surfaces was dose-dependent, with a minimum protein concentration of 0.1% FBS or 0.001% BSA needed to "rescue" cell viability.

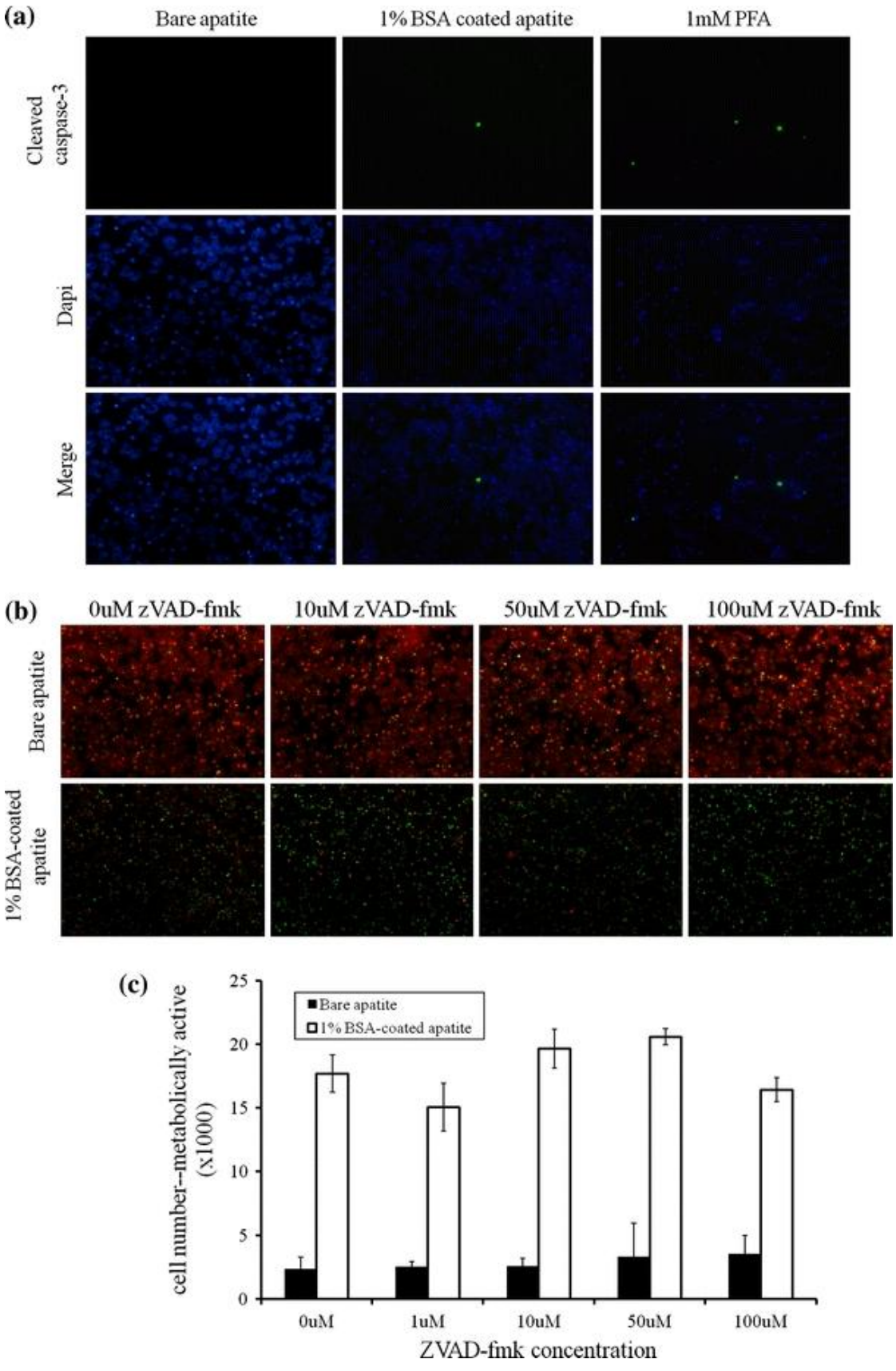
(a)
Bare apatite
1% BSA coated apatite
1mM PFA
Cleaved caspase-3
Dapi
Merge
(b)
0uM zVAD-fmk
10uM zVAD-fmk
50uM zVAD-fmk
100uM zVAD-fmk
Bare apatite
1% BSA-coated apatite
(c)
Bare apatite
1% BSA-coated apatite
cell number--metabolically active (x1000)
25
20
15
10
5
0
0uM
1uM
10uM
50uM
100uM
ZVAD-fmk concentration

Figure 4: MC3T3-E1 cell death on bare apatite surfaces is not mediated through a caspase-dependent apoptotic pathway. (A) MC3T3-E1 cells were cultured on bare apatite (left panel), 1% BSA-coated apatite (center panel), or bare apatite with 1mM PFA (right panel) for 1h and then analyzed for immunofluorescent staining of activated caspase-3 (Cleaved caspase 3 – green fluorescence). Cell nuclei were counterstained with DAPI (blue) and the images merged. (B) MC3T3-E1 cells cultured on bare apatite (black bars) or 1% BSA coated apatite surfaces (white bars) for 24h in the presence of the general caspase inhibitor zVAD-fmk. Cell viability was assessed with Live (green)/Dead (red) staining. (C) Quantification of cell viability on bare apatite vs. 1% BSA coated apatite in the presence of zVAD-fmk was assessed using fluorescent Alamar Blue assay. The number of viable cells (cell number--metabolically active(x1000)) was expressed with respect to the uM concentration of zVAD-fmk.

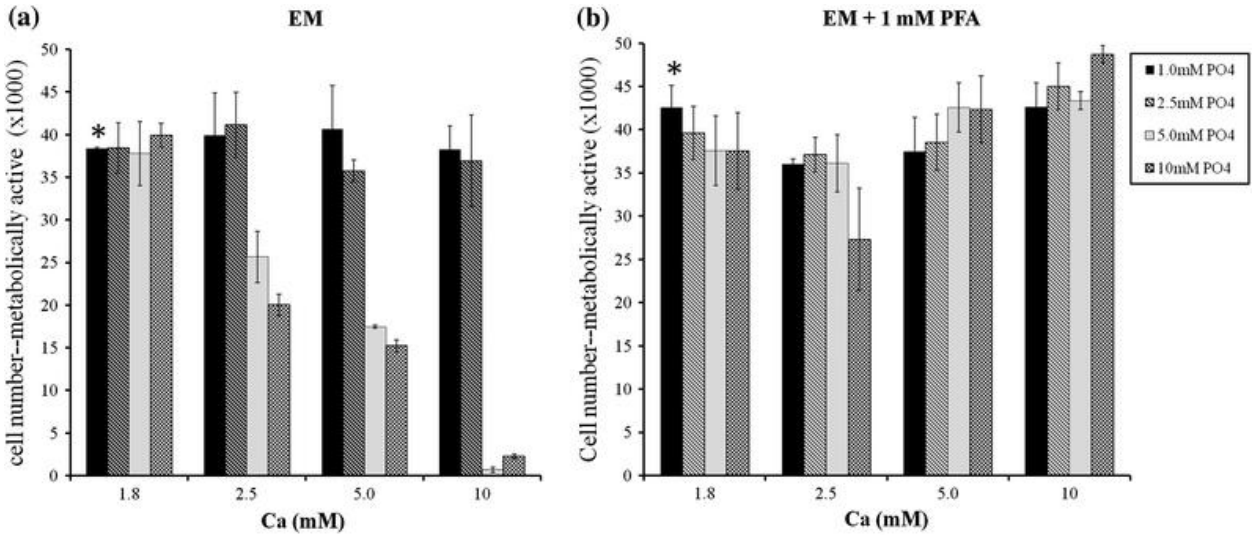

Figure 5: Extracellular Ca^{2+} and phosphate can affect MC3T3-E1 cell viability. (A) MC3T3-E1 cells were cultured on TCPS for 24 hours in EM supplemented with extracellular Ca^{2+} (total range: 1.8-10mM) and phosphate ions (total range: 1.0-10.0 mM). Unsupplemented EM containing basal Ca^{2+} and phosphate levels of 1.8mM and 1.0mM, respectively is shown with an "*". The number of viable cells (cell number – metabolically active (x1000)) was quantified using an Alamar Blue assay and expressed with respect to calcium and phosphate levels. In the presence of increased phosphate, increasing the amount of supplemented Ca^{2+} leads to an increase in cell death. (B) MC3T3-E1 cells were prepared as in (A), but in the presence of the Na-Pi co-transport inhibitor PFA. Alamar Blue viability assay demonstrated that extracellular calcium and phosphate ion-induced cell death could be inhibited with PFA.

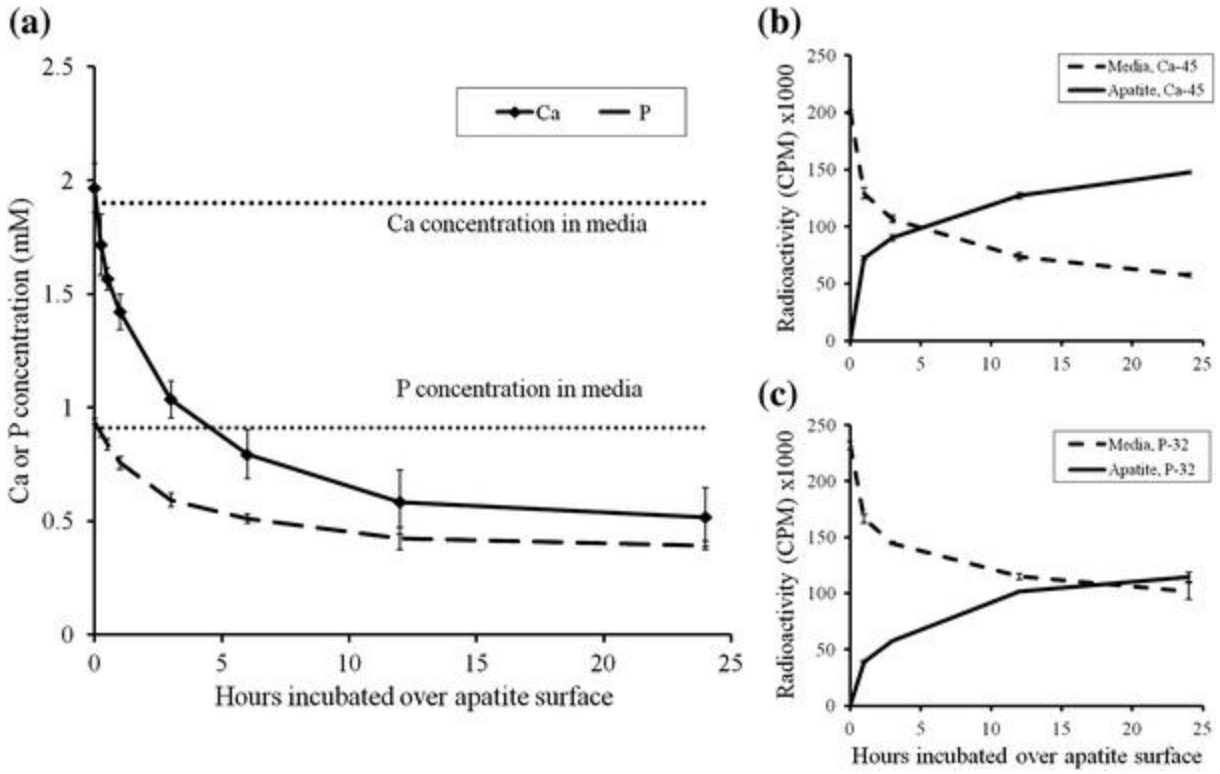

Figure 6: Apatite surfaces induce the "pull-down" of calcium and phosphate from the culture media. (A) Acellular apatite surfaces were incubated in serum-free α-MEM for up to 24 hours. At the indicated times (Hours incubated over apatite), the media was removed and subject to ICP-OES analysis to measure the concentrations of Ca and P ions within the media (Ca or P concentration (mM)). ICP-OES shows a progressive removal of Ca and P ions from the culture media within the first 6 hours, suggesting that these ions are "pulled" out of the media and deposit onto the apatite surface. Levels for Ca and P in alpha-MEM reported by the manufacturer were measured by ICP-OES prior to incubation on apatite surfaces and are shown (dotted lines). (B&C) To confirm the ICP-OES results, serum-free α-MEM was supplemented with radioactive Ca-45 (B) or P-32 (C) and incubated on acellular apatite surfaces for various lengths of time up to 24 hours (Hours incubated over apatite). The media was then removed, followed by solubilization of the apatite in HCl. Radioactivity, in counts per min (CPM) was measured in both media and apatite sample (Radioactivity (CPM)x1000). A time-dependent decrease in radioactivity within the media was observed (dashed lines), confirming the "pull-down" effect of Ca and P ions from the media onto the apatite surface. Solubilized apatite coatings showed increases in radioactivity (solid lines) that correlated almost exactly to the decrease in radioactivity in the media.

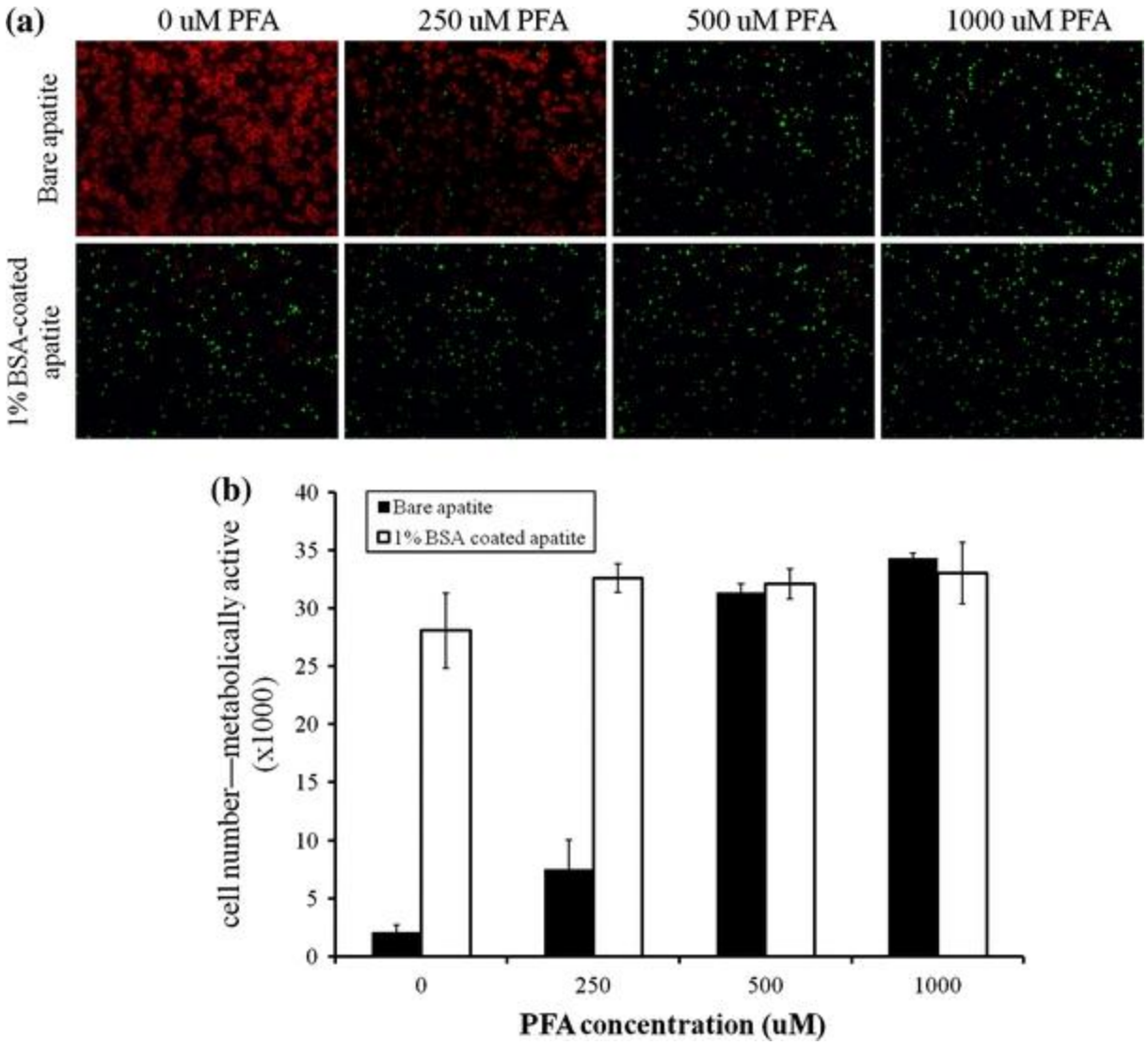

Figure 7: Blocking the uptake of phosphate ions can rescue the viability of MC3T3-E1 cells cultured on bare apatite. MC3T3-E1 cells were cultured for 24 hours on bare apatite in EM supplemented with the Na-Pi co-transport inhibitor phosphonoformate (PFA) at the indicated concentrations to block entry of phosphate into the cells. Viable cells (green fluorescence) and dead cells (red fluorescence) were detected using a Live/Dead Viability Cytoxicity stain. MC3T3-E1 cells were also cultured with PFA on apatite surfaces coated with 1% BSA (1% BSA coated apatite) as a control for the effects of this inhibitor. Increasing levels of viable cells on bare apatite treated with increasing levels of PFA suggests that blocking phosphate uptake can "rescue" MC3T3-E1 cells from apatite-induced cell death. (B) MC3T3-E1 cells were cultured on either bare apatite (black bars) or 1% BSA coated apatite (white bars) as a control, and the number of viable cells was determined via Alamar Blue assay (cell number – metabolically active (x1000)). Increasing amounts of PFA appears to increase MC3T3-E1 viability on bare apatite with a concentration of 500uM rescuing the majority of cells.

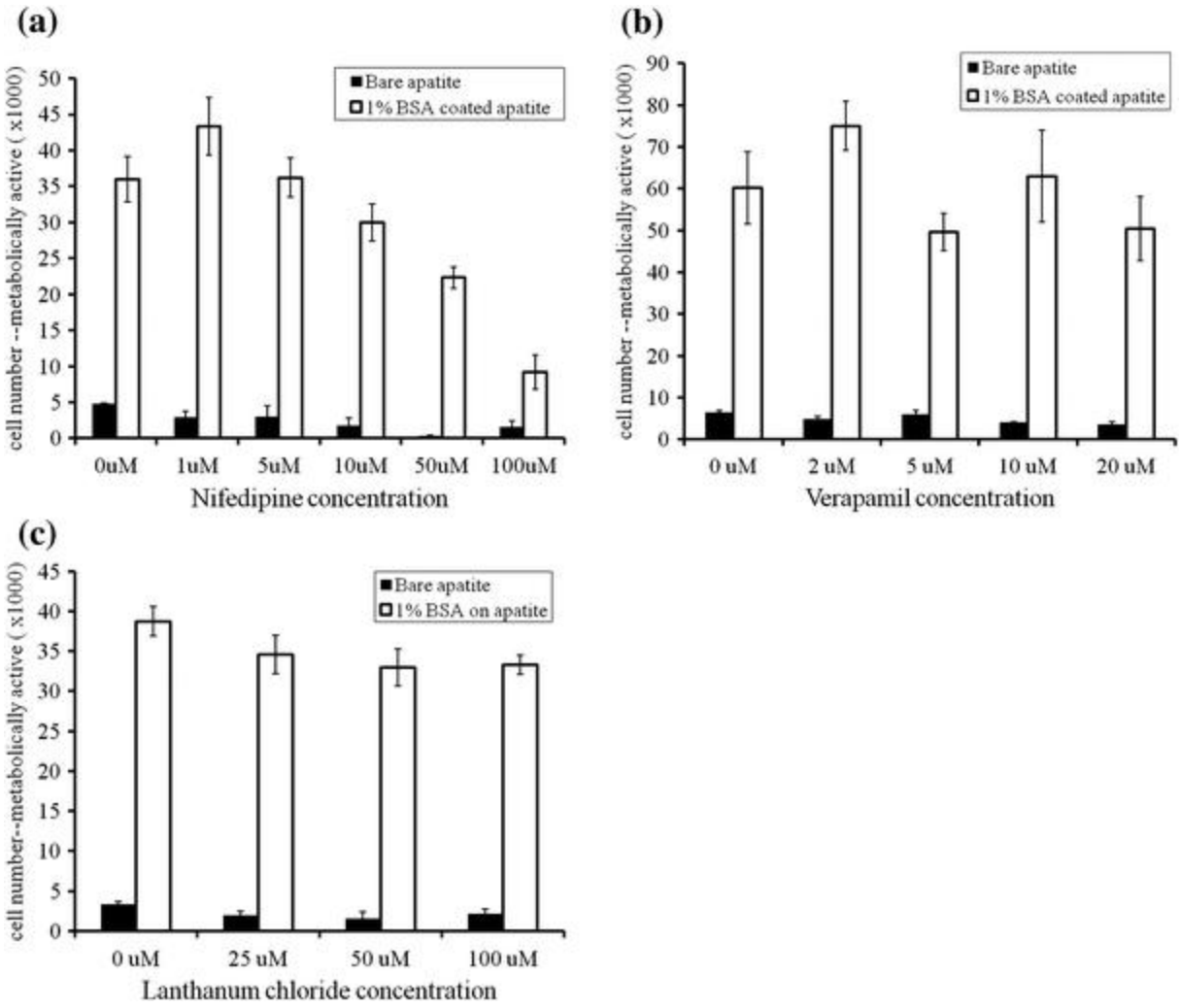

Figure 8: Blocking the uptake of calcium ions has no effect on the viability of MC3T3-E1 cells cultured on bare apatite. MC3T3-E1 cells were cultured for 24 hours on bare apatite in EM supplemented with the L-type calcium channel inhibitors (A) nifedipine, and (B) verapamil and the general calcium channel blocker (C) lanthanum chloride at the concentrations shown (black bars). MC3T3 cells were also cultured with these inhibitors on apatite surfaces coated with 1% BSA (1% BSA on apatite) as a control for the effects of this inhibitor (white bars). The number of viable cells (cell number – metabolically active (x1000)) was measured via Alamar Blue assay. At the given concentrations indicated below, treatment with calcium channel blockers was not able to "rescue" viability of MC3T3-E1 cells cultured on bare apatite surfaces. Treatment with higher concentrations of nifedipine (i.e. 10-100uM) indicated a possible toxic effect of this calcium channel blocker to control cells cultured on 1% BSA coated apatite, while lack of toxicity was observed for the given concentrations of verapamil and lanthanum chloride.

CHAPTER 3

INFLUENCE OF BIOMOLECULAR AND NON-BIOMOLECULAR SURFACE COATINGS ON ACCELERATED APATITE SURFACE ZETA POTENTIAL AND THEIR EFFECT ON CELLULAR RESPONSE

3.1 Introduction

Accelerated apatite biomaterials have been studied extensively for the regeneration of bone tissue, however, the exact mechanisms that contribute to their overall success remains largely unknown. When implanted in the body, biomaterials are known to undergo surface modifications immediately upon contact with surrounding body fluid at the implant site. One surface modification that is well-documented is the adsorption of blood proteins. This process is often considered the initial biological response that will ultimately influence the success or failure of the implant [102].

To understand the role of adsorbed proteins at the cell-apatite interface, we previously investigated the direct interaction between pre-osteoblast cells and bare apatite coatings in the absence of an intermediating protein layer [103]. This study demonstrated that in serum-free culture conditions, protein adsorption is a critical component of the apatite microenvironment, as significant cell death could be observed within three hours of cell seeding onto the bare apatite coatings. In contrast, when either a heterogeneous mix of proteins (FBS), or just a single protein (BSA) were pre-adsorbed onto the apatite surface, survival of the cultured cells could be restored. The mechanisms by which these adsorbed proteins improved the biocompatibility of accelerated apatite surface, however, have yet to be fully identified.

Apatite-based materials have high affinity for proteins [104]–[106], and it is suggested that the association between apatite surfaces and proteins are likely regulated by electrostatic interactions [107], [108]. The hydroxyapatite structure is known to have two protein binding sites that differ in electrostatic charge. C sites are calcium-rich, positively charged sites that bind to acidic protein domains (negatively charged), while P sites contain negatively charged phosphate groups that bind basic protein domains (positively charged) [105]. Several studies have shown that the apatite surface charge provided by these sites can dramatically influence cell behavior [109], [110]. For these reasons, we sought out to assess the native surface charge of accelerated apatite coatings and to investigate how protein adsorption modulates the net charge that is exposed to cultured cells. To accomplish this, several model proteins having different surface charge at physiological pH were chosen as adsorbates, and the resulting surface zeta potential and cell viability response to the treated apatite surfaces were measured. To account for potential biological effects of the proteins, polyamino acids and non-biomolecule surface coatings (carbon/gold) were also used to treat the apatite surface.

3.2 Materials and methods

3.2.1 Preparation of apatite coatings by biomimetic process

Apatite-coated substrates were prepared by a wet precipitation method through immersion in 5x concentrated SBF solutions as previously published [1], [103]. Briefly, substrates were initially incubated in a 5xSBF1, consisting of $CaCl_2$, $MgCl_2 \cdot 6H_2O$, $NaHCO_3$, $K_2HPO_4 \cdot 3H_2O$, Na_2SO4, KCl and NaCl in distilled deionized water for 24 hours at 37C. The substrates were then transferred to a 5xSBF2 solution that is similar to 5xSBF1, but devoid of the crystal growth inhibitors Mg^{2+} and HCO^{3-}. Incubation in 5xSBF2 was performed at 37C for 48

hours. Apatite-coated substrates were then rinsed gently 3 times with distilled deionized water and air-dried before further experimentation.

3.2.2 Biomolecule adsorption onto apatite-coated substrates

3.2.2.1 Protein adsorption

Stock protein solutions of bovine serum albumin (BSA), soybean trypsin inhibitor (STI), myoglobin, lysozyme, and histone H1 were prepared at a concentration of 1% (w/v) in sterile 1x PBS (Ca^{2+} and Mg^{2+} free, Mediatech CellGro, Manassas, VA). The protein stock solutions were sterile filtered through a 0.22 PES membrane and further diluted with 1x PBS to concentrations of 0.1%, 0.01%, and 0.001% (w/v). The proteins were chosen based on their isoelectric points (pI)—the pH at which their net charge is zero—in order to investigate the effect of protein charge on adsorption onto apatite surfaces, apatite surface zeta potential, and modulation of cell viability on apatite. Table 1 lists the molecules adsorbed to the apatite surfaces and their corresponding charge at physiological pH (~7.3-7.4). The apatite-coated substrates were immersed in protein solutions at a constant surface area to volume ratio of 3.9 cm^2/ml, and allowed to incubate 12 hours in a water-jacketed 37°C incubator. All substrates were rinsed three times with sterile 1x PBS immediately before seeding cells, measuring surface zeta potential, or quantifying protein adsorption using a BCA Assay (Thermo Scientific, Rockford, IL). BSA, myoglobin, lysozyme, and histone reagents were purchased from Sigma (St. Louis, MO). STI protein was purchased from (Invitrogen, Carlsbad, CA).

3.2.2.2 Polyamino acid adsorption

To control for potential confounding biological effects from the proteins on the cultured cells, polyamino acids were also adsorbed onto apatite surfaces and their effect on apatite surface charge and cell viability were assessed. As shown in Table 1, poly-L-lysine (PLL) is positively-charged, while poly-L-aspartate (PLA) and poly-L-glutamate (PLG) are negatively charged at physiological pH. Separate stock solutions of 1% (w/v) PLL, 1% PLA, and 1% PLG were prepared in 1x PBS, sterile filtered, and further diluted with sterile 1x PBS to concentrations of 0.1%, 0.01%, and 0.001% (w/v). Apatite-coated substrates were incubated in the various concentrations of polyamino acid solutions for 12 hours in a 37°C incubator, followed by triple rinsing with sterile 1x PBS to remove non-adsorbed polyamino acid. The amount of PLL adsorbed to the apatite coating was quantified using a ninhydrin assay. For this, ninhydrin was dissolved in a solution of isopropanol and 0.1 M acetate buffer (in a 3:2 ratio) to make a 1% ninhydrin working reagent. 1 ml of 1% ninhydrin working reagent was added to each PLL-treated apatite coated well of a 12-well tissue culture plate. The reagent was allowed to react with the adsorbed polyamino acid for 30 min in a 37°C oven. The reaction produced a colorimetric change in the reagent, which was quantified on a plate reader at 570 nm to determine the total amount of polyamino acid adsorbed to the apatite surface. For PLA and PLG, adsorption onto apatite was quantified by dissolving the PLA or PLG-treated apatite substrates with dilute hydrochloric acid, and UV-Vis absorbance was measured at 220 nm. The total amount in each sample was measured against a standard curve with known concentration of polyamino acid as determined by their respective quantification assays.

3.2.3 Carbon and gold-coated apatite substrates

Because biomolecules, such as the proteins and polypeptides used in this study, may potentially elicit unintended biological responses in cells, a non-biomolecular coating was sputtered onto apatite substrates in order to modulate their surface charge. A Balzers 160 carbon evaporator was used to deposit 1 or 2 layers of carbon on the apatite surfaces. Deposition of the carbon was performed using carbon thread with 1 mm thickness at a distance of 3.5 cm from the sample. Using these experimental parameters, a consistent layer of carbon with a thickness of approximately 20-40 nm on the apatite-coated substrates is expected, according to the manufacturer's specifications.

Similarly, gold sputter coating was also performed to modulate apatite surface charge. Using a Technics Hummer II sputtering system (Anatech, Alexandria, VA), the following deposition conditions were used to coat apatite samples: plate D/C mode, <50 mTorr argon gas, 10-12 mAmp current, voltage control position 12, and plate time of 30 or 120 seconds. With these experimental conditions, deposition of gold with a thickness of 10 nm (30 seconds) and 45 nm (120 seconds) was expected in accordance with the manufacturer's specifications.

3.2.4 Surface zeta potential measurements

Borosilicate glass microscope slides were cut to dimensions of 3.75 x 5 mm, cleaned in an ultrasonic bath and rinsed with distilled deionized water prior to coating with accelerated apatite and treated with various biomolecule or carbon coatings as described above. The samples were then mounted onto a surface zeta potential plate cell (Malvern, ZEN1020), placed in a cuvette containing an aqueous solution of tracer particles with known zeta potential, and then inserted into a Zetasizer Nano ZS (Malvern, Worcestershire, UK) where the surface zeta potential of triplicate apatite samples was determined. The Zetasizer Nano ZS measures the

electrophoretic mobility of the tracer particles, which is then related to the particles' zeta potential using the Smoluchowski approximation. The electrophoretic mobility of the tracer particles is greatly influenced by the presence of our apatite-coated surfaces. Therefore, by measuring the electrophoretic mobility of the tracer particles as a function of displacement from the sample surface, the apparent zeta potential of our apatite coatings can be extrapolated.

3.2.5 MC3T3-E1 cell culture and viability on apatite surfaces

MC3T3-E1 cells, purchased from ATCC (CRL-2594), were expanded under standard cell culture conditions in MC3T3-E1 Expansion Medium (EM) containing α-MEM, 10% FBS and 1% penicillin/streptomycin. As previously published [103], MC3T3-E1 cells were first transitioned to serum-free conditions by incubating in EM with 5% FBS for six hours, followed by twelve hours in serum-free EM. The cells were then harvested using 0.25% tryspin/2.21mM EDTA, and resuspended at a desired density in serum-free EM immediately before seeding onto bare apatite surfaces, apatite surfaces with adsorbed biomolecules (proteins, polyamino acids), or apatite surfaces coated with carbon. The cells were cultured on the variously treated apatite surfaces for 24 hours in at 37°C, 5% CO_2 incubator prior to analysis of cell viability. All cell culture reagents were purchased from Mediatech CellGro (Manassas, VA).

To assess the cellular response to the different adsorbing molecules on the apatite surface, MC3T3-E1 cells were seeded at a density of 10,000 cells/cm^2, and viability was quantified after 24 hours of culture on the apatite surfaces using an Alamar Blue assay (Invitrogen, Carlsbad, CA). At the desired experimental endpoint, the cell culture medium was replaced with a 10% solution of Alamar Blue reagent that was freshly prepared in serum-free EM, and the cells were incubated for one hour at 37°C. The EM containing the metabolized Alamar Blue reagent was

then removed and measured on a fluorometric plate reader at 535/590 nm (excitation/emission). The number of viable (i.e. metabolically active) cells was determined based on the measured fluorescence according to the manufacturer's protocol against a cell standard curve. Viability assays were repeated three times (n=3) and expressed as the average of viable cells ± SD.

3.3 Results

3.3.1 Apatite surfaces may adsorb negatively-charged biomolecules to a greater extent than neutrally- or positively-charged biomolecules

Various protein solutions, spanning a range of concentrations from 0.001% to 1% w/v, were incubated over apatite-coated surfaces, and the total amount of protein adsorbed to the surfaces was measured using a BCA protein quantification assay. The proteins used as the adsorbing molecules in this study (BSA, STI, myoglobin, lysozyme, and histone) differ primarily in pI value, and represent a range of relatively acidic (negatively charged) compounds to basic (positively charged) at physiological pH (~7.3-7.4).

For the model proteins used in this study, all showed a dose-dependent relationship between the initial concentration of the protein solution exposed to apatite and the amount of protein that adsorbed to the apatite surfaces. However, the total amount of protein that was adsorbed varied depending on the type of protein used. BCA assay results (Figure 9a) suggest that the negatively-charged (BSA, STI) and neutrally-charged proteins (myoglobin), adsorbed to apatite to the greatest degree, while the positively-charged proteins varied in adsorption depending on the type of protein. Consistent with previous results [103] negatively-charged BSA adsorbed to apatite surfaces in a logarithmic manner, reaching a maximum of 46.9±0.13 ug of protein/cm^2 when apatite substrates were exposed to a concentration of 1% (w/v) BSA

solution. STI protein, also negatively-charged, adsorbed to an even greater degree at the higher solution concentrations of 0.1% and 1.0% protein, reaching adsorption densities of 76.9±2.2 ug/cm^2 and 122±4.1 ug/cm^2, respectively. Compared to the negatively-charged proteins, the rate of myoglobin adsorption to apatite surfaces was more gradual at concentrations between 0.001% and 0.1% (w/v). However, a significant increase in adsorption was measured (53.8±1.9 ug/cm^2) at the highest concentration of myoglobin (1% w/v), and was found to be comparable to that of BSA protein. Lysozyme and histone, both positively-charged at physiological pH, demonstrated very different adsorption profiles when compared to negatively charged proteins, and to each other. Although both proteins demonstrated a gradual rise in adsorption over the increasing range of concentrations examined, apatite surfaces adsorbed significantly less lysozyme and histone compared to STI, BSA, or myoglobin. A concentration of 1% w/v histone allowed for an adsorption density of no greater than 34.4±1.9 ug/cm^2. Moreover, the apatite surfaces displayed an even lower adsorption capacity for lysozyme compared to that of histone, reaching 1.84±0.36 ug/cm^2 after exposure to 1% lysozyme solution.

In addition to proteins that vary in charge, acidic and basic polyamino acids were also adsorbed to apatite surfaces, and their degree of adsorption was assessed. Solutions of either poly-L-lysine (PLL), poly-L-glutamate (PLG), or poly-L-aspartic acid (PLA) were prepared at concentrations ranging from 0.001% to 1% and incubated over apatite surface for 12 hours at 37°C. As shown in Figure 9b, PLL showed a steady increase in adsorption to apatite as its concentration in solution increased from 0.001% to 1% (w/v). Exposure to the highest concentration of PLL (1% w/v) resulted in adsorption of 18.6±0.95 ug/cm^2, which was similar to the amount of BSA adsorbed to apatite from 0.01% BSA solutions (20.7±0.02 ug/cm^2). Similarly, the adsorption profile of PLA demonstrated a steady increase as the concentration of

the adsorbate solution incubated over apatite increased. However, the adsorption capacity for PLA reached a plateau at 0.1% as no further increase in adsorption was observed with 1% PLA solutions. At concentrations between 0.001% and 0.01%, the degree of adsorption of PLA was not significantly different from PLL adsorption. At 1%, however, approximately 50% more PLL was present on the apatite surface compared to PLA ($p < 0.01$).

3.3.2 Adsorption of differently charged proteins modulates the zeta potential of the apatite surface and influences cell viability

To determine whether the adsorption of proteins of different charge resulted in a measurable change in the overall apatite surface charge, apatite-coated substrates were exposed to solutions of 1% w/v BSA, STI, myoglobin, lysozyme, or histone, and the surface zeta potential was determined. As expected, the apatite charge varied depending on the type of protein adsorbed to the surface (Figure 10b). Bare apatite, which was only exposed to 1X PBS prior to measurement of charge, had a surface zeta potential of -23.6±0.31 mV. When treated with protein solutions, however, the apatite surface charge appeared to change in accordance with the native charge of the adsorbing protein molecule. For example, when exposed to the negatively-charged BSA protein solution, the apatite surface charge acquired a more negative zeta potential of -40.2±1.13 mV, while that for STI-treated surfaces showed a more moderate decrease to -29.6±3.6 mV. Similarly, adsorption of positively-charged histone mitigated the negative charge of the apatite surface from the -23.6±0.31 mV of bare apatite to -18.6±0.90 mV ($p < 0.01$). In contrast, exposure to the other positively-charged protein, lysozyme, did not significantly differ from bare apatite (-22.1±1.51 mV). Despite having a relatively neutral charge at pH 7, adsorption of myoglobin altered the apparent surface zeta potential of the apatite,

producing a slightly more negative surface charge (-29.3±2.2 mV) compared to bare apatite ($p < 0.05$).

To determine if there is a correlation between protein concentration and zeta potential, apatite surfaces were treated with BSA solutions ranging from 0.001% to 1% w/v for 12 hours, rinsed with 1x PBS and surface zeta potential measured. BSA was chosen due to its significant effect on the apatite surface zeta potential. Figure 10c shows that increasing the BSA concentration results in an accompanying step-wise decrease in the apatite surface zeta potential. Although exposure to 0.001% BSA solution did not alter the surface charge compared to bare apatite, raising the concentration to 0.01% led to a more negatively charged apatite surface (-28.0±0.85 mV, $p < 0.01$). Additional 10-fold and 100-fold increases in the BSA concentration further decreased the surface charge to -30.7±0.85 mV and -38.1±3.9 mV, respectively.

To investigate whether these proteins are also able to rescue cell viability when adsorbed to apatite, MC3T3-E1 viability was measured on protein-treated apatite surfaces in serum-free media. Consistent with the results presented in Chapter 2, cell viability (as determined by cellular metabolic activity) increased on BSA-treated apatite as the concentration of BSA exposed to the apatite surface was raised. A minimum concentration of 0.01% BSA was required to "rescue" nearly 50% of the initial cell seeding density (Figure 11). At the highest BSA concentration of 1% (w/v), greater than 84% of the initial cells seeded remained viable. In contrast, adsorption from 0.1% (w/v) STI solution was required to achieve 41.7±4.8% cell viability, and no significant increase in viability was observed with higher concentrations of STI. Neutrally-charged myoglobin, adsorbed to the apatite at 1% (w/v), resulted in a moderate improvement in cell viability, while concentrations below 1% were all unable to rescue cell

viability. The 1% myoglobin solution rescued approximately 46.7±2.6% of the original number of cells seeded, comparable to the viability from resulting from 0.01% BSA adsorption. Neutral or negative charges appeared to be vital as the positively-charged proteins had less of an effect on cell "rescue." On apatite treated with histone, a 22.6±3.1% survival rate was observed when the apatite surfaces were incubated in 1% histone solutions. However, exposure to histone solutions less than 1% led to very low cell viability, similar to bare apatite surfaces. The 22.6±3.1% survival rate on 1% histone-treated apatite surfaces was observed despite an adsorption density of 34.4±1.9 ug/cm^2 protein—an extent comparable to that of 0.1% BSA-treated apatite. Similarly, exposure of apatite surfaces to lysozyme solutions up to 1% w/v was unable to rescue cell viability—a result that may be related to the lack of significant lysozyme adsorption onto the apatite. In summary, despite the similar adsorption levels between 1% myoglobin, 1% histone, and 0.1% BSA, the 0.1% BSA-treated apatite had a significantly higher cell survival rate of 75.7±1.3%, suggesting again that the negatively-charged BSA protein at lower concentrations are capable of providing a more hospitable environment for cells on apatite.

3.3.3 Polyamino acids are also capable of modulating apatite surface charge and cell viability

In addition to protein, the influence of polyamino acid adsorption on apatite charge was assessed. Similar to the protein treatment results, exposure to negatively-charged, but not positively-charged, polyamino acid solutions for 12 hours altered the apparent zeta potential of apatite surfaces (Figure 10e). Apatite that was exposed to 1% PLL solutions exhibited a surface zeta potential of -25.4±1.8 mV, which was not statistically different from bare apatite (-23.6±0.31 mV). Exposure to 1% PLA or 1% PGA solutions, however, produced a surface charge that was significantly more negative. Adsorption of PLA resulted in a surface zeta

potential of -28.5±2.4 mV ($p < 0.05$ vs. bare apatite), while PLG generated a surface zeta potential of -31.1±2.5 mV ($p < 0.01$ vs. bare apatite). Both 1% PLA- and 1% PLG-treated apatite surfaces, however, were still significantly less negative than 1% BSA-treated apatite (-40.2±1.1 mV).

Negatively-charged polyamino acids adsorbed to apatite were also capable of rescuing cell viability as the proteins examined above, however to a lesser degree (Figure 10d and 12). Adsorbed PLL, at all concentrations tested, was unable to rescue cell viability, despite exhibiting reasonable adsorption levels on apatite after incubation in 1% PLL solution. The PLL surface coverage resulting from adsorption from 1% PLL was comparable to adsorption from 0.01% BSA solutions. However, 0.01% BSA-treated apatite surfaces demonstrated a 48.2±0.2% cell survival rate, compared to just 2.0±1.9% survival from 1% PLL-treated apatite. In contrast, negatively-charged polyamino acids (PLG and PLA), both showed improvement in cell viability when apatite surfaces were exposed to at least 0.01% polyamino acid solutions. No further improvement, however, was observed on apatite surfaces treated with higher concentrations of acidic polyamino acid. Specifically, adsorption from PLG solutions ranging from 0.01% to 1% resulted in a survival rate between 24.8±1.8% and 27.5±2.4%, while that from 0.01% to 1% PLA

3.3.4 Carbon and gold deposition onto apatite produces a more negatively-charged surface and improves MC3T3-E1 cell viability

In addition to protein and polyamino acid adsorption, apatite surfaces were modified with a non-biomolecular treatment through deposition of either carbon via evaporation, or gold via plasma sputter coating. For carbon-treated samples, one or two layers of carbon were deposited onto apatite substrates and the resultant surface zeta potential was measured. As shown in Figure

12b, the magnitude of the negative surface zeta potential increased as a function of the number carbon layers deposited on the apatite. A single carbon layer (Carbon 1x) generated a surface charge of -30.7±1.3 mV while two carbon coating layers (Carbon 2x) resulted in surface charge of -36.7±2.4 mV. The surface zeta potential of both "Carbon 1x" and "Carbon 2x" apatite samples were significantly more negative than that measured for bare apatite (-25.8 ±1.2 mV, $p < 0.05$ vs. Carbon 1x, $p < 0.01$ vs. Carbon 2x). Likewise, gold sputter coating onto the apatite substrates altered the surface zeta potential, with longer coating times producing a more negatively charged surface. Gold sputtering durations of 30 and 120 seconds resulted in measured surface zeta potentials of -31.2±1.8 mV and -37.4±1.4 mV, respectively.

The deposition of either carbon or gold onto apatite also influenced the viability of MC3T3-E1 cells that were cultured on apatite surfaces in serum-free conditions. For both types of deposition treatments, a similar trend was observed where cell viability increased as a function of the surface coating. For carbon-treated apatite, 34.5±3.8% of the initial cell seeding density remained viable with a single carbon layer, while 53.0±8.9% cell viability was observed with two carbon layers (Figure 12a). Similarly, gold-coated samples saw an increase in the percent viability to 35.5±0.9% after 30 seconds of gold sputtering, while the viability improved to 51.0±6.3% after 120 seconds of gold coating. Taken together, the surface zeta potential and cell viability results after carbon and gold deposition further suggest that modifying the native apatite zeta potential towards a more negative surface charge improves the cellular biocompatibility of the apatite microenvironment.

3.4 Discussion

Use of calcium phosphate-based biomaterials like accelerated apatite coatings is one approach that has had a history of success for both *in vitro* and *in vivo* applications for bone tissue engineering [1]–[4]. Despite this repeated success, surprisingly, little is known regarding the exact mechanism that produces the enhanced bioactivity within the apatite microenvironment. However, it is well known that when introduced into the body, many biomaterial implants will trigger a biological response upon exposure to blood and the surrounding tissue [102]. The nature of this response, and ultimately the biological performance of the implant, may be dictated by several material surface properties such as topography, surface charge, and/or the chemical constituents or chemical factors that are introduced with the implant. These properties are known to mediate protein adsorption and cell adhesion on the biomaterial implant surface, modulating specific signaling pathways to invoke certain cellular responses.

In the case of apatite-based materials, few studies have looked specifically at the contribution of the inherent surface charge at the cell-apatite interface. The hydroxyapatite crystal surface possesses two, oppositely charged sites that allow it to bind to both acidic and basic protein domains [105]. C sites, which are arranged on the *ac* or *bc* crystal faces, are rich in calcium ions resulting in a high local positive charge density that serve as binding sites acidic proteins. P sites are arranged on the *ab* crystal faces and contain a high density of negatively charged phosphate ions, providing binding sites for basic protein groups. As such, this study aimed to more carefully examine how modulation of the apatite surface potential influences cell behavior.

To accomplish this, several model proteins were first chosen based on their charge at physiological pH, and were exposed to apatite surfaces over night to allow for adsorption. Despite having an overall net negative surface zeta potential, accelerated apatite coatings showed a preference for adsorbing negatively-charged proteins, followed by neutrally-charged proteins (although to a slightly lower extent), while adsorption of positively-charged proteins varied depending on protein type. BSA and STI—which both have isoelectric points around 4.5-4.7 and hence have a net negative charge in normal *in vitro* culture conditions—adsorbed to the apatite surfaces to a high degree. Consistent with previous results [103], BSA adsorption onto apatite surfaces followed a dose-dependent correlation, with increasing initial protein concentration leading to increased amounts of BSA adsorbed. It has been suggested that although the net charges of both the apatite and BSA are negative, their strong interaction is primarily due to attractive electrostatic forces between the negatively-charged carboxylic groups of the BSA molecule and the localized positive charge found at the C sites of the apatite surface [111]. Following a similar trend, apatite that was exposed to increasingly higher concentrations of STI solution adsorbed progressively more STI protein. Like BSA, STI has been shown to strongly interact with the apatite by virtue of its acidic side groups' affinity for the positively-charged C sites of apatite [104], [112].

Myoglobin, a small globular protein (MW = 17.8 kDa) found in cardiac and skeletal muscle, has an isoelectric point of 7.3 and is therefore close to neutrally-charged at physiological pH. In this study, myoglobin was third to BSA and STI in adsorption density when the adsorbate solution had a concentration between 0.001% and 0.1%. However, with exposure to 1% solutions, myoglobin overtook BSA, exhibiting a higher adsorption level on the apatite surface. Our results are in agreement with previous work that has demonstrated that at similar protein

concentrations, adsorption of myoglobin to apatite particles was significantly higher than that of BSA [111], [113]. Because of the neutral surface charge of the myoglobin molecules, it is unlikely that the high adsorption capacity was due to electrostatic attractive forces at the positively-charged C sites of the apatite, as was the case for BSA. Instead, the authors attributed the myoglobin-apatite association to conformational changes of the protein upon adsorption to the apatite surface, allowing for van der Waals attractive forces to predominate over the interaction at the exposed *ac* or *bc* crystal faces of the apatite [113]. Furthermore, it was concluded that the higher adsorption capacity for myoglobin was due to its lower molecular mass compared to BSA (faster diffusion rate).

For positively-charged proteins, adsorption onto the apatite surface varied depending on the type of protein studied. Histone protein (pI = 11.1) demonstrated a similar adsorption profile as that for myoglobin and BSA, though at a slightly lower magnitude. In contrast, lysozyme (pI = 11.3) failed to adsorb to the apatite to a significant extent. As was observed with the other protein types, increasing the concentration of the lysozyme solution did result in increasing amounts of protein adsorbed, but apatite exposed to the highest concentration (1% w/v lysozyme) failed to adsorb greater than 2 ug of protein per cm^2. Kandori et al. demonstrated similar results, showing that the saturated adsorption amount of lysozyme was less compared to BSA [114]. Although histone and lysozyme are both positively-charged proteins with similar isoelectric points, this disparity in the degree of adsorption suggests that the overall net charges of the adsorbate (i.e. protein) and adsorbant (i.e. apatite) cannot be the only determinants used to predict the association between the protein molecule and apatite. For the histone-apatite interaction, other factors are very likely to be present. For example, histones, which have a critical role in the packaging of DNA in the cell nucleus, are characterized by relatively high

levels of lysine and arginine residues that allow it to bind tightly to the negatively charged phosphate backbone of DNA [115]. Therefore it is reasonable to assume that in this study, adsorbed histone molecules have a high affinity for exposed phosphates on the apatite surface, in spite of electrostatic repulsive forces that may be present between the positively-charged basic groups of the protein and the C sites of the apatite. Indeed, studies investigating the adsorption and elution characteristics of proteins in hydroxyapatite chromatography columns concluded that the adsorbing sites for basic proteins likely contain phosphate groups, as the cations from a low concentration $CaCl_2$ buffer effectively outcompeted the basic protein side groups for the apatite phosphate sites during elution [106].

Apatite surface zeta potential measurements after treatment with protein or polyamino acid solutions confirmed that the surface charge could be altered upon adsorption. Predictably, adsorption of acidic biomolecules resulted in a more negatively charged surface, while treatment with basic biomolecules produced a less negative surface charge. The change in surface zeta potential, however, did not always correlate with the amount of biomolecule adsorption observed on the apatite. For example, among the 1% acidic protein solutions tested, STI molecules adsorbed to apatite surfaces greater than 2.5 times more than BSA, but it was BSA-treated apatite surfaces that displayed the greater change in surface zeta potential. Additionally, 1% STI adsorption led to a surface charge that was very similar to 1% myoglobin, despite a greater than 2-fold difference in adsorption onto apatite.

The surface charge of apatites treated with basic protein solutions also demonstrated differences upon adsorption. While the change in histone-treated apatite surface zeta potential was statistically different versus bare apatite, lysozyme-treated apatite surface zeta potential was

not, despite both basic proteins having very similar pI. The disparity in surface charge may be due to the different degree to which each protein adsorbed to the apatite surface. Immersion of apatite surfaces in 1% w/v solution of lysozyme resulted in an adsorption density of less than 2 ug of protein per cm^2, while that for 1% w/v histone resulted in a density of 34.4±2.0 ug per cm^2. Taken together, these results suggest that surface modification by protein adsorption can modulate the surface potential of apatite, but the magnitude of that change is difficult to predict based solely on the known charge of the free protein. The differences in degree of adsorption, as well as the changes in surface zeta potential upon adsorption to apatite, may both be a result of conformational changes or denaturation of the proteins as interact with the substrate surface [116], [117]. For example, different proteins that may have similar pI may differ in the arrangement of their charged groups in their native conformation. These differences may significantly influence the adsorption dynamics of that protein onto apatite substrates. Upon adsorption to a charged biomaterial surface, protein unfolding may occur, particularly for "soft" proteins like the BSA and myoglobin proteins used in this study [111], [113], [118], which can result in differences in the strength of the adherence to the surface [119]. In addition to the rate or strength of adsorption, the denaturation or unfolding of the protein may alter the apparent zeta potential of the protein as presented on the apatite surface [120], which may explain why certain proteins in this study adsorb to and modulate the apatite surface charge with varying degree. In general, our observations are in agreement with Reynolds et al. [89], who demonstrated that the overall modification in apatite surface zeta potential is reflected by the charge of the adsorbing molecule from the various treatment conditions.

Regardless of the treatment that is used to modulate the apatite surface zeta potential, our results show that producing a more negatively charged surface improves cell viability. Although

bare apatite surfaces natively have a net negative charge, it is possible that they still present pockets of local, high positive charge density that is toxic to cells, as is traditionally seen with polycationic materials[121]. In general, by masking these areas of high positive charge density with negatively-charged biomolecules, cell survival could be restored on the apatite substrates. In our investigation, protein-treated apatites required a surface zeta potential of approximately -30 mV in order to obtain close to a 50% cell survival rate. Apatite treatment with 0.01% BSA, 1% STI, or 1% myoglobin had zeta potential measurements of -28.0±0.85 mV, -29.6±3.6 mV, and -29.3±2.2 mV, respectively, resulting in cell viability between 42-48% for all three surfaces.

It should be noted, however, that despite making the apatite surface less negative upon adsorption, histone treatment from 1% solutions resulted in a moderate improvement in cell viability compared to apatite samples with a similar surface potential (i.e. bare apatite, lysozyme-treated apatite, PLL-treated apatite). Although the DNA-binding and packaging properties of histones are well known, the function of extracellular histones is poorly understood. A limited number of studies, however, have demonstrated that extracellular histones may have beneficial antimicrobial activity and function as immune cell effectors [122]. Yet surprisingly, treatment of human keratinocytes with histone H1 above a certain concentration proved to be cytotoxic [123]. In the present study, however, histone proteins adsorbed onto apatite were found to reduce the toxicity of the apatite surface in serum-free media. Although the effect of free extracellular histone on MC3T3-E1 viability was not assessed here, it is possible that the cytotoxic properties observed by other researchers may be negated due to denaturation or protein unfolding upon adsorption to the apatite substrate. When unfolded on the surface, internal hydrophobic regions of the protein may be exposed and presented to the cultured cells. These exposed regions could potentially interact with cell membrane receptors that trigger pro-survival signaling despite

having a surface charge found to be associated with low cell viability. It is well known that activation of integrin receptors at the cell surface by certain extracellular protein sequences can directly initiate survival signaling through FAK, PI3K, and Akt pathways [124]. Elucidation of the sequences displayed by proteins when adsorbed to apatite is beyond the scope of this study, but certainly warrants future investigation.

As adsorbates that are less likely to elicit integrin-dependent FAK/Akt pathways, non-protein biomolecules were also found to modify the apatite surface zeta potential. As we observed for the protein experiments, adsorption of polyamino acids that resulted in a more negatively charged surface led to improved cell viability. The homo-polyamino acids poly-L-lysine, poly-L-glutamate, and poly-L-aspartic acid were each used in this study to either reduce or augment the negative zeta potential of apatite, without the potential confounding biological effects that may be associated with full-size proteins. Poly-L-lysine is an adhesive polyamino acid that is often used to enhance nonspecific cell adhesion to substrates, but is not known to interact with cell surface receptors that activate pro-survival signals in cytotoxic environments [125], [126]. Likewise, PLG- and PLA-coated substrates have been found to enhance cell adhesion [127], [128], but are not known to form focal adhesion contacts. As such, only electrostatic charge properties of the polyamino acids are expected to influence changes in cell function upon culturing onto the polyamino acid-treated apatite.

Polyamino acid treatments that resulted in an apatite zeta potential of approximately -30 mV again were shown to improve MC3T3-E1 viability, as was observed for the majority of the protein-treated apatite surfaces. At the maximum 1% concentration tested, both negatively-charged polyamino acids (PLG and PLA) reduced the apatite surface potential to -31.1±2.5 mV

and -28.5±2.4 mV, respectively. In contrast, positively-charged PLL did not significantly alter the apatite charge compared to bare apatite. This threshold zeta potential value resulting from the 1% PLG and PLA treatments coincides with that from the 0.01% BSA treatment, which was the minimum concentration of BSA needed to see any improvement in cell viability. For PLG and PLA-treated apatite, initial improvement in cell viability occurred at 0.01% concentration similar to BSA, although at significantly lower viability rate. Unlike BSA, however, increasing the polyamino acid concentration did not result in further improvement, reaching a plateau of 30.2±1.9% and 27.5±2.4% survival for PLG and PLA, respectively. In contrast, as little as 0.01% BSA treatment could produce a cell survival rate of 48.2±0.2%, suggesting that full-size proteins may offer additional beneficial effects for rescuing cell viability.

Previous studies have shown that carbon or gold coating onto biomaterial substrates results in a more negatively-charged surface zeta potential [129], [130]. In agreement with those studies, deposition of carbon or gold layers onto apatite surface showed that the change in surface charge was dependent on deposition thickness, and in both cases, the thicker the coating, the more negative the zeta potential. This change towards a more negatively-charged surface is due to the accumulation of electrons at the surface when the carbon or gold coatings come into contact with an electrolyte solution. Similar to the protein and polyamino acid-treated apatites, the decrease in surface zeta potential following carbon or gold deposition appeared to correlate with an improvement in the viability of cells cultured on the apatite substrates. Interestingly for both types of coatings, a "threshold" surface charge seemed to present—close to -30 mV—leading to an improved cell survival rate of approximately 35%. Doubling the coating thickness decreased the surface charge to ~ -36 to -38 mV and resulted in a 50% cell survival rate. As biologically inert, non-biomolecule coatings, carbon and gold deposition onto apatite seems to

confirm our hypothesis that the substrate surface charge plays a significant role in modulating cell function in the apatite microenvironment.

When taken together, our results from protein, polyamino acid, and carbon/gold treated surfaces suggest that there is certain surface zeta potential value—approximately -30 mV—that is required to achieve a marked improvement in cell viability. However, the percentage of viable cells at that -30 mV threshold varied depending on the type of surface treatment, suggesting that the interaction at the cell-apatite interface is multifaceted, particularly for complex biomolecule mediators such as proteins. Nevertheless, biomaterial surface charge would seem to be a key player in the overall biological performance of an implant.

Electrically stimulated bone growth is an area of biomedical research with a long history dating back to the 1960s [131], [132]. Fukuda et al, reported the piezoelectric properties of bone, revealing that mechanical loading led to the development of electric potentials in the bone tissue [133]. Since then, many studies have investigated the effect of applying electric fields to cultured cells *in vitro* and bone tissues *in vivo* [134]. More recently, the implants or substrates onto which cells are cultured have been manipulated themselves in order to alter their apparent surface charge as a means of improving their osteogenic potential. As insulators, ceramic biomaterials, as in hydroxyapatite, have been electrically modified by various electrical polarization methods such as thermoelectrical, electron beam, and electromagnetic radiation poling [135]–[138]. These earlier studies demonstrated that apatite materials can store an applied charge and act as an "electret"—material that has a "permanent" macroscopic electric field at its surface [108]—and investigated how polarization influences the physical properties of the apatite. Several studies suggest that negatively charged surfaces may be beneficial for

osteogenesis. For example, Yamashita *et al.* demonstrated that mineralization and crystal growth was accelerated on negative surfaces but not on positive surfaces of polarized hydroxyapatite [135]. Also, negatively polarized tantalum oxide implants were shown to have increased cartilage mineralization *in vivo* compared to positively charged implants [139]. The exact mechanisms, as to how these electrical modifications to apatite surfaces influence biological interactions remain unknown. However, it has been proposed that in addition to changes in electrostatic properties, polarization may also modulate hydrophobicity/hydrophilicity of the material [140]–[142]. Both the wettability and surface potential properties may in turn affect protein adsorption and subsequently cell attachment, morphology, migration and proliferation. Investigations of the *in vitro* cellular response to poled apatite substrates have shown that negatively polarized surfaces were better able to support osteoblast adhesion, proliferation and ECM production [88], [109], [143]. The results from the current investigation are generally in agreement with these earlier studies, demonstrating a more favorable cellular response on more negatively charged apatite surfaces.

3.5 Conclusion

Immediately upon implantation in the body, modifications occur at the substrate surface due to contact with the surrounding body fluid. The nature of these changes at the implant surface can greatly affect the cellular response and ultimately the biological performance of the implant. The purpose of the present study was to determine the contribution of the surface charge on cellular activity, specifically viability, upon adherence to accelerated apatite substrates. Several studies have investigated the polarizability of apatite biomaterials and the subsequent biological response to that induced surface charge. In contrast, this study focused on

the effect of the *native* surface potential presented by accelerated apatite coatings. It was found that various proteins and polyamino acids possessing different charge at physiological pH were able to modulate the surface zeta potential of apatite substrates upon adsorption. The change in apatite surface zeta potential was largely determined by the degree of adsorption as well as the inherent charge of the biomolecule. Non-biomolecule coatings of carbon or gold were also able to alter the apatite surface charge. In general, apatite surface treatments that resulted in a more negatively charged zeta potential, compared to un-treated controls, improved the viability of cells in a serum-free environment, suggesting that the electrical properties of apatite-based biomaterials are key contributors to the overall cellular response in the apatite microenvironment.

3.6 Figures and tables

Table 1. Molecular weights and isoelectric points of various proteins and polyamino acids

Compound	Type (charge at pH 7)	Molecular wt (kDa)	Isoelectric point (pI)
Poly-L-glutamic acid	Acidic polypeptide (-)	50 - 100	3
Poly-L-aspartatic acid	Acidic polypeptide (-)	5 -15	2.9
Bovine serum albumin	Acidic protein (-)	66.4	4.7
Soybean trypsin inhib	Acidic protein (-)	21	4.5
Myoglobin	Neutral protein	17.6	7.3
Histone H1 (lysine-rich)	Basic protein (+)	21.5	11.01
Lysozyme	Basic protein (+)	14.3	11.35
Poly-L-lysine	Basic polypeptide (+)	30-70	11.4

Figure 9

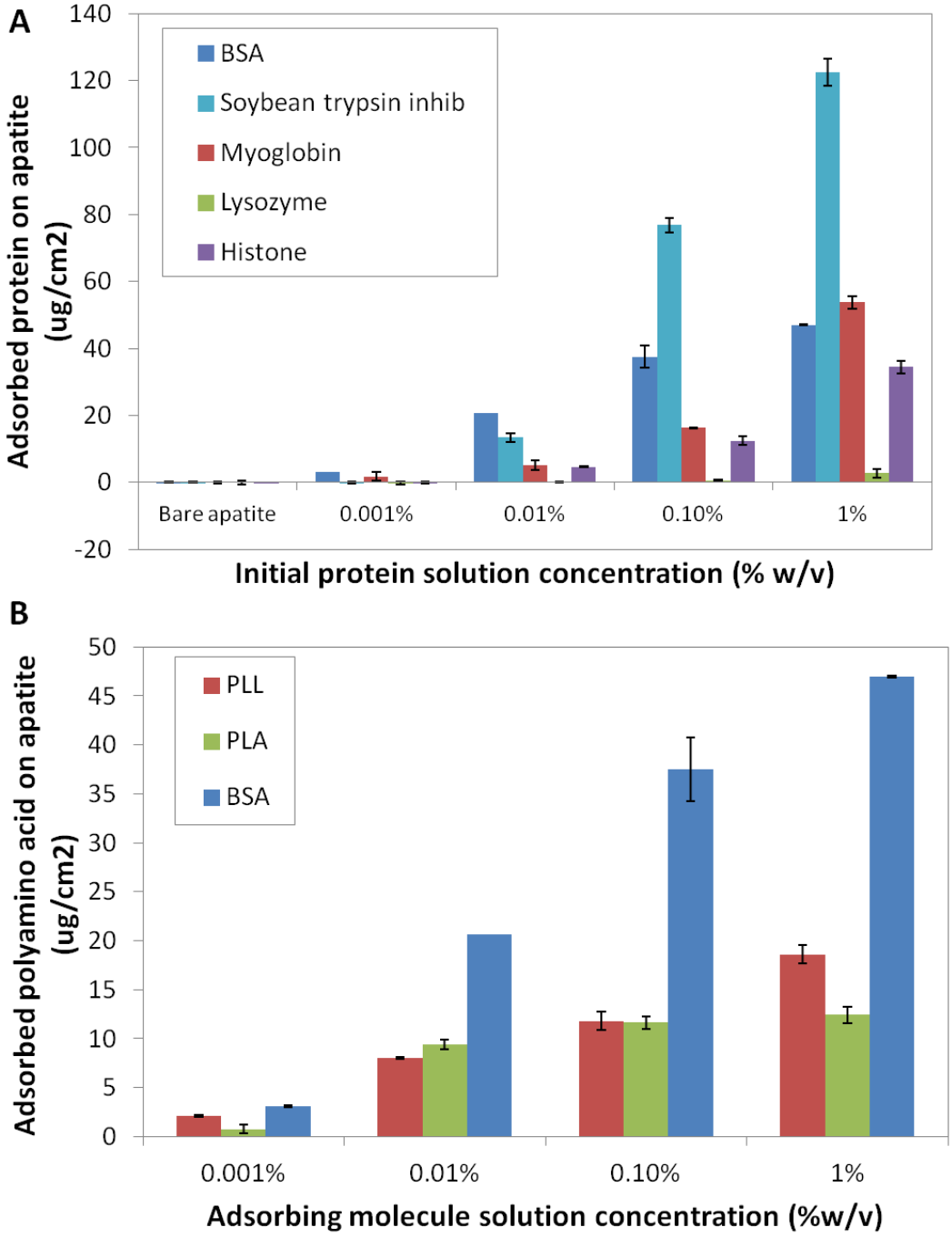
A
Adsorbed protein on apatite (ug/cm2)
140
120
100
80
60
40
20
0
-20
BSA
Soybean trypsin inhib
Myoglobin
Lysozyme
Histone
Bare apatite
0.001%
0.01%
0.10%
1%
Initial protein solution concentration (% w/v)
B
Adsorbed polyamino acid on apatite (ug/cm2)
50
45
40
35
30
25
20
15
10
5
0
PLL
PLA
BSA
0.001%
0.01%
0.10%
1%
Adsorbing molecule solution concentration (%w/v)

Figure 9: Quantification of protein and polyamino acid adsorption onto accelerated apatite surfaces. (a) Apatite surfaces were treated with various protein solutions at 0.001% to 1% concentration for 12h at 37C. After rinsing residual non-adsorbed protein from the apatite, the amount of protein adsorbed was quantified by BCA assay (n = 9). At the maximum concentration of 1% protein, negatively-charged proteins (BSA, STI) and neutrally-charged proteins (myoglobin) adsorbed to apatite to the greatest degree, while positively-charged proteins (lysozyme, histone) varied in adsorption depending on protein type.

(b) Apatite surfaces were treated with various polyamino acid solutions at 0.001% to 1% concentration for 12h at 37C. After rinsing residual non-adsorbed polyamino acid from the apatite, the amount adsorbed was quantified by Ninhydrin assay (PLL) or UV absorption (PLA). For comparison, negatively-charged BSA protein was also adsorbed to apatite and quantified by BSA assay. The amount of polyamino acid or protein was measured against a standard curve with known concentration of adsorbing molecule as determined by their respective quantification assays. The oppositely-charged PLL and PLA molecules adsorbed to apatite to a similar extent at concentrations between 0.001% and 0.1%. When the adsorbate solution concentration was 1%, more PLL adsorbed to apatite than PLA ($p < 0.01$).

Figure 10

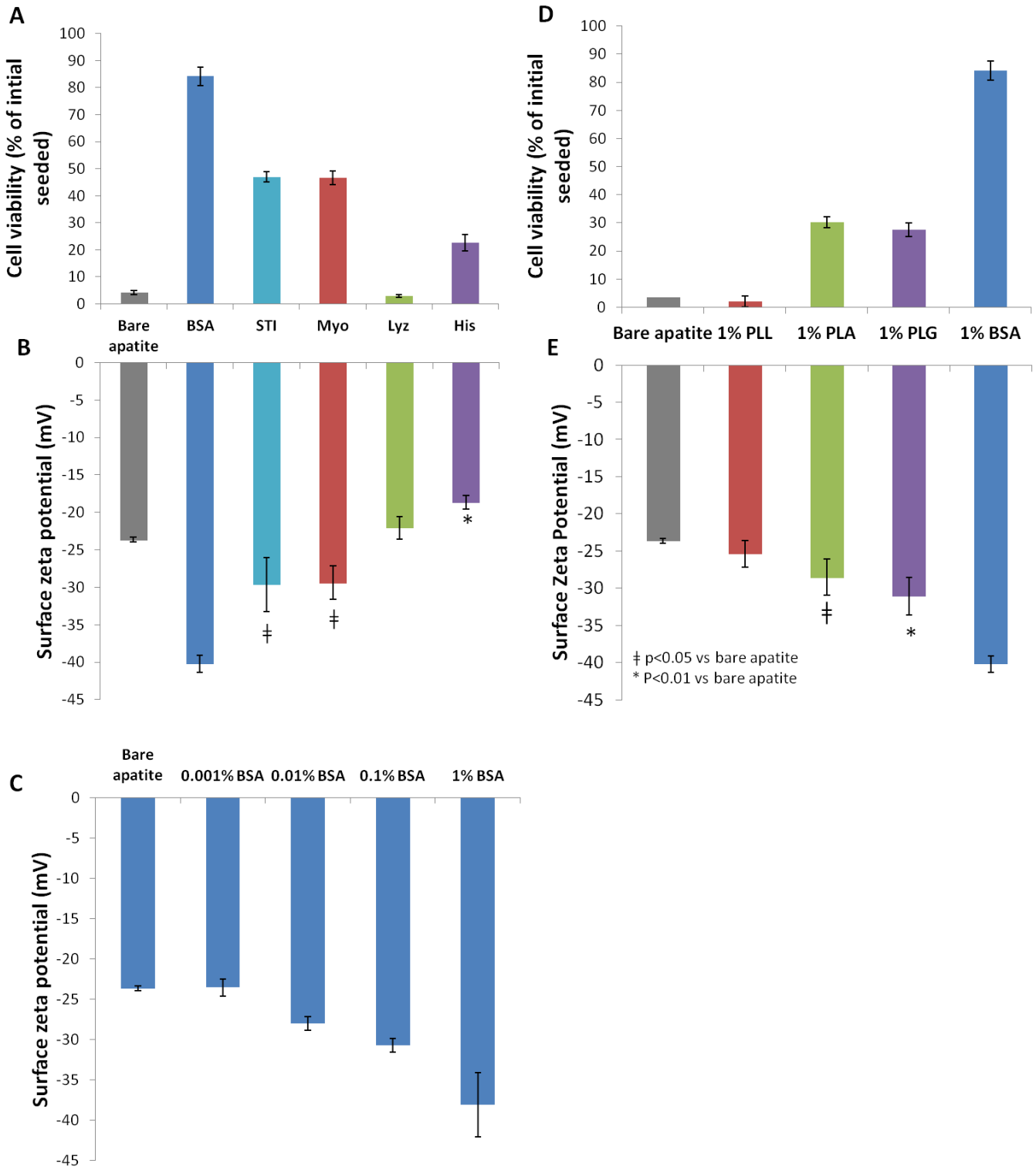
A
Cell viability (% of intial seeded)
Bare apatite
BSA
STI
Myo
Lyz
His
B
Surface zeta potential (mV)
‡
*
C
Bare apatite
0.001% BSA
0.01% BSA
0.1% BSA
1% BSA
Surface zeta potential (mV)
D
Cell viability (% of initial seeded)
Bare apatite
1% PLL
1% PLA
1% PLG
1% BSA
E
Surface Zeta Potential (mV)
‡ p<0.05 vs bare apatite
* P<0.01 vs bare apatite

Figure 10: Adsorbed proteins and polyamino acids with different isoelectric points modulate the apparent surface zeta potential of apatite and influence cell viability. (a) MC3T3-E1 cells were cultured on untreated apatite surfaces (bare apatite), or apatite treated with BSA, STI, myoglobin, lysozyme, and histone solutions ranging from 0.001% to 1% concentration. After 24 hours, cell viability was assessed by Alamar Blue assay. Apatites treated with acidic proteins (BSA, STI) displayed increasing cell viability as a function of protein concentration. Improvement in cell viability on myoglobin and histone-treated apatite was not observed until the adsorbing solution was 1% concentration. Cell viability on lysozyme treated apatite could not be rescued at any concentration tested.

(b) Apatite surfaces were treated with various protein solutions at 1% w/v concentration for 12h at 37C. After rinsing residual non-adsorbed protein from the apatite, the surface zeta potential of the protein-treated apatite surfaces was measured using a Zetasizer Nano ZS (Malvern, Worcestershire, UK). Apatite exposed to acidic proteins increased the negative surface charge of the apatite when compared to other apatite surfaces. Treatment with basic proteins either did not significantly change (lysozyme) or slightly reduced (histone) the negative charge of the apatite compared to untreated apatite controls.

(c) Apatite surfaces were treated with BSA solutions ranging from 0.001% to 1% concentration for 12h at 37C. After rinsing residual non-adsorbed BSA from the apatite, the surface zeta potential of the protein-treated apatite surfaces was measured using a Zetasizer Nano ZS (Malvern, Worcestershire, UK). Increasing the BSA concentration exposed to apatite resulted in accompanying decrease in the apatite surface zeta potential towards more negative values.

(d) MC3T3-E1 cells were cultured on untreated apatite surfaces (bare apatite), or apatite treated with PLL, PLG, or PLA solutions ranging from 0.001% to 1% concentration. After 24 hours, cell viability was assessed by Alamar Blue assay. Apatites treated with acidic polyamino acids (PLG, PLA) improved cell viability at concentrations greater than 0.01%. Cell viability on PLL-treated apatite could not be rescued at any concentration tested. Cell viability on BSA-treated apatite was included for reference.

(e) Apatite surfaces were treated with various polyamino acid solutions at 1% w/v concentration for 12h at 37C. After rinsing residual non-adsorbed polyamino acid molecules from the apatite, the surface zeta potential was measured using a Zetasizer Nano ZS (Malvern, Worcestershire, UK). Similarly to protein treatment, exposure to negatively-charged, but not positively-charged polyamino acids significantly made the surface ZP more negative compared to untreated controls.

Figure 11

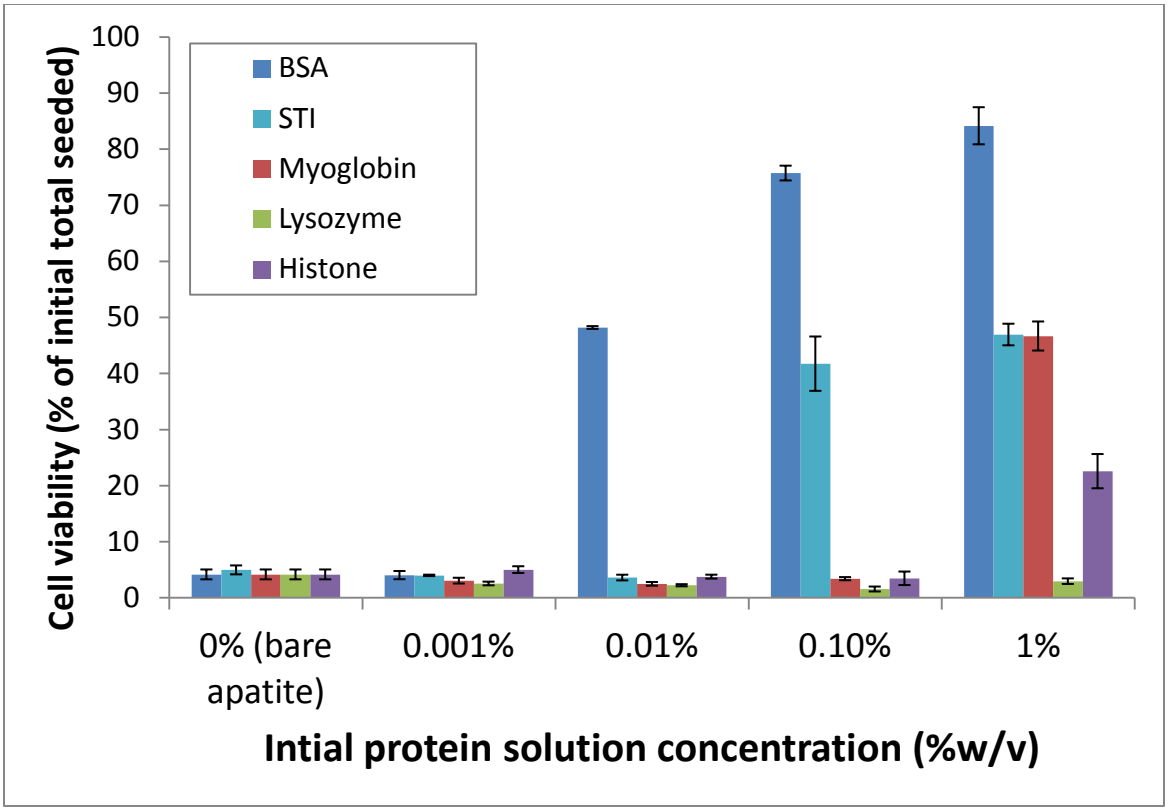

Figure 11: Negatively-charged proteins are most effective in rescuing MC3T3-E1 cell viability on apatite surfaces. MC3T3-E1 cells were cultured on untreated apatite surfaces (bare apatite), or apatite treated with BSA, STI, myoglobin, lysozyme, and histone solutions ranging from 0.001% to 1% concentration. After 24 hours, cell viability was assessed by Alamar Blue assay. Apatites treated with acidic proteins (BSA, STI) displayed increasing cell viability as a function of protein concentration. Improvement in cell viability on myoglobin and histone-treated apatite was not observed until the adsorbing solution was 1% concentration. Cell viability on lysozyme treated apatite could not be rescued at any concentration tested.

Figure 12

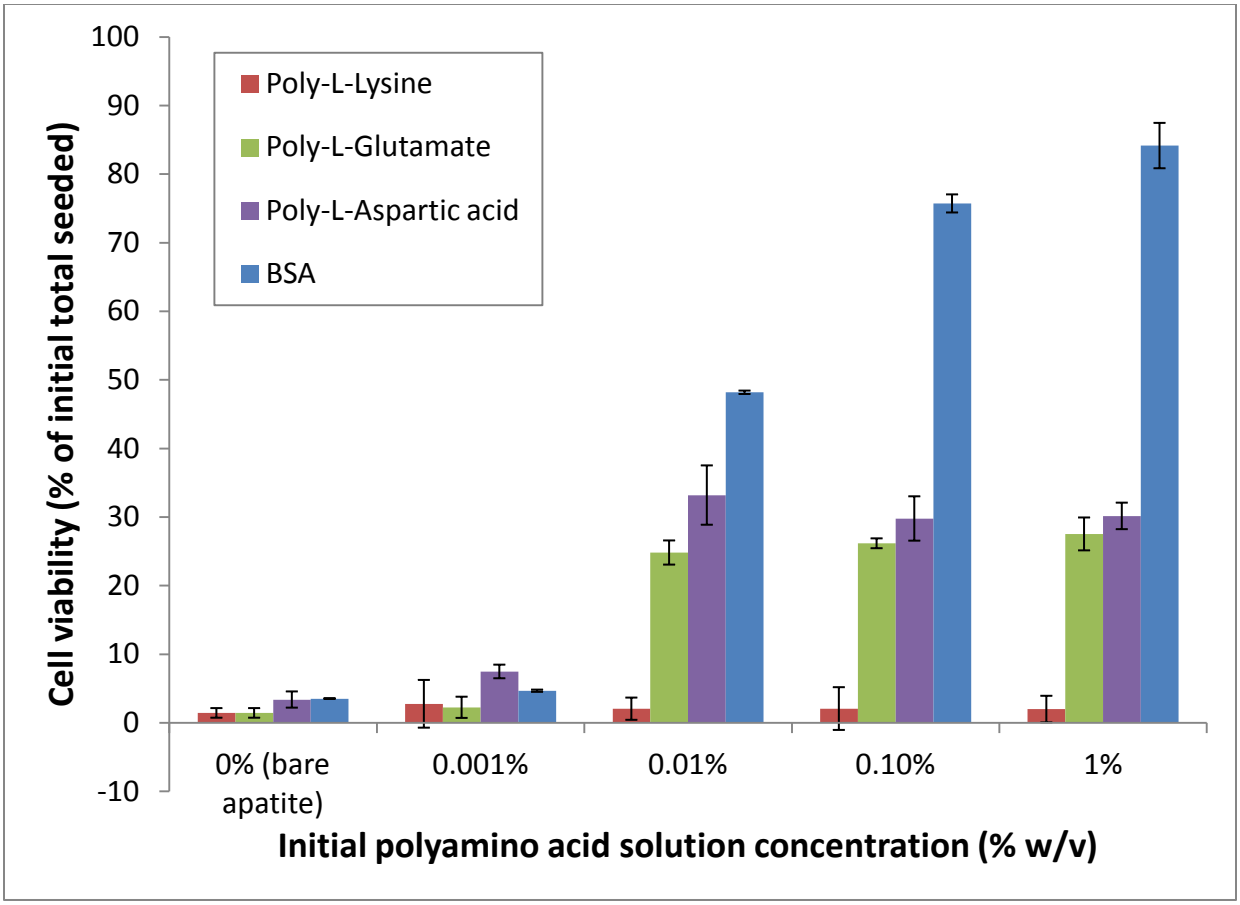

Figure 12: Adsorption of acidic polyamino acids, but not basic polyamino acids can rescue 3T3-E1 cell viability on apatite. MC3T3-E1 cells were cultured on untreated apatite surfaces (bare apatite), or apatite treated with PLL, PLG, or PLA solutions ranging from 0.001% to 1% concentration. After 24 hours, cell viability was assessed by Alamar Blue assay. Apatites treated with acidic polyamino acids (PLG, PLA) improved cell viability at concentrations greater than 0.01%. Cell viability on PLL-treated apatite could not be rescued at any concentration tested. Cell viability on BSA-treated apatite was included for reference.

Figure 13

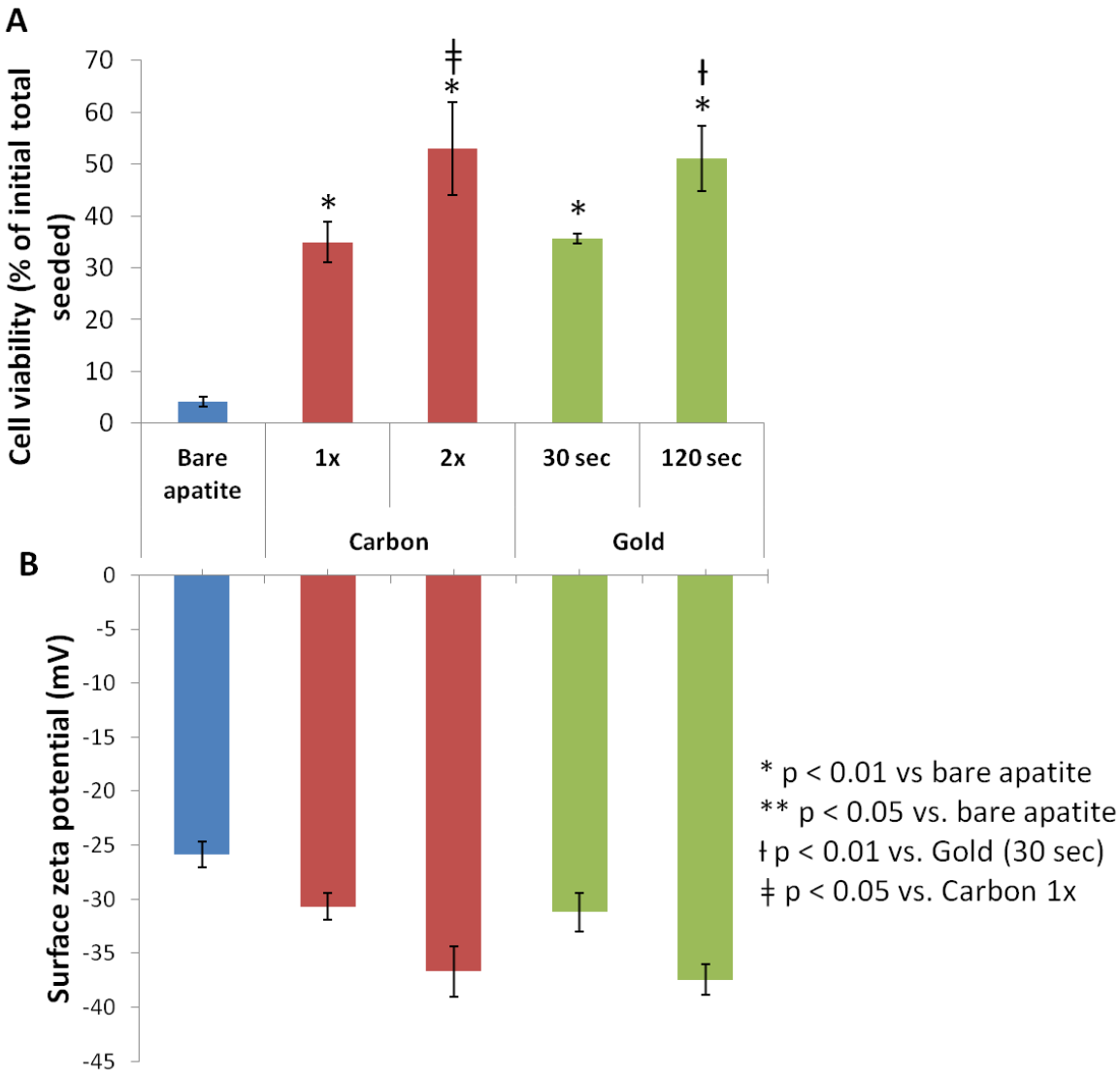

Figure 13: Carbon and gold deposition on apatite results in a more negatively-charged surface ZP, improving cell viability on apatite surfaces. (a) MC3T3-E1 cells were cultured in serum-free media on untreated apatite surfaces (bare apatite), apatite coated with one or two carbon layers (Carbon-1x, Carbon-2x), or apatite coated with gold (Gold-30 sec, Gold-120 sec). After 24 hours, the cell viability in response to the coated apatite surfaces was assessed by Alamar Blue assay. For both types of deposition treatments, cell viability improved significantly compared to bare apatite ($p<0.01$), and this improvement increased as a function of the coating thickness**.** (b) Carbon or gold coatings with varying thickness were deposited onto apatite surfaces. For carbon coating, one or two layers (Carbon-1x and Carbon-2x, respectively) were deposited via evaporation, while for gold coating, plasma sputtering was performed for 30 or 120 seconds (Gold-30 sec and Gold 120 sec, respectively). Zeta potential was measured using a

Zetasizer Nano ZS (Malvern, Worcestershire, UK). Both carbon and gold deposition decreased the apatite surface zeta potential towards more negative levels.

CHAPTER 4

MONOCYTE INTERACTIONS WITHIN ACCELERATED APATITE MICROENVIRONMENTS AND ITS INFLUENCE ON OSTEOBLASTIC DIFFERENTIATION

4.1 Introduction

The host inflammatory response against apatite materials is often considered the primary factor in the context of the material's biocompatibility, and therefore may significantly influence the implant's long-term clinical success or failure. Previous studies have demonstrated that *in vivo* implantation of apatite materials does not elicit significant long-term inflammatory response, leading to successful integration with host bone tissue [144]. Consequently, calcium phosphate-based materials are considered highly biocompatible and capable of facilitating bone formation *in vivo*. However, at initial implantation, an acute inflammatory reaction may occur in response to the surgical procedure itself and/or to the presence of the foreign implant material, which is marked by an infiltration of monocytes, neutrophils, and other polymorphonuclear leukocytes at the implantation site around the biomaterial-tissue interface [145]. As a result, the initial short-term reaction should be considered when investigating mechanisms related to the performance of apatite-based implant materials.

The hypothesis of this study is that upon implantation, accelerated apatite coatings may activate or be exposed to a mild or short-term inflammatory reaction that plays a role in the pro-osteogenic performance of these materials *in vivo*. To explore this hypothesis *in vitro*, the interaction between monocytes and accelerated apatite coatings was investigated. Monocytes, which play a central role in host defense and immune regulation, are one of the first

inflammatory cell types recruited to the site of implantation. When inactivated, circulating monocytes are non-adherent until presented with appropriate stimuli, resulting in adhesion at the implant site, differentiation into macrophages, and release of chemoattractant signals [146]. Furthermore, current research has shown that monocytes/macrophages have a central role in the regulation of bone development and healing. Chang *et al.* demonstrated that the presence of resident bone tissue macrophages—OsteoMacs, which are typically co-isolated with calvarial osteoblast cultures—is required for significant osteoblast mineralization and osteocalcin gene expression [147]. Although it was demonstrated that OsteoMacs are an integral component of bone tissue, the exact mechanism that allows them to regulate osteoblast function was not fully elucidated. The ability of macrophages to secrete osteoinductive factors such as TGF-β [148], osteopontin [149], 1,25-dihydroxyvitamin D_3 [150], and BMP2 [151], has been suggested as potential means for their capacity to regulate bone formation. As such, the purpose of this preliminary study is to determine what influence accelerated apatites may have on U937 human monocyte cell line or primary human monocyte isolates, and whether this interaction may mediate a pro-osteogenic response *in vitro*.

Assessment of monocyte response to both 2D and 3D apatite microenvironments was performed by evaluating production of various soluble mediators (cytokines) that may influence surrounding cells. The monocyte/macrophage system has been shown to release inflammatory factors that play a role in natural bone fracture healing [152]. For example, when activated these cells may secrete several types of mediators such as pro-inflammatory (TNF-α, IL-1β), multifunctional (IL-6), or anti-inflammatory IIL-10) cytokines. Additionally, activated monocytes/macrophages have been shown to produce growth factors that can influence the proliferation/differentiation of other cells through paracrine signaling, such as those from the

TGF superfamily and PDGF [153]–[155]. Therefore it merits exploring the potential factors that activated monocytes may produce in the presence of accelerated apatite, and whether these factors influence osteoblast differentiation *in vitro*. The results of this study may challenge the paradigm that a lack of inflammatory response is paramount to the success of biomaterial implants. On the contrary, it may be proven that a minimal or short-term inflammatory response to apatite materials may be desired, and that this reaction is critical for successful bone healing and tissue formation.

4.2 Materials and methods

4.2.1 Preparation of apatite coatings by biomimetic process

Apatite-coated substrates were prepared by a wet precipitation method through immersion in 5x concentrated SBF solutions as previously published [1], [103]. Briefly, substrates were initially incubated in a 5xSBF1, consisting of $CaCl_2$, $MgCl_2 \cdot 6H_2O$, $NaHCO_3$, $K_2HPO_4 \cdot 3H_2O$, Na_2SO4, KCl and NaCl in distilled deionized water for 24 hours at 37C. The substrates were then transferred to a 5xSBF2 solution that is similar to 5xSBF1, but devoid of the crystal growth inhibitors Mg^{2+} and HCO^{3-}. Incubation in 5xSBF2 was performed at 37C for 48 hours. Apatite-coated substrates were then rinsed gently 3 times with distilled deionized water and air-dried before further experimentation.

4.2.2 PLGA scaffold fabrication

PLGA scaffolds were prepared by a solvent casting/porogen leaching method using 85:15 D,L-poly(lactic-co-glycolic acid) (inherent viscosity = 0.61 dL/g, LACTEL Absorbable Polymers, Birmingham, AL). Briefly, 1.0 g of a 17.5% PLGA in chloroform solution was mixed

with 1.5 g of 200-300 um diameter sucrose particles, and pressed between Teflon molds to create 0.5 mm thick polymer sheets. The sheets were then frozen over night and lyophilized for ~ 8 hours in a lyophilizer to remove solvent from the scaffolds. After lyophilization, the scaffolds were immersed in three changes of ddH_2O for 1 hour each in order to leach the sucrose particles. After air-drying, a biopsy punch was used to obtain 6 mm diameter circular scaffolds. Non-apatite coated scaffolds were prepared for cell culture with plasma etching using argon glow discharge to improve wetting, followed by sterilization in 70% ethanol for 30 minutes. Residual ethanol was rinsed from the scaffolds using three changes of sterile ddH_2O. At this point, a subset of the sterile PLGA scaffolds was prepared for apatite-coating. For this, scaffolds were immersed in SBF1 solution for 24 hours, followed by SBF2 for 48 hours. At the end of the apatite coating process, the scaffolds were rinsed three times with sterile ddH_2O and allowed to air dry in a laminar flow hood over night.

4.2.3 Cell culture and monocyte viability on accelerated apatite

U937 monocytes were expanded under standard cell culture conditions in U937 expansion medium containing RPMI 1640, 10% FBS and 1% penicillin/streptomycin. Prior to cell culture experiments, monocytes were primed with 100 ng/ml interferon-γ (IFN-γ) for 16-24 hours, followed by activation with 1 ug/ml lipopolysaccharide (LPS) for 24 hours [156]. Primary human osteoblast cells were expanded in cell culture growth medium containing DMEM (4.5 mg/L glucose, pyruvate, L-glutamine), 20 mM HEPES, 10% FBS, 1% penicillin/streptomycin, and 100 ug/ml L-ascorbic acid. Osteogenic differentiation media consists of normal growth medium supplemented with 10 mM betaglycerophosphate (BGP).

For monocyte/osteoblast co-culture experiments, human osteoblasts were first harvested using 0.25% trypsin/2.21 mM EDTA and resuspended at a cell density of $5x10^6$ cells/mL. A total of 10 uL of cell suspension was seeded onto each apatite-coated scaffold. Immediately following seeding of osteoblast cells, U937 human monocytes were resuspended at a cell density of $5x10^5$ cells/mL and 10 uL of the cell suspension was gently pipetted onto the apatite-coated scaffolds already seeded with osteoblasts. A 1:10 monocyte:osteoblast seeding ratio was obtained under this process. Cells were allowed to adhere to the scaffolds for 1 hour in a water-jacketed, 5% CO_2 incubator, at which point additional cell growth media was added to the wells to completely immerse the scaffolds.

To assess the effect of the apatite presence on monocyte viability, U937 cells were seeded onto 2D apatite-coated TPCS at 10,000 cells/cm^2, and viability and adhesion was determined at select time points up to 24 hours using either a Live/Dead cell viability staining kit (Invitrogen, Carlsbad, CA) or an Alamar Blue assay (Invitrogen). For Live/Dead staining, cells were incubated at the desired time points with a solution of Calcein AM and Ethidium homodimer-1 (EthD-1) as outlined by the manufacturer to determine living (green) and dead (red) cells as observed under fluorescence microscopy. For quantification of viability, Alamar Blue reagent, which is metabolically processed by living cells, was added directly to the U937 culture medium at the selected time points and incubated with the cells for 1 hour at 37C. The culture medium containing the metabolized Alamar Blue was then removed and measured at 535/590 nm (ex/em).

4.2.4 Assessment of osteoblast mineralization in response to monocyte conditioned media

Monocyte conditioned media was prepared from either primary human monocytes (generously donated from Dr. Anahid Jewett) or activated U937 human monocyte cells that were cultured on 2D apatite coatings or TCPS for 24 hours. After 24 hours, the media from these cultures were centrifuged and the supernatant was collected and stored as aliquots at -80C. Osteoblast cultures were prepared by seeding primary human osteoblasts in normal osteoblast growth medium at a cell density of 10,000 cells/cm^2 on TCPS. After reaching confluency, the cell culture medium was replaced with medium containing a 3:2 ratio of normal osteoblast growth medium:monocyte conditioned medium. Control wells were treated with media containing a 3:2 ratio of normal osteoblast growth medium:normal monocyte growth medium. The control and conditioned medium-treated wells were changed with fresh medium every three days.

Mineralization in the osteoblast cultures was assessed after 14, 21, and 28 days with Von Kossa staining. For this, wells were gently rinsed with PBS after removal of cell culture medium and then fixed with 4% paraformaldehyde. After washing away residual paraformaldehyde with ddH_2O, wells were incubated in a 5% silver nitrate solution and exposed to UV light for 20-30 minutes when dark brown mineral staining was observed. The silver nitrate stain was rinsed with ddH_2O and imaging was performed using brightfield microscopy.

4.2.5 Osteocalcin gene expression via quantitative real-time PCR

Osteocalcin (OCN) gene expression was assessed from co-cultures of primary human osteoblast cells and U937 monocytes or human osteoblast cells alone on 3D apatite-coated PLGA scaffolds according to the protocol described above. At 14, 21, and 28 days, cells on the scaffolds were lysed with RLT buffer containing 1% β-mercaptoethanol and total RNA was

homogenized and isolated using a QiaShredder Kit and RNeasy Mini Kit, respectively (Qiagen, Valencia, CA). Total RNA concentration and purity was determined spectrophotometrically at 260 and 280 nm. Purified RNA was converted to cDNA using a first-strand cDNA synthesis kit (Promega, WI, USA) according to the manufacturer's protocol. cDNA concentration was quantified spectrophotometrically at 260 nm. A QuantiTect PCR Probe Kit (Qiagen) was used to prepare cDNA samples (n =2, duplicate for each reaction) for quantitative real-time RT-PCR in order to assess gene expression of osteocalcin (Hs00609452_g1, Applied Biosystems, Carlsbad, CA) and GAPDH (Hs99999905_m1, Applied Biosystems) as a housekeeping gene. Relative gene expression was determined using the comparative C_T ($\Delta\Delta C_T$) method. The osteocalcin gene expression from osteoblast-monocyte co-culture scaffolds was expressed as a fold-difference ± SD versus the osteocalcin gene expression from osteoblast cells on scaffolds.

4.2.6 Cytokine detection by antibody array

Cytokine release in response to 2D apatite coatings from U937 monocytes were detected using a Human Cytokine Array 3.0 (Affymetrix, Santa Clara, CA), which can detect 36 different human inflammatory cytokines simultaneously. Following activation as described above, U937 monocytes were seeded onto 2D apatite coatings or TCPS at a cell density of 10,000 cells/cm^2. After 24 hours of culture, the cell culture medium from each sample was centrifuged to pellet the cells and the supernatant collected for the cytokine antibody array, which was performed according to the manufacturer's instructions. Quantification of the expression of detected cytokines was performed using ImageJ image processing and analysis software. Cytokine expression from monocytes cultured on apatite was expressed as a fold difference ± SD versus cytokine expression from monocytes cultured on TCPS controls (n = 4).

Detection of cytokine release was also performed on 3D apatite-coated PLGA scaffolds containing a co-culture of U937 monocytes and human osteoblast cells. Briefly, three sets of culture conditions were examined: 3D apatite-coated PLGA scaffolds were seeded, as described above, with either (1) both human osteoblasts and U937 monocytes, (2) human osteoblasts alone or (3) U937 monocytes alone. After 24 hours of co-culture on the scaffolds, cell culture medium from the samples were collected for cytokine detection using the Human Cytokine Array 3.0 kit and quantified with ImageJ. Cytokine expression from the co-culture condition was expressed as a fold-difference ± SD versus expression of either mono-culture (osteoblasts alone or monocytes alone).

4.3 Results

4.3.1 Protein adsorption on apatite surfaces is required for U937 monocyte cell viability

Previous results investigating the cell-apatite interaction have demonstrated that the adsorption of proteins onto the apatite surface is critical for cell survival of adherent cell types [103]. Consistent with this data, bare apatite surfaces induced cell death of the normally non-adherent U937 human monocyte cells. Live/dead fluorescent staining demonstrated that 24 hours of culture on bare apatite resulted in the death of nearly all cells (Figure 14). However, when the apatite surfaces were incubated with increasing concentrations of FBS as a source of protein prior to cell seeding, significant increases in cell viability was observed. The increase in viability demonstrated a dose-dependent correlation with the concentration of protein pre-incubated on the apatite. Pre-incubation with at least a 1% FBS concentration was required to qualitatively observe viability in at least half of the total cell population. Further increases in

adsorbed protein on the apatite improved the quantity of viable cells (green staining), and reduced the number of non-viable cells (red staining).

4.3.2 Conditioned media from primary human monocytes or U937 monocytes cultured on accelerated apatite surfaces promote biomineralization of primary human osteoblasts in 2D culture

Inflammation is marked by an influx of circulating monocytes that will release specific factors and/or differentiate in response to the presence of a foreign body [146]. To assess the ability of monocytes to produce osteogenic factors in response to the presence of accelerated apatite, primary human monocytes and a human monocyte cell line (U937) were cultured on apatite coatings or TCPS for 24 hours. Following removal of the monocyte cells, the conditioned medium was given to human osteoblast cells cultured on TCPS and their mineralization was assessed via Von Kossa staining after 28 days (Figure 15). Osteoblasts cultured in the presence of monocyte conditioned medium demonstrated significantly more areas of dark brown/black staining, indicating an increase in mineral formation. The increase in positive Von Kossa staining was apparent in osteoblast cultures treated with conditioned media from both monocyte cell types, regardless if the monocytes were exposed to TCPS or apatite coatings. In contrast osteoblasts that were treated with control medium consisting of a 3:2 ratio of osteoblast growth medium:monocyte growth medium did not display any positive mineralization staining.

Despite producing similar increases in osteoblast mineralization, U937 monocytes cultured on different substrates (apatite coatings vs. TCPS) had different cytokine expression profiles. Using a human cytokine antibody array, secretion of 36 commonly known

inflammatory cytokines by U937 monocytes was determined after 24-hour culture on either apatite coatings or TCPS. The cytokines expressed by the U937 monocytes in response to the two different substrates are displayed in Table 2, and depicts the fold difference in cytokine expression by monocytes cultured on apatite versus the TCPS control. Of the 36 inflammatory cytokines detectable by the antibody array, only seven were expressed by U937 monocytes. In response to the presence of the apatite coating, U937 monocytes showed fold increases in expression of VEG-F (18.77±19.12), IFN-γ (7.00±4.05), MIP-1b (3.20±0.31), MIP-1a (2.13±0.92), IP-10 (1.84±0.92), and slight decreased expression of IL-8 (-1.18±0.16) and RANTES (-1.57±0.35).

4.3.3 U937 monocyte response to 3D apatite-coated PLGA scaffold microenvironments

As a more relevant *in vitro* model that better mimics the *in vivo* apatite microenvironment, U937 monocytes were co-cultured with human osteoblast cells on apatite-coated 3D PLGA scaffolds that have previously been shown to significantly improve bone regeneration when implanted *in vivo* [4]. When given the appropriate environmental cues, circulating monocytes will adhere to the site of implantation at the onset of inflammation in response to the presence of the foreign body or the surgical procedure itself. As shown in Figure 16, U937 monocytes adhered to 3D apatite-coated PLGA scaffolds (structure shown in Figure 16A) *in vitro* with a majority of the seeded cells remaining viable (Figure 16B). Fewer non-viable cells were also dispersed throughout the scaffold structure (Figure 16C).

Having established the ability of U937 monocytes to adhere as an initial reaction to 3D apatite-coated PLGA scaffolds, we next aimed to assess any further functional response that could mediate the differentiation of human osteoblast cells in co-culture with the adhered U937

monocytes. Primary human osteoblast cells alone or osteoblasts with activated U937 monocytes were seeded onto apatite-coated PLGA scaffolds and cultured for 14, 21, and 28 days. At the designated time points, RNA from the scaffold cultures were harvested and processed for quantitative real-time PCR to assess gene expression of OCN as a marker for osteogenic differentiation. Figure 17 demonstrates that after just 14 and 21 days of culture no significant difference can be observed in OCN gene expression between osteoblasts cultured with U937 monocytes and osteoblasts alone. However, by 28 days the osteoblast/monocyte co-culture exhibited a 7.4±3.9 fold increase over the osteoblast-only culture, suggesting that the presence of the monocytes may enhance OCN gene expression of osteoblasts on 3D apatite-coated PLGA scaffolds.

To identify the cytokines released in response to the co-culture environment, media was collected from 3D apatite-coated PLGA scaffolds seeded with both human osteoblasts and U937 monocytes and analyzed by a cytokine array kit. Table 3 presents the cytokine expression observed from the co-cultured cells as a fold-difference with respect to each 3D mono-culture condition (osteoblasts alone or monocytes alone). Relative to U937 monocyte mono-cultures, the co-culture containing both cell types showed significant increases in MMP3 (6.97±0.43), RANTES (3.67±0.28), IL-8 (3.01±1.00), and moderate increases in Leptin (1.81±0.15), ICAM-1 (1.69±0.20), and IL-1ra (1.60±0.14). Relative to osteoblast mono-cultures, significant increases in the co-culture were seen for Leptin (5.85±0.25), and ICAM-1 (4.64±0.32), while moderate increases in the co-culture were seen for MMP3 (2.56±0.30), RANTES (2.25±0.22), IL-8 (1.63±0.80), and IL-1ra (1.51±0.13).

Taken together, these results suggest that the cellular response to the 3D apatite co-culture condition differs relative to the response of either cell type cultured alone. The presence of the additional cell type in the apatite microenvironment results in differential production of inflammatory cytokines that may play a role in bone remodeling.

4.4 Discussion

Few studies have closely examined the direct interaction between inflammatory cells and the accelerated apatite microenvironment and how this interaction may contribute to enhancing osteoblast differentiation *in vitro* and bone formation *in vivo*. As a preliminary investigation, this study represents an early attempt to improve our understanding of the inflammatory cell response to both a 2D and 3D apatite microenvironment *in vitro*. For this, monocyte adherence to apatite surfaces, as well as the subsequent cytokine production and ability to promote osteoblast differentiation were evaluated.

In the current study, non-activated U937 monocytes adhered to 2D apatite surfaces at a higher rate relative to TCPS surfaces after 24 hours in normal 10% serum-supplemented culture medium (data not shown). This result may indicate that the apatite surface may provide an appropriate stimulus necessary for monocyte activation, which is primarily marked by monocyte adhesion and release of soluble inflammatory mediators [157]. The specific physical interaction between monocytes and the apatite surface was not evaluated here, but it is likely to be mediated by adsorbed proteins [107], [114], [158], [159]. When biomaterials are first implanted *in vivo* or immersed in conventional cell culture conditions *in vitro*, one of the immediate events to take place is serum protein adsorption onto the surface, a phenomenon that is known to occur on

apatite materials [160]. Shortly thereafter, platelets and the clotting process will release chemokines, guiding circulating monocytes to this protein-coated material *in vivo* [146].

How adsorbed proteins mediate the interaction between monocytes and the apatite has not, to our knowledge, been previously explored. In this study, the absence of adsorbed protein on the apatite surface resulted in significant monocyte cell death—a response similar to that of adherent cell types, such as MC3T3-E1 pre-osteoblasts, to the bare apatite surface [103]. However, as was previously demonstrated, cell death could be mitigated in a dose-dependent manner relative to the amount of serum protein adsorbed to the apatite surface. It was speculated previously that the improvement in cell viability may be due to the activation of pro-survival signals upon attachment to proteins presented on the apatite surface. Furthermore, the effect of protein adsorption on the apatite surface zeta potential may also or alternatively play a direct role in the enhanced cell survival. As was shown in Chapter 3 of this thesis, apatite surface modifications that resulted in a more negative surface zeta potential could improve cell viability upon attachment.

The physicochemical properties of the apatite dictate the type, amount, and conformation of the adsorbed proteins, which in turn may directly influence monocyte adhesion behavior and activity. Serum albumin is the predominant protein found in plasma, making up 60-75% of the total protein. Although albumin is generally believed to "passivate" the surface and reduce the acute inflammatory response to biomaterials, evidence suggests that monocytes will still adhere to albumin-coated surfaces [159]. In contrast, fibrinogen—another primary plasma protein—has been shown to be a critical factor in the initiation of the inflammatory response to implanted biomaterials. It has been suggested that upon adsorption, fibrinogen will denature on the

material surface, and that the degree of this denaturation helps determine the degree of acute inflammation [161]. Monocytes have also been shown to bind other blood and ECM proteins such as fibronectin [162], immunoglobulins [163], factor X [164], and complement [165], via integrin and immunoglobulin family of receptors, which may modulate macrophage activation and secretion. Further investigation is required to fully understand the nature of the adsorbed protein layer presented to monocytes that promote adhesion and survival on the apatite surface.

Having established the ability of monocytes to interact with accelerated apatite by adhering to the surface (which necessitates adsorbed proteins to maintain viability), determining whether that interaction may contribute to osteoblast differentiation *in vitro* was subsequently investigated. For this, monocytes were first cultured in a 2D apatite microenvironment, from which the resulting conditioned media was collected and delivered to osteoblast cultures. The results demonstrated that conditioned media from monocytes cultured on either TCPS or 2D apatite were both capable of promoting mineralization in osteoblast cultures, suggesting that the presence of the apatite coating may not offer a significant advantage for enhancing monocyte production of osteogenic factors *in vitro*. However, it should be noted that the monocytes in this experiment were primed with activation factors (IFN-γ, LPS) prior to exposure to the apatite-coated or non-coated substrates. It has been shown that monocytes are quite sensitive to LPS and respond by releasing many different types of growth factors and cytokines [166], [167]. Therefore the possibility exists that chemical activation of the monocytes with IFN-γ/LPS is sufficient to enable the production and release of growth factors/cytokines that are capable of influencing osteoblast function, regardless of the substrate onto which the monocytes are cultured. Future work is certainly needed to assess the pro-osteogenic potential of conditioned media from monocytes cultured on apatite without pre-activation using LPS.

Nevertheless, the above results suggest that the monocyte conditioned media may contain factors that are capable of regulating osteoblast function. To help identify those possible factors, a cytokine antibody array was performed. A difference was indeed observed in the cytokine expression profiles of monocytes cultured on apatite versus those on TCPS, despite the fact that the conditioned media from both groups induced similar levels of osteoblast mineralization as described above. The seven inflammatory cytokines detected in both monocyte groups have all been shown to play some role in regulating bone regeneration or remodeling. In this study, VEG-F, IFN-γ, MIP-1a and MIP-1b were upregulated to various degrees while RANTES was slightly downregulated by U937 monocytes on 2D apatite relative to non-coated TCPS.

VEGF, which is an important angiogenic factor, regulates bone remodeling through the recruitment of endothelial, osteoblast, and osteoclast cells, and by autocrine regulation of chondrocyte function [168]. IFN-γ has been shown to regulate the differentiation of hMSCs into osteoblasts, but in combination with TNF-α, TGF-β and IL-17—inflammatory cytokines that were not detected in this study using the antibody array. The IFN-γ detected in the present study is more likely to be a residual factor during the pre-activation of the monocytes prior to seeding on the apatite coatings.

MIP-1a and MIP-1b are associated with regulation of osteoclast differentiation, and thus may be players in resorption and remodeling during bone tissue healing *in vivo* [169], [170]. Stimulation of osteoblasts with IP-10 has been shown to induce alkaline phosphatase (ALP) activity and β-*N*-acetylhexosaminidase release (Hex) [171], markers for osteoblastic activity and endochondral ossification, respectively. A decrease in RANTES secretion by monocytes on apatite was shown here, in accordance with previous studies by Hamlet, et al. who showed

RANTES down-regulation in response to CaP-modified surfaces [172]. RANTES is a chemokine that has been shown to play a role as an osteoclast migration and differentiation.

Taken together, these differences in cytokine expression suggest that U937 monocytes may respond differently to 2D apatite surfaces versus TCPS. Again, in spite of these differences, U937 monocytes cultured in the current 2D *in vitro* systems were able to secrete factors that were capable of stimulating osteoblast mineralization, which may have been made possible through pre-activation of the monocytes with IFN-γ and LPS.

The 2D *in vitro* apatite microenvironment may provide us an initial understanding of monocyte-apatite interactions, but is likely quite different from the interactions present in the *in vivo* apatite microenvironment, which has a proven track record in stimulating new bone formation in animal models [4]. As such, 3D apatite-coated PLGA scaffolds were used as a substrate for both inactivated monocytes and osteoblast cells, in co-culture, as a better *in vitro* representation of the 3D apatite microenvironment examined in the previous *in vivo* studies. The two cell types were cultured on the scaffolds concurrently throughout the duration of the experiment to allow for the presence of both paracrine signaling and cell-cell contact—two elements that are likely to be factors in the *in vivo* setting. The monocyte/osteoblast co-culture showed increased OCN gene expression after 28 days when compared to osteoblasts cultured alone and without pro-osteogenic culture medium supplements such as β-glycerophosphate. In accordance with the 2D apatite experiments, this again suggests that the inclusion of monocytes may play a role in osteoblastic differentiation.

To identify paracrine factors expressed in the 3D apatite co-culture system, a cytokine array was performed similarly to the 2D apatite experiment. Unlike the 2D apatite experiment

however, the cytokines detected in the 3D co-culture could be produced by the osteoblasts as well, and not solely by the monocytes. When osteoblasts and U937 monocytes were cultured together on the 3D apatite-coated scaffolds, a different inflammatory cytokine expression profile emerged compared to cultures of either cell type alone, suggesting that the presence of the additional cell type may significantly influence cell behavior or activity. Several cytokines displayed increased expression in the co-culture compared to each mono-culture (MMP3, RANTES, IL-8, Leptin, ICAM-1 and IL-1ra) and are all associated with bone remodeling. MMP-3, an enzyme involved in matrix degradation, is secreted by both osteoblasts and monocyte-derived cells [173]–[175], and has been shown to participate in bone resorption and the reorganization of collagen prior to mineralization. Furthermore, matrix degradation by MMP-3 may also result in the release of other factors that further promote the bone remodeling process.

For several of the identified pro-inflammatory cytokines, a review of the literature reveals paradoxical functions in the bone remodeling process. For example, IL-8 is a known chemoattractant for neutrophils, monocytes, leukocytes, but has also been reported to suppress bone resorption by osteoclasts [176]. Similarly, leptin, which is known to stimulate IL-8 production, may have both a stimulatory and suppressive effect on bone formation [177]. Studies investigating the role of soluble ICAM-1 in osteoclast activity suggest that it may protect osteoblasts against cell death and does not appear to influence osteoclast differentiation *in vitro*, despite being a recognized stimulator of TNF-α, IL-6, and MIP-1a—known modulators of osteoclast activity [178]–[181].

IL-1 receptor antagonist (IL-1ra), as its name implies, inhibits the osteoclastogenic activity of IL-1 [182]. Suppression of IL-1 may also activate mechanisms that promote bone formation, independent of the inhibition of bone resorption resulting from reduced osteoclastic activity [183]. In summary, although the exact mechanisms have not been elucidated, it is evident that the presence of a second cell type can effect cytokine expression of both U937 monocytes and human osteoblast cells cultured on 3D apatite-coated scaffolds. These differences in cytokine expression demonstrate the ability of cells to utilize paracrine signaling as one of several potential methods of intercellular communication. This, in turn, may positively regulate bone healing, given the release of appropriate pro-osteogenic factors into the surrounding environment.

Another potential means of communication between cell types in co-culture is through cell-cell contact. Although not specifically examined in this study, others have investigated the physical interactions between monocytes or monocyte-derived cells and osteoblasts. In a study on vascular calcification, co-culture of osteoblast-like cells with peripheral blood monocytes resulted in enhanced ALP activity and matrix mineralization [184]. Furthermore, conditioned media from monocytes activated with oxidized LDL in a transwell co-culture did not produce the same effect, suggesting that cell-cell contact between the monocytes and osteoblast-like cells was required. LPS-activated monocytes, however, produced conditioned media capable of increasing ALP activity in the osteoblast-like cells, proving the potency of LPS as an activator of monocytes. Although investigated for a different physiological system, this study suggests that both cell-cell contact as well as intercellular communication by soluble factors may influence the differentiation of osteoblast cells.

In the normal bone remodeling process, direct cell-cell contact has been shown to play a central role, and is likely mediated by cell surface receptors and ligands presented by osteoblasts and osteoclast precursors (including monocyte/macrophages). For example, osteoblasts express RANKL, the ligand recognized by RANK receptors of osteoclast precursors. Binding of RANKL to RANK initiates osteoclast differentiation, which marks the onset of the resorption phase in the bone remodeling process. Following bone resorption by mature osteoclasts, so-called "coupling factors" are expressed and act on pre-osteoblast cells to stimulate their differentiation and activation, signaling the transition to the bone forming phase [185]. Not only has direct cell-cell contact been observed between osteoclasts and osteoblasts *in vivo* [186], but a potential mechanism has been demonstrated where bidirectional osteoblast-osteoclast signaling is mediated by the coupling of Eph tyrosine kinase receptors and EphrinB ligands presented on osteoblasts and osteoclasts, respectively [187]. When ligand and receptor interact, simultaneous inhibition of osteoclastogenesis and stimulation of osteoblast differentiation occurs, facilitating the transition from bone resorption to bone formation.

4.4.1 Limitations of the current study and future considerations

The preliminary work investigating the behavior of inflammatory cells in response to accelerated apatite microenvironments presented here is certainly not without limitations. Firstly, the majority of the experiments in this study utilized the U937 monocyte cell line. Although it is widely used and an established *in vitro* model for human monocytes/macrophage differentiation, it is an immortalized cell line and thus may not be well representative of cells in the natural *in vivo* environment. Future work will be better served using normal primary human

monocytes to complement the primary human osteoblasts used in the study, which may better mimic the cellular behavior found *in vivo*.

Secondly, several of the preliminary experiments that focused on the 2D apatite-cellular response used pre-stimulatory factors such as IFN-γ and LPS, which have been proven to be potent triggers of U937 activation. Artificial *in vitro* stimulation using these chemical factors may produce confounding results when attempting to understand organically-derived, biomaterials-based stimulation of monocyte activation. Further investigation is needed to optimize the IFN-γ/LPS concentrations to model the levels that are secreted by inflammatory cells during the inflammatory response *in vivo.* Additional studies without the use of IFN-γ/LPS stimulation, as was performed for the 3D apatite experiments, may also be warranted to more precisely examine the effect of apatite materials on monocyte function in osteogenesis.

The current study might be considered an oversimplification of a highly complex system as the *in vivo* response to a foreign body is dynamic and involves many cells, proteins, and factors that work collectively to wage an appropriate inflammatory reaction. A defined sequence of events takes place that begins with initial blood protein-material interactions. As was described earlier in this discussion, the cellular response to the apatite surface will be mediated by an adsorbed protein layer likely composed of the primary plasma proteins albumin, immunoglobulins, and fibrinogen. However, in addition to these primary proteins, adsorption other plasma components such as complement factors and platelets are also likely to contribute to the overall cell-apatite surface interaction.

Complement activation involves a cascade of enzymatic cleavages that produces protein fragments with biological activity involved in the host immune response. The complement

components C3a, C5a, and C3b have been shown to stimulate monocytes/macrophages to secrete inflammatory cytokines [188]. Furthermore, in response to this activation, macrophages have been known to respond to ceramic implants *in vivo*, participating in the implant's biodegradation. The complement system may also have a role in bone development, independent of its role in immune function. Recent studies have shown that under proper stimulation, C3 is produced by bone marrow stromal cells and primary osteoblasts *in vitro* [189]. Complement components C3, factor B, C5, and C9 have also been localized to areas of endochondral bone formation, providing an impetus for cartilage turnover to bone [190], [191]. Taken together, the role of complement should be considered for further investigation not only as regulators of monocyte/macrophage activation, but also as mediators of bone remodeling and formation in response to apatite biomaterials.

Platelets are cell fragments found in blood that are involved in coagulation and are also likely to play a role in the blood-material interaction *in vivo*. Studies investigating the role of coagulation factors in the osteoconductivity of polarized hydroxyapatite materials demonstrated that negatively-charged surfaces were more likely than positively- or non-charged hydroxyapatite surfaces to enhance platelet adhesion [192]. It was suggested that the interaction between the platelets and hydroxyapatite surface was mediated by increased fibrin adsorption as a result of an accumulation of Ca^{2+} ions on the negatively-charged hydroxyapatite surface. This subsequently created a positively charged ion layer that enhanced the electrostatic attraction of fibrin to the surface. Platelets were previously shown to interact with fibrin and become activated via integrin $\alpha_{IIb}\beta_3$ [193], resulting in platelet production of growth factors, such as PDGF and TGF-β, that play a role in bone cell recruitment [194]. The efficacy of platelets in

bone healing has further been suggested from the extensive clinical use of platelet-rich plasma therapy for enhancement of bone graft integration [195], [196].

Although this preliminary study has focused primarily on monocyte-apatite interactions, we should be reminded that cellular recruitment in response to a foreign implant will take place by multiple cell types found *in vivo*, not limited to just monocytes/macrophages. Following the initial blood-material interaction, inflammatory events occur that progress towards the recruitment of other myeloid cells, the first being neutrophils during the acute phase. Apatite-based materials were shown to activate neutrophil adhesion and secretion of pro-inflammatory factors (IL-1α), chemotactic factors (IL-8 and MIP-1a), and MMP-9 [197]. Release of these factors could potentially lead to subsequent activation of other polymorphonuclear cells or monocytes/macrophages, while MMP-9 may be critical for tissue remodeling in response to hydroxyapatite implants *in vivo* [198].

Lymphocytes are another immune cell population that is likely to be recruited to the site of implantation. Their infiltration is typically identified with the onset of chronic inflammation following the initial acute phase response by neutrophils and monocytes/macrophages. For biocompatible biomaterials, the chronic inflammatory response is normally short-lived (on the order of a few weeks) and confined to the implantation site. Work by Matesanz *et al.* suggests that apatite materials may be capable of tempering the immune response mediated by lymphocytes. Nanocrystalline hydroxyapatite surfaces were shown to induce macrophage production of pro-inflammatory cytokines (IL-6 and TNF-α), but significantly decreased their proliferation and phagocytic activity, as well as induced apoptosis of SR.D10 T lymphocytes *in*

vitro [199]. This modulation of the immune response may aid in the long-term acceptance of apatite biomaterials *in vivo*.

Aside from their primary function in the immune response, lymphocytes may also participate in the regulation of bone remodeling, with evidence suggesting they may play a dual role in both resorption and formation phases [200]. For example, T lymphocytes have been shown to stimulate osteoclastogenesis via RANK/RANKL binding, and through the secretion of pro-resorptive cytokines, to initiate the resorption phase. In contrast, there is evidence that T lymphocytes also produce various interleukins that function to protect against bone loss by inhibiting osteoclast formation. A role for B lymphocytes in the regulation of new bone induction and regeneration has also been suggested [201], and both B and T lymphocytes are known to be critical in normal bone homeostasis. Given the role of lymphocytes in bone regulation, these immune cells should also be considered when investigating pro-osteogenic properties of apatite materials upon implantation *in vivo*.

A heterogeneous population of immune cells known as myeloid-derived suppressor cells (MDSCs) has come to the forefront in recent years. These cells, which inhibit T lymphocyte and NK cell activity, typically emerge during chronic inflammation or the development of cancer [202]. Myeloid precursors that give rise to MDSCs normally differentiate into typical myeloid-derived immune cells (neutrophils, macrophages, dendritic cells, etc.) under non-pathological conditions. However, at the onset of infection, cell differentiation will diverge towards the immunosuppressive phenotype and infiltrate the site of inflammation. The expansion and activation of MDSC is usually mediated by paracrine factors—including GM-CSF, IL-6, IL-10, IL-1, and VEGF—or by cell-cell contact.

MDSCs are influenced by mesenchymal stem cells—precursors of bone forming cells—and have been shown to interact with other bone cells during bone metastasis. Their response to foreign biomaterial implants, however, has not been extensively studied, but it has been shown that MDSCs express integrin receptors [203] that may be capable of interacting with adsorbed proteins on apatite and other biomaterial surfaces. MDSCs may also participate in bone remodeling processes since they have been shown to express markers that overlap with those of osteoclast progenitors, and thus may have the potential to differentiate into bone resorbing osteoclasts [204]. The understanding of MDSCs as potential regulators of bone regulation, however, is still relatively nascent, and their interaction with biomaterial implants is even more limited. Nevertheless, exploration in this field is rapidly developing and it may be proven that these regulators of immune function may ultimately play a significant role in biomaterials-based tissue regeneration.

4.5 Conclusion

The mechanisms underlying accelerated apatite's ability to provide a pro-osteogenic environment are not well understood, especially when coupled with *in vivo* physiological processes such as inflammation and the immune response. The findings of this preliminary study, however, bring to light a possible role of the inflammatory response in the bone-regenerating capacity of apatite *in vivo*. Although there are many factors involved in a complex and dynamic inflammatory reaction, the current study aimed to establish the initial cellular interactions between monocytes and apatite coatings. Monocyte adherence *in vivo* is central to an inflammatory response and is typically associated with the release growth factors/cytokines to the surrounding environment, which may attract and/or trigger other cell types associated with

inflammation or tissue healing. In the current study, it was found that apatite coatings on 2D surfaces as well as 3D polymer scaffolds could promote monocyte adhesion in the absence of soluble monocyte activation factors. Furthermore, the presence of monocytes or monocyte conditioned media was shown to promote the differentiation of osteoblasts *in vitro*. Finally, the cellular production of cytokines, in response to the apatite material, was also assessed to help identify potential inflammatory factors that may also function in the healing of bone.

4.6 Figures and tables

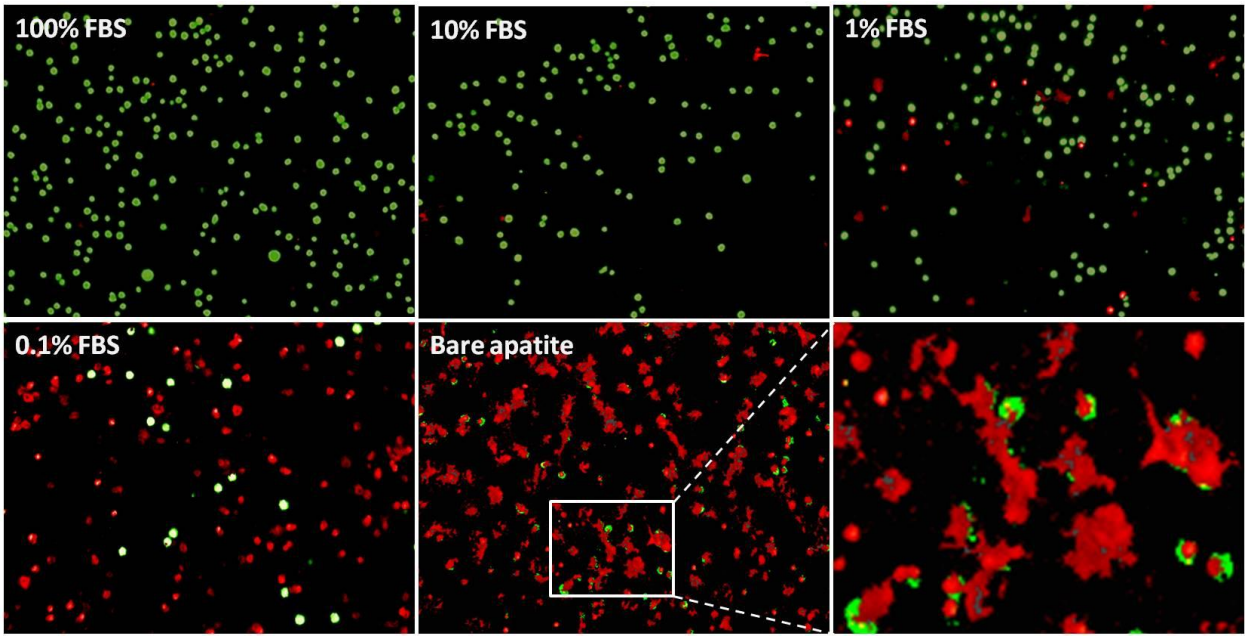

Figure 14: Adsorbed proteins on apatite surfaces are critical for U937 monocyte survival. U937 monocytes were seeded onto uncoated apatite surfaces (i.e. Bare apatite) or apatite surfaces pre-coated with FBS solutions with concentration from 0.1% to 100% (w/v). Live/dead viability staining shows a dose-dependent response with respect to the amount of protein pre-adsorbed onto the apatite prior to cell seeding, with an increasing number of live cells (green fluorescence) and a fewer number of dead cells (red fluorescence) being observed as protein concentration increases. The bottom right panel shows the extracellular release of DNA from the cells at higher magnification.

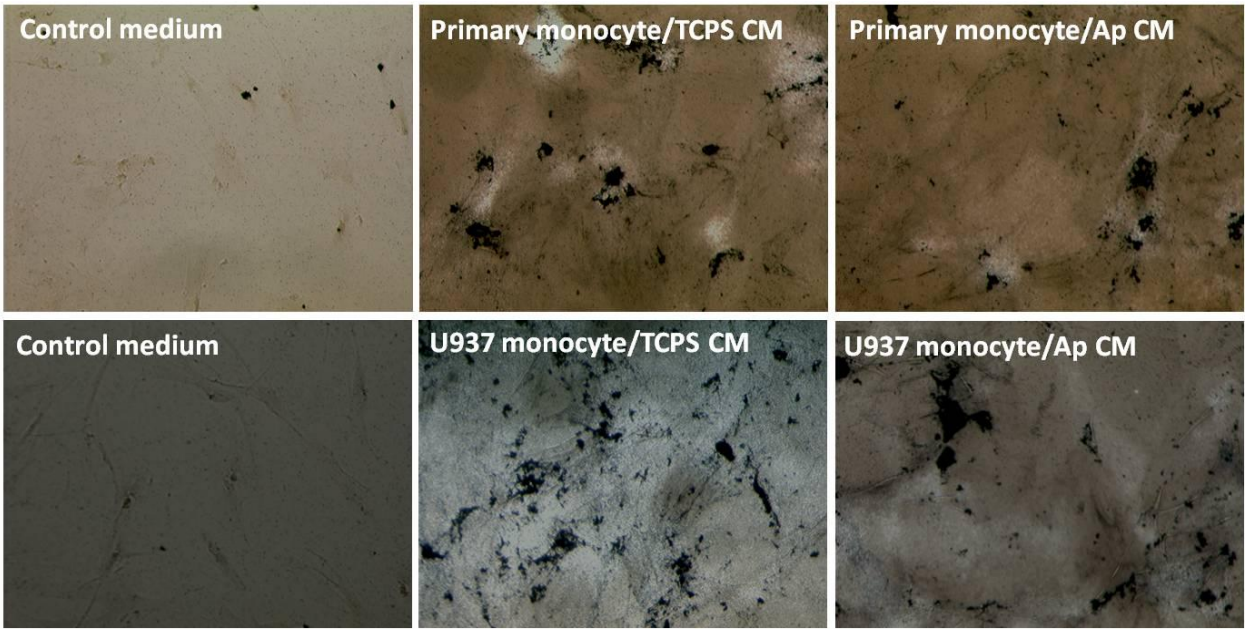

Figure 15: Monocyte conditioned media from primary human monocytes or U937 monocytes are capable of inducing *in vitro* osteoblast mineralization. Primary human monocytes and U937 monocytes were cultured on 2D apatite-coated TCPS or control TCPS for 24 hours. The cells were then removed from the media, which was subsequently used as conditioned media (CM) for primary human osteoblasts. Von Kossa staining for assessing biomineralization was performed on the osteoblasts after 28 days. Osteoblasts incubated in conditioned media from both types of monocytes exhibited increased biomineralization (black staining) relative to control medium, regardless of the substrate the monocytes were subjected to (TCPS vs. apatite-coated TCPS).

Table 2: Cytokines expressed by U937 monocytes on 2D apatite

Cytokine	Expression on apatite (24h) (fold change ± SD vs. TCPS)
VEG-F	**18.77 ± 19.12**
IFN-y	**7.00 ± 4.05**
MIP1b	**3.20 ± 0.31**
MIP1a	**2.13 ± 0.92**
IP-10	1.84 ± 0.92
IL-8	-1.18 ± 0.16
RANTES	-1.57 ± 0.35

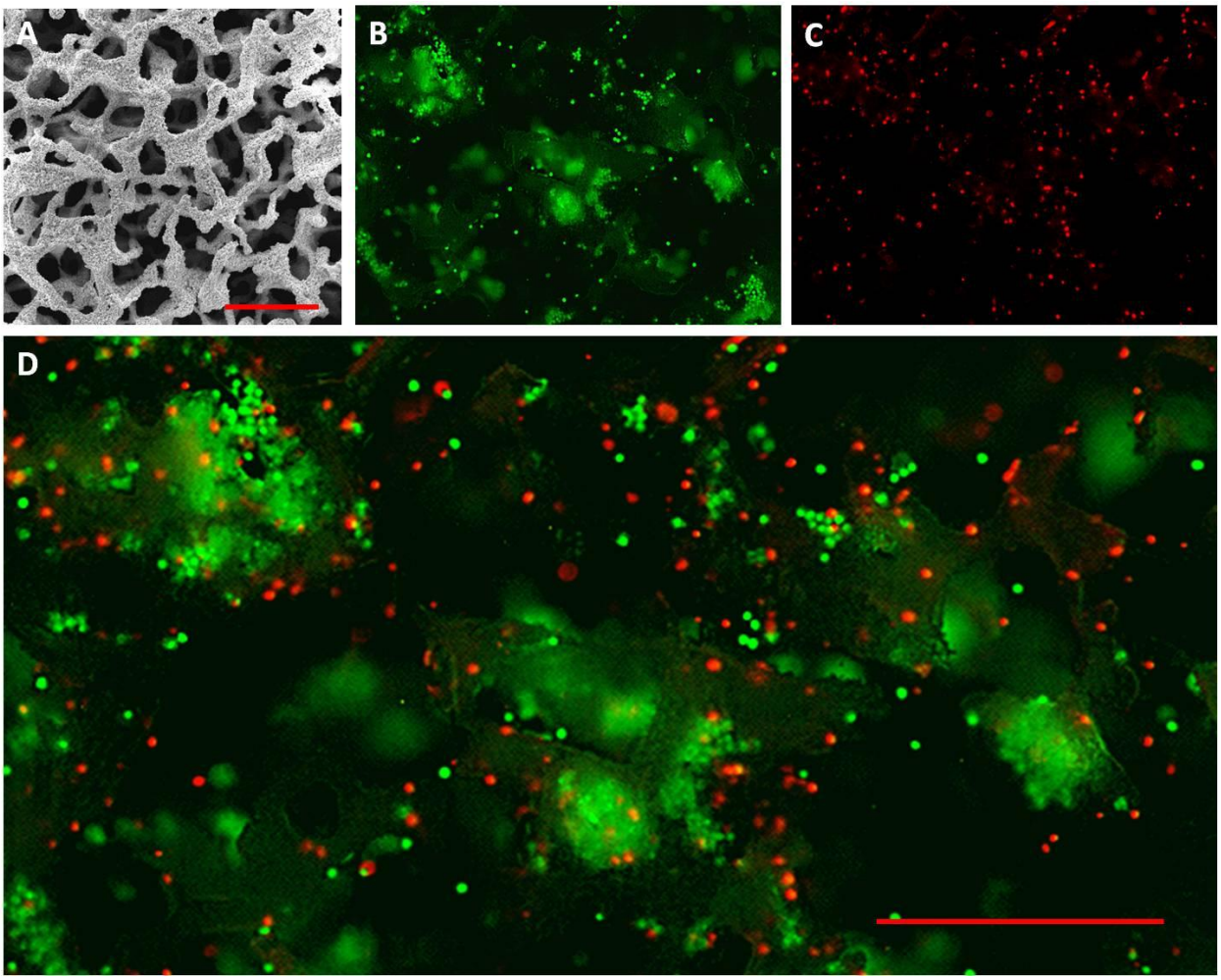

Figure 16: U937 monocytes adhere to 3D apatite-coated PLGA scaffolds. (A) SEM micrograph of the porous structure of apatite-coated PLGA scaffolds. (B-D) U937 monocytes were seeded onto 3D apatite-coated PLGA scaffolds at a cell density of 50,000 cells/scaffold and cell viability was assessed after 24 hours using a Live/Dead fluorescent staining kit. Live/dead fluorescent imaging demonstrated mostly viable cells (B) with few dead cells (C) in response to the 3D apatite-coated environment. (D) Merged Live/Dead fluorescent image with viable cells in green, dead cells in red. (scale bar = 500 um)

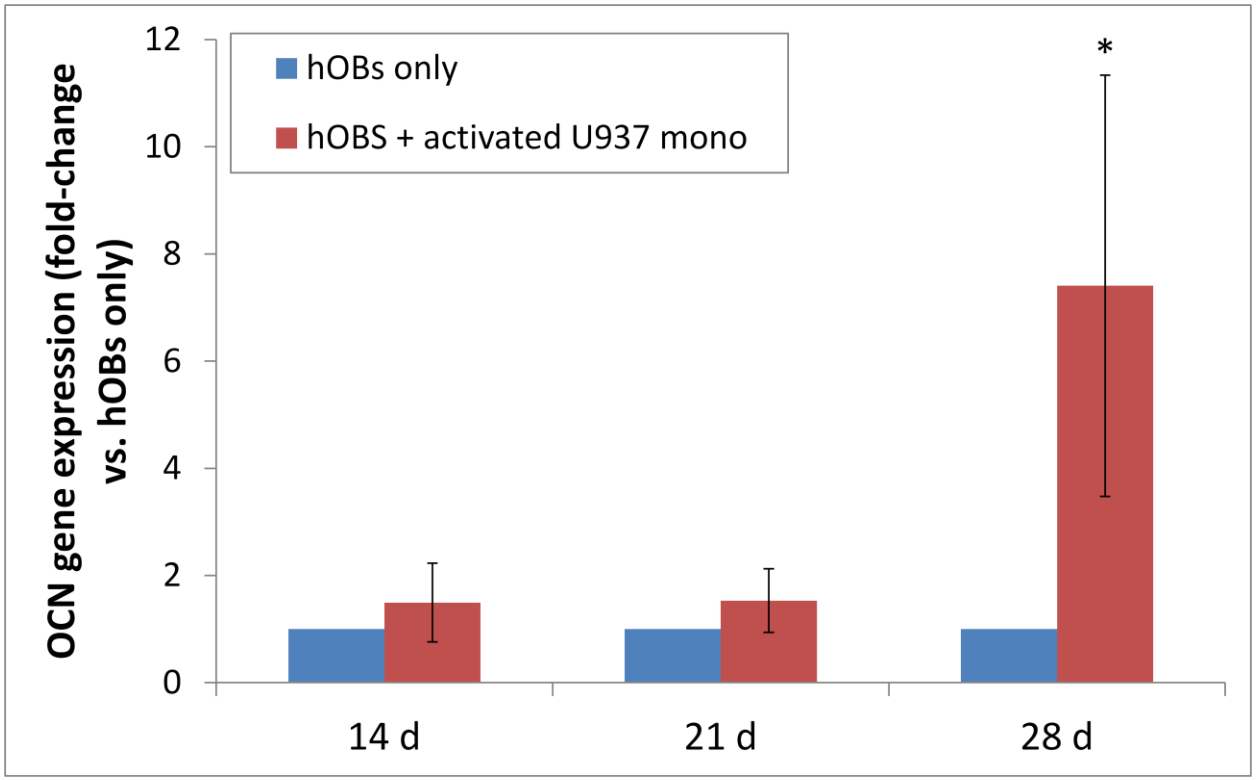

Figure 17: Primary human osteoblasts cultured with U937 monocytes on 3D apatite-coated express higher levels of OCN than osteoblasts alone. Primary human osteoblasts (hOBs) were cultured on 3D apatite-coated PLGA scaffolds either alone, or in co-culture with activated U937 monocytes. At 14, 21, and 28 days, RNA lysate was harvested from the scaffolds and OCN gene expression was measured by quantitative real-time PCR. After 14 and 21 days no significant difference can be observed in OCN gene expression (expressed as fold-change vs. hOBs alone) between hOBs cultured with U937 monocytes and hOBs alone. By 28 days the hOBs/monocyte co-culture exhibited a 7.4±3.9 fold increase over hOBs only culture.

(* $p < 0.05$)

Table 3: Cytokine expression from hOBS + U937 monocytes on 3D apatite-coated PLGA scaffolds

Cytokine	Expression from co-culture vs. mono-culture (fold-difference ± SD)		Potential role in bone healing
	hOBs+U937 vs. U937	hOBs+U937 vs. hOBs	
MMP3	**6.97 ± 0.43**	**2.56 ± 0.30**	Bone remodeling/resorption; osteoclast/osteoblast paracrine effect
RANTES	**3.67 ± 0.28**	**2.25 ± 0.22**	Osteoclastogenesis; chemotaxis of osteoblasts
IL-8	**3.01 ± 1.00**	1.63 ± 0.80	Osteoclastogenesis; pro-angiogenic
Leptin	1.81 ± 0.15	**5.85 ± 0.25**	Osteogenesis
ICAM-1	1.69 ± 0.20	**4.64 ± 0.32**	Osteoclast function
IL-1ra	1.60 ± 0.14	1.51 ± 0.13	Inhibition of IL-1 (osteoclastic factor)

CHAPTER 5

5.1 CONCLUSION

In this thesis, three features of the accelerated apatite microenvironment were separately examined to evaluate their influence on the cellular response. First, accelerated apatite coatings significantly alter the local calcium and phosphate ionic concentrations that are potentially exposed to cells within the microenvironment. This conclusion may not seem unexpected considering that the vast majority of the apatite literature has reported on the dissolution properties of apatite, resulting in the release of calcium and phosphate. Contrary to these reports, the results presented in Chapter 2 reveal that accelerated apatite coatings, when immersed in standard cell culture media, adsorb free calcium and phosphate, thus depleting the concentration of these ions originally present in the surrounding medium. This suggests that the apatite material prepared from a modified accelerated biomimetic approach has dissolution properties that may differ from other apatite-based materials. It is possible that the accelerated apatite surface, which has a Ca/P ratio of 1.48, undergoes changes to reach a more thermodynamically stable phase, such as stoichiometric hydroxyapatite (Ca/P ratio = 1.67). Although the exact structural and compositional changes that occur to the accelerated apatite upon immersion are unknown, these preliminary findings support the hypothesis of Aim 1 that accelerated apatite materials create an altered ionic microenvironment for cells.

The "pull-down" of calcium and phosphate ions to the apatite surface may have implications for the cellular or biological response to apatite-coated implants. Osteoprogenitor cells seeded onto apatite-coated scaffolds may be exposed to local elevated levels of calcium and phosphate due to the flux of these ions towards the apatite coating's surface. The actual

concentrations of calcium and phosphate near the surface of the apatite were not determined, but the effect of increasing levels of both ions has been reported to promote osteoblastic differentiation, up to a certain ion concentration threshold. It was confirmed here that concentrations above that threshold induces significant cell death. The intracellular uptake of phosphate was directly linked to the combined calcium/phosphate ion-induced cell death as viability could be restored upon treatment with phosphate transport inhibitors. Certainly, future studies are needed to determine whether elevated, but sub-lethal levels of calcium and phosphate are present adjacent to the surface and contribute to the overall osteogenic potential within the accelerated apatite microenvironment.

In Chapter 2, the direct interaction between osteoblast progenitor cells and the bare apatite surface was evaluated, and it was determined that adsorbed proteins are critical for cell survival. This result suggests that the unmodified, bare apatite surface may not be as biocompatible as is traditionally thought for most apatite materials. Cell death could be prevented, however, by pre-treating the cells with a phosphate transport inhibitor—a similar response by cells that were exposed to lethal doses of free exogenous calcium and phosphate ions. This finding suggests that uptake of phosphate may be responsible for the observed cell death on bare apatites. The role of adsorbed proteins in mitigating this response may be through the prevention of phosphate uptake, or by other means such as altering surface charge (Chapter 3), or eliciting pro-survival signaling via integrin-mediated pathways.

To evaluate the influence of apatite surface charge on cell viability, the surface zeta potential of bare accelerated apatites, as well as apatites modified with various surface coatings, was quantified and the resulting cellular response assessed. Both biomolecular and non-

biomolecular coatings were able to alter the apatite surface charge in a near-linear fashion with respect to coating thickness. The change in magnitude of the surface charge was also largely dependent on the degree of adsorption and inherent charge of the various biomolecules used to modify the apatite. It was also confirmed that apatites have varying affinities for different biomolecules, which may be governed not only by the molecules' charge, but also the structure, deformability, and presence of specific binding sites on the surface of the adsorbed molecules. In general, apatite surface treatments that resulted in a more negatively charged zeta potential, compared to un-treated controls, improved the viability of cells upon adherence in a serum-free environment.

When designing *in vitro* experiments to assess the biological interaction with a biomaterial, the *in vivo* biological response should always be considered since, ultimately, synthetically bioengineered constructs for tissue regeneration will be introduced into the body. With this in mind, the potential role of the immune response in regulating osteoblast differentiation was assessed by examining the cellular response of monocytes to 2D and 3D apatite-coated systems. Our initial *in vitro* results suggest that monocytes have the potential to enhance the biomineralization of osteoblast cultures and up-regulate the expression of mature osteogenic markers such as osteocalcin. Furthermore, co-cultures of monocytes and osteoblasts in a 3D apatite microenvironment displayed altered expression profiles of cytokines that have a potential role in regulating bone remodeling. These preliminary findings suggest the possibility that inflammatory cell-apatite interactions play a central role in the pro-osteogenic capacity of accelerated apatite coatings.

In summary, elucidating the immunopotentiating properties of apatite materials has considerable implications for the development of better bone tissue engineering constructs. That understanding, however, concomitantly requires an awareness of how changes to the physicochemical properties of apatite lead to controllable biological reactions. For example, future work studying apatite coatings may be able to modulate apatite's ability to adsorb ions or proteins. As a consequence, it may be possible to control ionic concentrations or surface charges that are presented at the apatite surface, and thereupon mediate a more effective cellular or biological response. Accordingly, an apatite-driven strategy thus can be designed to exploit the function of cells either *in vitro* or *in vivo* for stimulation of bone healing (e.g. monocytes/macrophages producing a "cocktail" of pro-osteogenic cytokines in response to apatite material *in situ*).

5.2 Future directions and suggested experiments

This thesis presents a preliminary investigation of three central components in the accelerated apatite microenvironment and their contribution in mediating *in vitro* cell-apatite interactions. However, many questions still remain that should be considered in order to fully understand the *in vitro* biological response as well as how it translates to the *in vivo* environment. Therefore, the following is a discussion on potential future considerations that may be explored to further the advancement of apatite-based materials for bone regeneration.

Influence of ion "pull-down" on osteoblast function

When immersed in standard cell culture media, accelerated apatite coatings caused the depletion of calcium and phosphate ions from the surrounding medium. It is speculated that this adsorption, or "pull-down," creates high local concentrations of calcium and phosphate near the

apatite surface where adherent cells are seeded. Further experimentation is needed to determine the ionic concentration adjacent to the apatite coating surface, and compare the measured concentration against the literature values that are reported to induce osteoblastic differentiation. Furthermore, is it possible to modulate the ion "pull-down" effect through modification of the apatite coating in order to finely tune or customize the osteoblastic response based on the ability to control local ion concentrations?

Source of phosphate that mediates cell death on bare apatite

In regard to the cell interaction with bare apatite surfaces, significant cytotoxicity was observed, but could be prevented through the inhibition of cellular phosphate uptake. It is unclear whether the source of phosphate that gains entry to the cell is from the apatite surface itself, or potentially from increased local ion concentrations near the apatite surface that is a result of the "pull-down" effect. Further radioactive P-32 cell uptake studies can be performed to determine this source by measuring the intracellular radioactivity of cells exposed to P-32 modified coatings or P-32 doped cell media.

Role of adsorbed proteins in preventing phosphate-induced cell death on apatite

Tracking P-32 will also help clarify whether adsorbed proteins on apatite contribute to cell survival by inhibiting phosphate-induced cell death, or solely by alternative methods (i.e. masking of surface charge or induction of integrin-mediated pro-survival signaling pathways).

"Pull-down" (adsorption) of other ions onto accelerated apatite surfaces

Although only calcium and phosphate were assessed regarding the ion "pull-down" effect, cell culture media and body fluids also contain other ions such as magnesium, sodium,

potassium, chloride, and sulfate. How accelerated apatite influences the concentrations of these ions in the microenvironment is unknown, although it can be speculated that they too can be adsorbed to apatite surfaces due to electrostatic interactions. Further studies can be performed using ICP methods to quantify these ions as was previously done for calcium and phosphorus.

Influence of accelerated apatite surface charge on cell transmembrane potential

It is possible that the exposure of a cell to a charged surface like apatite coatings may alter the potential difference across the cell membrane. This transmembrane potential is regulated by ion channels that transverse the plasma membrane. The surface charge of the apatite may change the open or closed state of these ion channels, which may have implications in regulating cellular activity such as cell death, proliferation, or differentiation. Recent studies have demonstrated that changes in membrane potential are a functional determinant of MSC differentiation [205]. Additionally, our preliminary findings suggest that there is a surface charge threshold (~ -30 mV) that delineates cell survival versus cell death. Is it possible to correlate specific surface charge values to the open/closed states of these ion channels in a quantifiable manner, and does this manipulation of ion channel state influence cell viability? Moreover, can this knowledge be used to modify apatite surfaces (i.e. with surface coatings, change in crystal structure or composition) in order to achieve a specific charge that will elicit a predictable or desired response?

Accelerated apatite interactions with other cellular and chemical mediators of inflammation

As was discussed in Chapter 4 of this thesis, certain changes in cytokine expression by monocyte cultures and monocyte/osteoblast co-cultures were observed in response to accelerated apatite coatings. More specific assays such as ELISA or multiplexed MAGPIX analysis can be

performed to quantify these changes in expression. Once identified, recombinant forms of these cytokines can be delivered to osteoblasts or osteoprogenitors to determine their osteoinductive potential.

BIBLIOGRAPHY

[1] Y.-F. Chou, W.-A. Chiou, Y. Xu, J. C. Y. Dunn, and B. M. Wu, "The effect of pH on the structural evolution of accelerated biomimetic apatite.," *Biomaterials*, vol. 25, no. 22, pp. 5323–31, Oct. 2004.

[2] Y.-F. Chou, W. Huang, J. C. Y. Dunn, T. a Miller, and B. M. Wu, "The effect of biomimetic apatite structure on osteoblast viability, proliferation, and gene expression.," *Biomaterials*, vol. 26, no. 3, pp. 285–95, Jan. 2005.

[3] Y.-F. Chou, J. C. Y. Dunn, and B. M. Wu, "In vitro response of MC3T3-E1 pre-osteoblasts within three-dimensional apatite-coated PLGA scaffolds.," *J. Biomed. Mater. Res. B. Appl. Biomater.*, vol. 75, no. 1, pp. 81–90, Oct. 2005.

[4] C. M. Cowan, Y.-Y. Shi, O. O. Aalami, Y.-F. Chou, C. Mari, R. Thomas, N. Quarto, C. H. Contag, B. Wu, and M. T. Longaker, "Adipose-derived adult stromal cells heal critical-size mouse calvarial defects.," *Nat. Biotechnol.*, vol. 22, no. 5, pp. 560–7, May 2004.

[5] M. G. M. G. Penido and U. S. Alon, "Phosphate homeostasis and its role in bone health.," *Pediatr. Nephrol.*, vol. 27, no. 11, pp. 2039–48, Nov. 2012.

[6] "American Association of Orthopaedic Surgeons." [Online]. Available: www.aaos.org.

[7] C. Laurencin, Y. Khan, and S. F. El-Amin, "Bone graft substitutes.," *Expert Rev. Med. Devices*, vol. 3, no. 1, pp. 49–57, Jan. 2006.

[8] W. G. DE LONG, T. A. EINHORN, K. KOVAL, M. MCKEE, W. SMITH, R. SANDERS, and T. WATSON, "Bone grafts and bone graft substitutes in orthopaedic trauma surgery : A critical analysis," *J. Bone Joint Surg. Am.*, vol. 89A, no. 3, pp. 649–658.

[9] B. Stevens, Y. Yang, A. Mohandas, B. Stucker, and K. T. Nguyen, "A review of materials, fabrication methods, and strategies used to enhance bone regeneration in engineered bone tissues.," *J. Biomed. Mater. Res. B. Appl. Biomater.*, vol. 85, no. 2, pp. 573–82, May 2008.

[10] S. Jalota, S. B. Bhaduri, and A. C. Tas, "Osteoblast proliferation on neat and apatite-like calcium phosphate-coated titanium foam scaffolds," *Mater. Sci. Eng. C*, vol. 27, no. 3, pp. 432–440, Apr. 2007.

[11] S. Jalota, S. B. Bhaduri, and A. C. Tas, "In vitro testing of calcium phosphate (HA, TCP, and biphasic HA-TCP) whiskers.," *J. Biomed. Mater. Res. A*, vol. 78, no. 3, pp. 481–90, Sep. 2006.

[12] T. Mygind, M. Stiehler, A. Baatrup, H. Li, X. Zou, A. Flyvbjerg, M. Kassem, and C. Bünger, "Mesenchymal stem cell ingrowth and differentiation on coralline hydroxyapatite scaffolds.," *Biomaterials*, vol. 28, no. 6, pp. 1036–47, Feb. 2007.

[13] C. Klein, K. de Groot, W. Chen, Y. Li, and X. Zhang, "Osseous substance formation induced in porous calcium phosphate ceramics in soft tissues," *Biomaterials*, vol. 15, no. 1, pp. 31–34, Jan. 1994.

[14] U. Ripamonti, "Osteoinduction in porous hydroxyapatite implanted in heterotopic sites of different animal models," *Biomaterials*, vol. 17, no. 1, pp. 31–35, Jan. 1996.

[15] P. Habibovic, U. Gbureck, C. J. Doillon, D. C. Bassett, C. A. van Blitterswijk, and J. E. Barralet, "Osteoconduction and osteoinduction of low-temperature 3D printed bioceramic implants.," *Biomaterials*, vol. 29, no. 7, pp. 944–53, Mar. 2008.

[16] B. Clarke, "Normal bone anatomy and physiology.," *Clin. J. Am. Soc. Nephrol.*, vol. 3 Suppl 3, no. Supplement_3, pp. S131–9, Nov. 2008.

[17] S. Weiner, I. Sagi, and L. Addadi, "Structural biology. Choosing the crystallization path less traveled.," *Science*, vol. 309, no. 5737, pp. 1027–8, Aug. 2005.

[18] M. I. KAY, R. A. YOUNG, and A. S. POSNER, "CRYSTAL STRUCTURE OF HYDROXYAPATITE.," *Nature*, vol. 204, pp. 1050–2, Dec. 1964.

[19] P. W. Brown and B. Constantz, *Hydroxyapatite and Related Materials*. CRC Press, 1994, p. 368.

[20] R. Z. LeGeros, "Calcium phosphates in oral biology and medicine.," *Monogr. Oral Sci.*, vol. 15, pp. 1–201, Jan. 1991.

[21] R. Zapanta LeGeros, "Apatites in biological systems," *Prog. Cryst. Growth Charact.*, vol. 4, no. 1–2, pp. 1–45, Jan. 1981.

[22] C. S. Adams, K. Mansfield, R. L. Perlot, and I. M. Shapiro, "Matrix regulation of skeletal cell apoptosis. Role of calcium and phosphate ions.," *J. Biol. Chem.*, vol. 276, no. 23, pp. 20316–22, Jun. 2001.

[23] S.-H. Kwon, Y.-K. Jun, S.-H. Hong, and H.-E. Kim, "Synthesis and dissolution behavior of β-TCP and HA/β-TCP composite powders," *J. Eur. Ceram. Soc.*, vol. 23, no. 7, pp. 1039–1045, Jun. 2003.

[24] P. Ducheyne, S. Radin, M. Heughebaert, and J. C. Heughebaert, "Calcium phosphate ceramic coatings on porous titanium: effect of structure and composition on electrophoretic deposition, vacuum sintering and in vitro dissolution," *Biomaterials*, vol. 11, no. 4, pp. 244–254, May 1990.

[25] E. Mavropoulos, A. M. Rossi, N. C. C. da Rocha, G. A. Soares, J. C. Moreira, and G. T. Moure, "Dissolution of calcium-deficient hydroxyapatite synthesized at different conditions," *Mater. Charact.*, vol. 50, no. 2–3, pp. 203–207, Mar. 2003.

[26] T. L. Livingston, S. Gordon, M. Archambault, S. Kadiyala, K. McIntosh, A. Smith, and S. J. Peter, "Mesenchymal stem cells combined with biphasic calcium phosphate ceramics promote bone regeneration," *J. Mater. Sci. Mater. Med.*, vol. 14, no. 3, pp. 211–218, Mar. 2003.

[27] M. H. Mankani, S. A. Kuznetsov, B. Fowler, A. Kingman, and P. G. Robey, "In vivo bone formation by human bone marrow stromal cells: effect of carrier particle size and shape.," *Biotechnol. Bioeng.*, vol. 72, no. 1, pp. 96–107, Jan. 2001.

[28] R. LeGeros, A. Chohayeb, and A. Shulman, "Apatitic calcium phosphates: possible dental restorative materials," *J Dent Res*, vol. 61, p. 343, 1982.

[29] M. P. Ginebra, T. Traykova, and J. A. Planell, "Calcium phosphate cements as bone drug delivery systems: a review.," *J. Control. Release*, vol. 113, no. 2, pp. 102–10, Jun. 2006.

[30] C. D. Friedman, P. D. Costantino, S. Takagi, and L. C. Chow, "BoneSource hydroxyapatite cement: a novel biomaterial for craniofacial skeletal tissue engineering and reconstruction.," *J. Biomed. Mater. Res.*, vol. 43, no. 4, pp. 428–32, Jan. 1998.

[31] D. Knaack, M. E. Goad, M. Aiolova, C. Rey, A. Tofighi, P. Chakravarthy, and D. D. Lee, "Resorbable calcium phosphate bone substitute.," *J. Biomed. Mater. Res.*, vol. 43, no. 4, pp. 399–409, Jan. 1998.

[32] S. Larsson and T. Bauer, "Use of injectable calcium phosphate cement for fracture fixation: a review," *Clin. Orthop. Relat. Res.*, 2002.

[33] M. D. Weir and H. H. K. Xu, "Human bone marrow stem cell-encapsulating calcium phosphate scaffolds for bone repair.," *Acta Biomater.*, vol. 6, no. 10, pp. 4118–26, Oct. 2010.

[34] J. Wang, A. van Apeldoorn, and K. de Groot, "Electrolytic deposition of calcium phosphate/chitosan coating on titanium alloy: growth kinetics and influence of current density, acetic acid, and chitosan.," *J. Biomed. Mater. Res. A*, vol. 76, no. 3, pp. 503–11, Mar. 2006.

[35] C. Yang, "Effect of calcium phosphate surface coating on bone ingrowth onto porous-surfaced titanium alloy implants in rabbit tibiae," *J. Oral Maxillofac. Surg.*, vol. 60, no. 4, pp. 422–425, Apr. 2002.

[36] S. Yang, K. F. Leong, Z. Du, and C. K. Chua, "The design of scaffolds for use in tissue engineering. Part I. Traditional factors.," *Tissue Eng.*, vol. 7, no. 6, pp. 679–89, Dec. 2001.

[37] S. Yang, K.-F. Leong, Z. Du, and C.-K. Chua, “The design of scaffolds for use in tissue engineering. Part II. Rapid prototyping techniques.,” *Tissue Eng.*, vol. 8, no. 1, pp. 1–11, Feb. 2002.

[38] R. Murugan and S. Ramakrishna, “Nano-featured scaffolds for tissue engineering: a review of spinning methodologies.,” *Tissue Eng.*, vol. 12, no. 3, pp. 435–47, Mar. 2006.

[39] W. L. Murphy, D. H. Kohn, and D. J. Mooney, “Growth of continuous bonelike mineral within porous poly(lactide-co-glycolide) scaffolds in vitro.,” *J. Biomed. Mater. Res.*, vol. 50, no. 1, pp. 50–8, Apr. 2000.

[40] L. Sun, C. C. Berndt, K. A. Gross, and A. Kucuk, “Material fundamentals and clinical performance of plasma-sprayed hydroxyapatite coatings: a review.,” *J. Biomed. Mater. Res.*, vol. 58, no. 5, pp. 570–92, Jan. 2001.

[41] J. H. Chern Lin, M. L. Liu, and C. P. Ju, “Structure and properties of hydroxyapatite-bioactive glass composites plasma sprayed on Ti6Al4V,” *J. Mater. Sci. Mater. Med.*, vol. 5, no. 5, pp. 279–283, May 1994.

[42] J.-M. Choi, H.-E. Kim, and I.-S. Lee, “Ion-beam-assisted deposition (IBAD) of hydroxyapatite coating layer on Ti-based metal substrate,” *Biomaterials*, vol. 21, no. 5, pp. 469–473, Mar. 2000.

[43] L. Clèries, E. Martínez, J. . Fernández-Pradas, G. Sardin, J. Esteve, and J. . Morenza, “Mechanical properties of calcium phosphate coatings deposited by laser ablation,” *Biomaterials*, vol. 21, no. 9, pp. 967–971, May 2000.

[44] M. . Ball, S. Downes, C. . Scotchford, E. . Antonov, V. . Bagratashvili, V. . Popov, W.-J. Lo, D. . Grant, and S. . Howdle, “Osteoblast growth on titanium foils coated with hydroxyapatite by pulsed laser ablation,” *Biomaterials*, vol. 22, no. 4, pp. 337–347, Feb. 2001.

[45] J. Ma, C. Wang, and K. W. Peng, “Electrophoretic deposition of porous hydroxyapatite scaffold,” *Biomaterials*, vol. 24, no. 20, pp. 3505–3510, Sep. 2003.

[46] O. Albayrak, O. El-Atwani, and S. Altintas, “Hydroxyapatite coating on titanium substrate by electrophoretic deposition method: Effects of titanium dioxide inner layer on adhesion strength and hydroxyapatite decomposition,” *Surf. Coatings Technol.*, vol. 202, no. 11, pp. 2482–2487, Feb. 2008.

[47] A. Oyane, H.-M. Kim, T. Furuya, T. Kokubo, T. Miyazaki, and T. Nakamura, “Preparation and assessment of revised simulated body fluids.,” *J. Biomed. Mater. Res. A*, vol. 65, no. 2, pp. 188–95, May 2003.

[48] Y. Yang, K.-H. Kim, and J. L. Ong, “A review on calcium phosphate coatings produced using a sputtering process--an alternative to plasma spraying.,” *Biomaterials*, vol. 26, no. 3, pp. 327–37, Jan. 2005.

[49] T. Kokubo, S. Ito, Z. T. Huang, T. Hayashi, S. Sakka, T. Kitsugi, and T. Yamamuro, “Ca,P-rich layer formed on high-strength bioactive glass-ceramic A-W.,” *J. Biomed. Mater. Res.*, vol. 24, no. 3, pp. 331–43, Mar. 1990.

[50] T. Kokubo, H. Kushitani, S. Sakka, T. Kitsugi, and T. Yamamuro, “Solutions able to reproduce in vivo surface-structure changes in bioactive glass-ceramic A-W.,” *J. Biomed. Mater. Res.*, vol. 24, no. 6, pp. 721–34, Jun. 1990.

[51] T. Kokubo and H. Takadama, “How useful is SBF in predicting in vivo bone bioactivity?,” *Biomaterials*, vol. 27, no. 15, pp. 2907–15, May 2006.

[52] T. Kokubo, “Apatite formation on surfaces of ceramics, metals and polymers in body environment,” *Acta Mater.*, vol. 46, no. 7, pp. 2519–2527, Apr. 1998.

[53] T. Kokubo, “Bioactive glass ceramics: properties and applications,” *Biomaterials*, vol. 12, no. 2, pp. 155–163, Mar. 1991.

[54] H. Takadama, “Round-robin test of SBF for in vitro measurement of apatite-forming ability of synthetic materials,” *Phosphorus Res. Bull.*, vol. 17, p. 119, 2004.

[55] F. Barrere, C. a van Blitterswijk, K. de Groot, and P. Layrolle, “Influence of ionic strength and carbonate on the Ca-P coating formation from SBFx5 solution.,” *Biomaterials*, vol. 23, no. 9, pp. 1921–30, May 2002.

[56] F. Barrere, C. . van Blitterswijk, K. de Groot, and P. Layrolle, “Nucleation of biomimetic Ca–P coatings on Ti6Al4V from a SBF×5 solution: influence of magnesium,” *Biomaterials*, vol. 23, no. 10, pp. 2211–2220, May 2002.

[57] I. Wulur, “Microstructural control of biomimetically grown bonelike minerals on two dimensional and three dimensional polymer surfaces,” University of California, Los Angeles, 2002.

[58] P. Habibovic, F. Barrère, C. A. Blitterswijk, K. Groot, and P. Layrolle, “Biomimetic Hydroxyapatite Coating on Metal Implants,” *J. Am. Ceram. Soc.*, vol. 85, no. 3, pp. 517–522, Dec. 2004.

[59] F. Barrère, C. M. van der Valk, G. Meijer, R. A. J. Dalmeijer, K. de Groot, and P. Layrolle, “Osteointegration of biomimetic apatite coating applied onto dense and porous metal implants in femurs of goats.,” *J. Biomed. Mater. Res. B. Appl. Biomater.*, vol. 67, no. 1, pp. 655–65, Oct. 2003.

[60] C. Du, G. . Meijer, C. van de Valk, R. . Haan, J. . Bezemer, S. . Hesseling, F. . Cui, K. de Groot, and P. Layrolle, "Bone growth in biomimetic apatite coated porous Polyactive® 1000PEGT70PBT30 implants," *Biomaterials*, vol. 23, no. 23, pp. 4649–4656, Dec. 2002.

[61] B. Boyan, "Role of material surfaces in regulating bone and cartilage cell response," *Biomaterials*, vol. 17, no. 2, pp. 137–146, Jan. 1996.

[62] S. Oh, N. Oh, M. Appleford, and J. Ong, "Bioceramics for tissue engineering applications-A review," *Am. J. Biochem. …*, vol. 2, no. 2, pp. 49–56, 2006.

[63] A. J. Engler, S. Sen, H. L. Sweeney, and D. E. Discher, "Matrix elasticity directs stem cell lineage specification.," *Cell*, vol. 126, no. 4, pp. 677–89, Aug. 2006.

[64] M. Okamoto, Y. Dohi, H. Ohgushi, H. Shimaoka, M. Ikeuchi, A. Matsushima, K. Yonemasu, and H. Hosoi, "Influence of the porosity of hydroxyapatite ceramics on in vitro and in vivo bone formation by cultured rat bone marrow stromal cells.," *J. Mater. Sci. Mater. Med.*, vol. 17, no. 4, pp. 327–36, Apr. 2006.

[65] G. R. Beck, "Inorganic phosphate as a signaling molecule in osteoblast differentiation.," *J. Cell. Biochem.*, vol. 90, no. 2, pp. 234–43, Oct. 2003.

[66] M. M. Dvorak, A. Siddiqua, D. T. Ward, D. H. Carter, S. L. Dallas, E. F. Nemeth, and D. Riccardi, "Physiological changes in extracellular calcium concentration directly control osteoblast function in the absence of calciotropic hormones.," *Proc. Natl. Acad. Sci. U. S. A.*, vol. 101, no. 14, pp. 5140–5, Apr. 2004.

[67] S. Maeno, Y. Niki, H. Matsumoto, H. Morioka, T. Yatabe, A. Funayama, Y. Toyama, T. Taguchi, and J. Tanaka, "The effect of calcium ion concentration on osteoblast viability, proliferation and differentiation in monolayer and 3D culture.," *Biomaterials*, vol. 26, no. 23, pp. 4847–55, Aug. 2005.

[68] Y. K. Liu, Q. Z. Lu, R. Pei, H. J. Ji, G. S. Zhou, X. L. Zhao, R. K. Tang, and M. Zhang, "The effect of extracellular calcium and inorganic phosphate on the growth and osteogenic differentiation of mesenchymal stem cells in vitro: implication for bone tissue engineering.," *Biomed. Mater.*, vol. 4, no. 2, p. 025004, Apr. 2009.

[69] C. J. Van Noorden, "The history of Z-VAD-FMK, a tool for understanding the significance of caspase inhibition.," *Acta Histochem.*, vol. 103, no. 3, pp. 241–51, Jul. 2001.

[70] K. M. Woo, J. Seo, R. Zhang, and P. X. Ma, "Suppression of apoptosis by enhanced protein adsorption on polymer/hydroxyapatite composite scaffolds.," *Biomaterials*, vol. 28, no. 16, pp. 2622–30, Jun. 2007.

[71] G. R. Nakayama, M. C. Caton, M. P. Nova, and Z. Parandoosh, “Assessment of the Alamar Blue assay for cellular growth and viability in vitro,” *J. Immunol. Methods*, vol. 204, no. 2, pp. 205–208, May 1997.

[72] D. G. . Nelson, J. . Barry, C. . Shields, R. Glena, and J. D. . Featherstone, “Crystal morphology, composition, and dissolution behavior of carbonated apatites prepared at controlled pH and temperature,” *J. Colloid Interface Sci.*, vol. 130, no. 2, pp. 467–479, Jul. 1989.

[73] P. Ducheyne, S. Radin, and L. King, “The effect of calcium phosphate ceramic composition and structure on in vitro behavior. I. Dissolution.,” *J. Biomed. Mater. Res.*, vol. 27, no. 1, pp. 25–34, Jan. 1993.

[74] T. Suzuki, R. Ohashi, Y. Yokogawa, K. Nishizawa, F. Nagata, Y. Kawamoto, T. Kameyama, and M. Toriyama, “Initial anchoring and proliferation of fibroblast L-929 cells on unstable surface of calcium phosphate ceramics,” *J. Biosci. Bioeng.*, vol. 87, no. 3, pp. 320–327, Jan. 1999.

[75] R. S. Hotchkiss, A. Strasser, J. E. McDunn, and P. E. Swanson, “Cell death.,” *N. Engl. J. Med.*, vol. 361, no. 16, pp. 1570–83, Oct. 2009.

[76] J. E. Chipuk and D. R. Green, “Do inducers of apoptosis trigger caspase-independent cell death?,” *Nat. Rev. Mol. Cell Biol.*, vol. 6, no. 3, pp. 268–75, Mar. 2005.

[77] H. Steller, “Mechanisms and genes of cellular suicide,” *Science (80-.).*, vol. 267, no. 5203, pp. 1445–1449, Mar. 1995.

[78] J. R. WILLIAMS, J. B. LITTLE, and W. U. SHIPLEY, “Association of mammalian cell death with a specific endonucleolytic degradation of DNA,” *Nature*, vol. 252, no. 5485, pp. 754–755, Dec. 1974.

[79] P. Golstein and G. Kroemer, “Cell death by necrosis: towards a molecular definition.,” *Trends Biochem. Sci.*, vol. 32, no. 1, pp. 37–43, Jan. 2007.

[80] A. El-Ghannam, P. Ducheyne, and I. M. Shapiro, “Effect of serum proteins on osteoblast adhesion to surface-modified bioactive glass and hydroxyapatite.,” *J. Orthop. Res.*, vol. 17, no. 3, pp. 340–5, May 1999.

[81] K. Guth, C. Campion, T. Buckland, and K. A. Hing, “Effect of Silicate-Substitution on Attachment and Early Development of Human Osteoblast-Like Cells Seeded on Microporous Hydroxyapatite Discs,” *Adv. Eng. Mater.*, vol. 12, no. 1–2, pp. B26–B36, Feb. 2010.

[82] K. L. Kilpadi, P. L. Chang, and S. L. Bellis, “Hydroxylapatite binds more serum proteins, purified integrins, and osteoblast precursor cells than titanium or steel.,” *J. Biomed. Mater. Res.*, vol. 57, no. 2, pp. 258–67, Nov. 2001.

[83] A. A. Sawyer, K. M. Hennessy, and S. L. Bellis, “Regulation of mesenchymal stem cell attachment and spreading on hydroxyapatite by RGD peptides and adsorbed serum proteins.,” *Biomaterials*, vol. 26, no. 13, pp. 1467–75, May 2005.

[84] Q. Chen, M. Kinch, T. Lin, K. Burridge, and R. Juliano, “Integrin-mediated cell adhesion activates mitogen-activated protein kinases,” *J. Biol. Chem.*, vol. 269, no. 43, pp. 26602–26605, Oct. 1994.

[85] F. G. Giancotti, “Integrin Signaling,” *Science (80-.).*, vol. 285, no. 5430, pp. 1028–1033, Aug. 1999.

[86] R. Globus, S. Doty, J. Lull, E. Holmuhamedov, M. Humphries, and C. Damsky, “Fibronectin is a survival factor for differentiated osteoblasts,” *J. Cell Sci.*, vol. 111, no. 10, pp. 1385–1393, May 1998.

[87] V. Grigoriou, I. M. Shapiro, E. A. Cavalcanti-Adam, R. J. Composto, P. Ducheyne, and C. S. Adams, “Apoptosis and survival of osteoblast-like cells are regulated by surface attachment.,” *J. Biol. Chem.*, vol. 280, no. 3, pp. 1733–9, Jan. 2005.

[88] M. Ohgaki, T. Kizuki, M. Katsura, and K. Yamashita, “Manipulation of selective cell adhesion and growth by surface charges of electrically polarized hydroxyapatite.,” *J. Biomed. Mater. Res.*, vol. 57, no. 3, pp. 366–73, Dec. 2001.

[89] E. Reynolds and A. Wong, “Effect of adsorbed protein on hydroxyapatite zeta potential and Streptococcus mutans adherence.,” *Infect. Immun.*, vol. 39, no. 3, pp. 1285–1290, 1983.

[90] M. E. Barbour, R. P. Shellis, D. M. Parker, G. C. Allen, and M. Addy, “Inhibition of hydroxyapatite dissolution by whole casein: the effects of pH, protein concentration, calcium, and ionic strength.,” *Eur. J. Oral Sci.*, vol. 116, no. 5, pp. 473–8, Oct. 2008.

[91] J. A. Juhasz, S. M. Best, A. D. Auffret, and W. Bonfield, “Biological control of apatite growth in simulated body fluid and human blood serum.,” *J. Mater. Sci. Mater. Med.*, vol. 19, no. 4, pp. 1823–9, Apr. 2008.

[92] Z. Meleti, I. . Shapiro, and C. . Adams, “Inorganic phosphate induces apoptosis of osteoblast-like cells in culture,” *Bone*, vol. 27, no. 3, pp. 359–366, Sep. 2000.

[93] J. J. Bergh, Y. Shao, E. Puente, R. L. Duncan, and M. C. Farach-Carson, “Osteoblast Ca(2+) permeability and voltage-sensitive Ca(2+) channel expression is temporally regulated by 1,25-dihydroxyvitamin D(3).,” *Am. J. Physiol. Cell Physiol.*, vol. 290, no. 3, pp. C822–31, Mar. 2006.

[94] S. E. Guggino, D. Lajeunesse, J. A. Wagner, and S. H. Snyder, “Bone remodeling signaled by a dihydropyridine- and phenylalkylamine-sensitive calcium channel.,” *Proc. Natl. Acad. Sci.*, vol. 86, no. 8, pp. 2957–2960, Apr. 1989.

[95] W. Chang, C. Tu, T. H. Chen, L. Komuves, Y. Oda, S. A. Pratt, S. Miller, and D. Shoback, "Expression and signal transduction of calcium-sensing receptors in cartilage and bone.," *Endocrinology*, vol. 140, no. 12, pp. 5883–93, Dec. 1999.

[96] J. Caverzasio, T. Selz, and J.-P. Bonjour, "Characteristics of phosphate transport in osteoblastlike cells," *Calcif. Tissue Int.*, vol. 43, no. 2, pp. 83–87, Aug. 1988.

[97] C. S. Adams and I. M. Shapiro, "Mechanisms by which Extracellular Matrix Components Induce Osteoblast Apoptosis," Aug. 2009.

[98] R. Saunders, K. H. Szymczyk, I. M. Shapiro, and C. S. Adams, "Matrix regulation of skeletal cell apoptosis III: mechanism of ion pair-induced apoptosis.," *J. Cell. Biochem.*, vol. 100, no. 3, pp. 703–15, Feb. 2007.

[99] X. Li, H.-Y. Yang, and C. M. Giachelli, "Role of the sodium-dependent phosphate cotransporter, Pit-1, in vascular smooth muscle cell calcification.," *Circ. Res.*, vol. 98, no. 7, pp. 905–12, Apr. 2006.

[100] F. Barrère, C. a van Blitterswijk, and K. de Groot, "Bone regeneration: molecular and cellular interactions with calcium phosphate ceramics.," *Int. J. Nanomedicine*, vol. 1, no. 3, pp. 317–32, Jan. 2006.

[101] T. Suzuki, T. Yamamoto, M. Toriyama, K. Nishizawa, Y. Yokogawa, M. R. Mucalo, Y. Kawamoto, F. Nagata, and T. Kameyama, "Surface instability of calcium phosphate ceramics in tissue culture medium and the effect on adhesion and growth of anchorage-dependent animal cells.," *J. Biomed. Mater. Res.*, vol. 34, no. 4, pp. 507–17, Mar. 1997.

[102] B. D. Ratner and S. J. Bryant, "Biomaterials: where we have been and where we are going.," *Annu. Rev. Biomed. Eng.*, vol. 6, no. 1, pp. 41–75, Jan. 2004.

[103] E. J. Tsang, C. K. Arakawa, P. A. Zuk, and B. M. Wu, "Osteoblast interactions within a biomimetic apatite microenvironment.," *Ann. Biomed. Eng.*, vol. 39, no. 4, pp. 1186–200, Apr. 2011.

[104] M. Gorbunoff, "The interaction of proteins with hydroxyapatite: I. Role of protein charge and structure," *Anal. Biochem.*, vol. 432, pp. 425–432, 1984.

[105] T. Kawasaki, "Theory of chromatography of rigid molecules on hydroxyapatite columns with small loads: I. The case when virtually all molecules are adsorbed on to a single type of crystal site," *J. Chromatogr. A*, vol. 93, pp. 313–335, 1974.

[106] G. Bernardi, M. Giro, and C. Gaillard, "Chromatography of polypeptides and proteins on hydroxyapatite columns: some new developments," *... Biophys. Acta (BBA)-Protein ...*, vol. 278, pp. 409–420, 1972.

[107] K. Wang, C. Zhou, Y. Hong, and X. Zhang, “A review of protein adsorption on bioceramics.,” *Interface Focus*, vol. 2, no. 3, pp. 259–77, Jun. 2012.

[108] S. Tofail, Ed., *Biological Interactions with Surface Charge in Biomaterials*. The Royal Society of Chemistry, 2011, pp. P001–262.

[109] S. Bodhak, S. Bose, and A. Bandyopadhyay, “Electrically polarized HAp-coated Ti: in vitro bone cell-material interactions.,” *Acta Biomater.*, vol. 6, no. 2, pp. 641–51, Feb. 2010.

[110] F. R. Baxter, C. R. Bowen, I. G. Turner, and a C. E. Dent, “Electrically active bioceramics: a review of interfacial responses.,” *Ann. Biomed. Eng.*, vol. 38, no. 6, pp. 2079–92, Jun. 2010.

[111] K. Kandori, K. Miyagawa, and T. Ishikawa, “Adsorption of immunogamma globulin onto various synthetic calcium hydroxyapatite particles.,” *J. Colloid Interface Sci.*, vol. 273, no. 2, pp. 406–13, May 2004.

[112] R. W. Romberg, P. G. Werness, B. L. Riggs, and K. G. Mann, “Inhibition of hydroxyapatite crystal growth by bone-specific and other calcium-binding proteins.,” *Biochemistry*, vol. 25, no. 5, pp. 1176–80, Mar. 1986.

[113] K. Kandori, A. Fudo, and T. Ishikawa, “Adsorption of myoglobin onto various synthetic hydroxyapatite particles,” *Phys. Chem. Chem. Phys.*, vol. 2, no. 9, pp. 2015–2020, 2000.

[114] K. Kandori, M. Mukai, A. Yasukawa, and T. Ishikawa, “Competitive and cooperative adsorptions of bovine serum albumin and lysozyme to synthetic calcium hydroxyapatites,” *Langmuir*, no. 199, pp. 2301–2305, 2000.

[115] C. von Holt, “Histones in perspective.,” *Bioessays*, vol. 3, no. 3, pp. 120–4, Sep. 1985.

[116] H. Zeng, K. K. Chittur, and W. R. Lacefield, “Analysis of bovine serum albumin adsorption on calcium phosphate and titanium surfaces.,” *Biomaterials*, vol. 20, no. 4, pp. 377–84, Feb. 1999.

[117] S. Elangovan, H. C. Margolis, F. G. Oppenheim, and E. Beniash, “Conformational changes in salivary proline-rich protein 1 upon adsorption to calcium phosphate crystals.,” *Langmuir*, vol. 23, no. 22, pp. 11200–5, Oct. 2007.

[118] I. Lynch and K. Dawson, “Protein-nanoparticle interactions,” *Nano Today*, vol. 3, no. 1, pp. 40–47, 2008.

[119] V. Balasubramanian, N. K. Grusin, R. W. Bucher, V. T. Turitto, and S. M. Slack, “Residence-time dependent changes in fibrinogen adsorbed to polymeric biomaterials.,” *J. Biomed. Mater. Res.*, vol. 44, no. 3, pp. 253–60, Mar. 1999.

[120] K. Yamada, S. Yoshii, S. Kumagai, I. Fujiwara, K. Nishio, M. Okuda, N. Matsukawa, and I. Yamashita, "High-Density and Highly Surface Selective Adsorption of Protein–Nanoparticle Complexes by Controlling Electrostatic Interaction," *Jpn. J. Appl. Phys.*, vol. 45, no. 5A, pp. 4259–4264, May 2006.

[121] D. Fischer, Y. Li, B. Ahlemeyer, J. Krieglstein, and T. Kissel, "In vitro cytotoxicity testing of polycations: influence of polymer structure on cell viability and hemolysis.," *Biomaterials*, vol. 24, no. 7, pp. 1121–31, Mar. 2003.

[122] F. Rose, K. Bailey, and J. Keyte, "Potential role of epithelial cell-derived histone H1 proteins in innate antimicrobial defense in the human gastrointestinal tract," *Infect. ...*, vol. 66, no. 7, pp. 3255–3263, 1998.

[123] F. Jacobsen, a Baraniskin, J. Mertens, D. Mittler, a Mohammadi-Tabrisi, S. Schubert, M. Soltau, M. Lehnhardt, B. Behnke, S. Gatermann, H. U. Steinau, and L. Steinstraesser, "Activity of histone H1.2 in infected burn wounds.," *J. Antimicrob. Chemother.*, vol. 55, no. 5, pp. 735–41, May 2005.

[124] D. G. Stupack, "Get a ligand, get a life: integrins, signaling and cell survival," *J. Cell Sci.*, vol. 115, no. 19, pp. 3729–3738, Oct. 2002.

[125] J.-W. Han, H.-J. Lee, G.-U. Bae, and J.-S. Kang, "Promyogenic function of Integrin/FAK signaling is mediated by Cdo, Cdc42 and MyoD.," *Cell. Signal.*, vol. 23, no. 7, pp. 1162–9, Jul. 2011.

[126] E. a Cowles, L. L. Brailey, and G. a Gronowicz, "Integrin-mediated signaling regulates AP-1 transcription factors and proliferation in osteoblasts.," *J. Biomed. Mater. Res.*, vol. 52, no. 4, pp. 725–37, Dec. 2000.

[127] D. Vautier, V. Karsten, C. Egles, J. Chluba, P. Schaaf, J.-C. Voegel, and J. Ogier, "Polyelectrolyte multilayer films modulate cytoskeletal organization in chondrosarcoma cells.," *J. Biomater. Sci. Polym. Ed.*, vol. 13, no. 6, pp. 713–32, Jan. 2002.

[128] K. Cai, K. Yao, X. Hou, Y. Wang, Y. Hou, Z. Yang, X. Li, and H. Xie, "Improvement of the functions of osteoblasts seeded on modified poly(D,L-lactic acid) with poly(aspartic acid).," *J. Biomed. Mater. Res.*, vol. 62, no. 2, pp. 283–91, Nov. 2002.

[129] J. Siegel, R. Krajcar, Z. Kolská, V. Hnatowicz, and V. Svorčík, "Annealing of gold nanostructures sputtered on polytetrafluoroethylene.," *Nanoscale Res. Lett.*, vol. 6, p. 588, Jan. 2011.

[130] P. Slepička, T. Hubáček, and Z. Kolská, "The Properties and Application of Carbon Nanostructures," in *Polymer Science*, F. Yilmaz, Ed. InTech, 2013, pp. 175–202.

[131] D. D. Levy, "A pulsed electrical stimulation technique for inducing bone growth.," *Ann. N. Y. Acad. Sci.*, vol. 238, pp. 478–90, Jan. 1974.

[132] J. A. Spadaro, "Electrically stimulated bone growth in animals and man. Review of the literature.," *Clin. Orthop. Relat. Res.*, vol. 122, no. 122, pp. 325–32, 1977.

[133] E. Fukada and I. Yasuda, "On the piezoelectric effect of bone," *J. Phys. Soc. Japan*, vol. 12, no. 10, pp. 1158–1162, 1957.

[134] K. Yonemori, S. Matsunaga, Y. Ishidou, S. Maeda, and H. Yoshida, "Early effects of electrical stimulation on osteogenesis.," *Bone*, vol. 19, no. 2, pp. 173–80, Aug. 1996.

[135] K. Yamashita, N. Oikawa, and T. Umegaki, "Acceleration and Deceleration of Bone-Like Crystal Growth on Ceramic Hydroxyapatite by Electric Poling," *Chem. Mater.*, vol. 8, no. 12, pp. 2697–2700, Jan. 1996.

[136] P. W. Chudleigh, "Mechanism of charge transfer to a polymer surface by a conducting liquid contact," *J. Appl. Phys.*, vol. 47, no. 10, p. 4475, 1976.

[137] T. Plecenik, S. a. M. Tofail, M. Gregor, M. Zahoran, M. Truchly, F. Laffir, T. Roch, P. Durina, M. Vargova, G. Plesch, P. Kus, and a. Plecenik, "Direct creation of microdomains with positive and negative surface potential on hydroxyapatite coatings," *Appl. Phys. Lett.*, vol. 98, no. 11, p. 113701, 2011.

[138] D. Aronov, G. Rosenman, a. Karlov, and a. Shashkin, "Wettability patterning of hydroxyapatite nanobioceramics induced by surface potential modification," *Appl. Phys. Lett.*, vol. 88, no. 16, p. 163902, 2006.

[139] M. Morgunov, "Application of electrets in traumatology and orthopedy," *Electrets, 1994.(ISE 8), …*, pp. 863–868, 1994.

[140] L. G. J. Fokkink and J. Ralston, "Contact angles on charged substrates," *Colloids and Surfaces*, vol. 36, no. 1, pp. 69–76, Jan. 1989.

[141] M. Paneru, C. Priest, R. Sedev, and J. Ralston, "Static and dynamic electrowetting of an ionic liquid in a solid/liquid/liquid system.," *J. Am. Chem. Soc.*, vol. 132, no. 24, pp. 8301–8, Jun. 2010.

[142] M. Nakamura, A. Nagai, T. Hentunen, J. Salonen, Y. Sekijima, T. Okura, K. Hashimoto, Y. Toda, H. Monma, and K. Yamashita, "Surface electric fields increase osteoblast adhesion through improved wettability on hydroxyapatite electret.," *ACS Appl. Mater. Interfaces*, vol. 1, no. 10, pp. 2181–9, Oct. 2009.

[143] Y. Dekhtyar, N. Polyaka, and R. Sammons, "Electrically Charged Hydroxyapatite Enhances Immobilization and Proliferation of Osteoblasts," *14th Nord. Conf. …*, pp. 23–25, 2008.

[144] T. Matsumoto, M. Okazaki, a Nakahira, J. Sasaki, H. Egusa, and T. Sohmura, "Modification of apatite materials for bone tissue engineering and drug delivery carriers.," *Curr. Med. Chem.*, vol. 14, no. 25, pp. 2726–33, Jan. 2007.

[145] D. W. Grainger, "All charged up about implanted biomaterials.," *Nat. Biotechnol.*, vol. 31, no. 6, pp. 507–9, Jun. 2013.

[146] J. M. Anderson, A. Rodriguez, and D. T. Chang, "Foreign body reaction to biomaterials.," *Semin. Immunol.*, vol. 20, no. 2, pp. 86–100, Apr. 2008.

[147] M. Chang and L. Raggatt, "Osteal tissue macrophages are intercalated throughout human and mouse bone lining tissues and regulate osteoblast function in vitro and in vivo," *J. Immunol.*, vol. 181, no. 2, pp. 1232–1244, 2008.

[148] S. M. WAHL, N. McCARTNEY-FRANCIS, J. B. ALLEN, E. B. DOUGHERTY, and S. F. DOUGHERTY, "Macrophage Production of TGF-b and Regulation by TGF-b," *Ann. N. Y. Acad. Sci.*, vol. 593, no. 1 Transforming, pp. 188–196, Jun. 1990.

[149] F. Takahashi, K. Takahashi, K. Shimizu, R. Cui, N. Tada, H. Takahashi, S. Soma, M. Yoshioka, and Y. Fukuchi, "Osteopontin is Strongly Expressed by Alveolar Macrophages in the Lungs of Acute Respiratory Distress Syndrome," *Lung*, vol. 182, no. 3, Aug. 2004.

[150] M. Kreutz, R. Andreesen, S. Krause, A. Szabo, E. Ritz, and H. Reichel, "1,25-dihydroxyvitamin D3 production and vitamin D3 receptor expression are developmentally regulated during differentiation of human monocytes into macrophages," *Blood*, vol. 82, no. 4, pp. 1300–1307, Aug. 1993.

[151] Y. Honda, T. Anada, S. Kamakura, M. Nakamura, S. Sugawara, and O. Suzuki, "Elevated extracellular calcium stimulates secretion of bone morphogenetic protein 2 by a macrophage cell line," *Biochem. Biophys. Res. Commun.*, vol. 345, no. 3, pp. 1155–1160, 2006.

[152] T. Miclau, R. A. Schneider, B. F. Eames, and J. A. Helms, "Fetal Bone Formation and Adult Fracture Repair," no. 7, pp. 45–55.

[153] C. Gretzer, A. Eriksson, and B. Allden, "Monocyte activation on titanium-sputtered polystyrene surfaces in vitro: the effect of culture conditions on interleukin-1 release," *Biomaterials*, vol. 17, no. 9, pp. 851–858, 1996.

[154] P. Thomsen and C. Gretzer, "Macrophage interactions with modified material surfaces," *Curr. Opin. Solid State Mater. Sci.*, vol. 5, no. 2–3, pp. 163–176, Apr. 2001.

[155] L. C. Gerstenfeld, C. M. Edgar, S. Kakar, K. A. Jacobsen, and T. A. Einhorn, "Osteogenic Growth Factors and Cytokines and Their Role in Bone Repair."

[156] B. M. P. Hayes, J. Wang, and M. A. Norcross, “Regulation of Interleukin-l2 Expression in Human Monocytes: Selective Priming by Interferon-y of Lipopolysaccharide-Inducible p35 and p40 Genes,” *Blood*, vol. 86, no. 2, pp. 646–650, 1995.

[157] B. a Imhof and M. Aurrand-Lions, “Adhesion mechanisms regulating the migration of monocytes.,” *Nat. Rev. Immunol.*, vol. 4, no. 6, pp. 432–44, Jun. 2004.

[158] T. a. Horbett, “Principles underlying the role of adsorbed plasma proteins in blood interactions with foreign materials,” *Cardiovasc. Pathol.*, vol. 2, no. 3, pp. 137–148, Jul. 1993.

[159] L. Tang and J. Eaton, “Natural responses to unnatural materials: A molecular mechanism for foreign body reactions.,” *Mol. Med.*, vol. 5, pp. 351–358, 1999.

[160] K. Anselme, “Osteoblast adhesion on biomaterials.,” *Biomaterials*, vol. 21, no. 7, pp. 667–81, Apr. 2000.

[161] L. Tang, Y. Wu, and R. B. Timmons, “Fibrinogen adsorption and host tissue responses to plasma functionalized surfaces.,” *J. Biomed. Mater. Res.*, vol. 42, no. 1, pp. 156–63, Oct. 1998.

[162] D. L. Brown, D. R. Phillips, C. H. Damsky, and I. F. Charo, “Synthesis and expression of the fibroblast fibronectin receptor in human monocytes.,” *J. Clin. Invest.*, vol. 84, no. 1, pp. 366–70, Jul. 1989.

[163] I. MELLMAN, T. KOCH, G. HEALEY, W. HUNZIKER, V. LEWIS, H. PLUTNER, H. MIETTINEN, D. VAUX, K. MOORE, and S. STUART, “Structure and function of Fc receptors on macrophages and lymphocytes,” *J. Cell Sci.*, vol. 1988, no. Supplement 9, pp. 45–65, Jan. 1988.

[164] D. Altieri and T. Edgington, “The saturable high affinity association of factor X to ADP-stimulated monocytes defines a novel function of the Mac-1 receptor,” *J. Biol. Chem.*, vol. 263, no. 15, pp. 7007–7015, May 1988.

[165] T. Ueda, P. Rieu, J. Brayer, and M. A. Arnaout, “Identification of the complement iC3b binding site in the beta 2 integrin CR3 (CD11b/CD18).,” *Proc. Natl. Acad. Sci.*, vol. 91, no. 22, pp. 10680–10684, Oct. 1994.

[166] D. Webb, Y. Shimizu, and G. Van Seventer, “LFA-3, CD44, and CD45: physiologic triggers of human monocyte TNF and IL-1 release,” *Science (80-.).*, vol. 249, no. 4974, pp. 1295–1297, 1990.

[167] M. Guha and N. Mackman, “LPS induction of gene expression in human monocytes.,” *Cell. Signal.*, vol. 13, no. 2, pp. 85–94, Feb. 2001.

[168] F. Bronner, M. Farach-Carson, and A. Mikos, *Engineering of functional skeletal tissues*. Springer, 2007.

[169] L. Chen, E. E. Tredget, P. Y. G. Wu, and Y. Wu, "Paracrine factors of mesenchymal stem cells recruit macrophages and endothelial lineage cells and enhance wound healing.," *PLoS One*, vol. 3, no. 4, p. e1886, Jan. 2008.

[170] D. R. Haynes, T. N. Crotti, and H. Zreiqat, "Regulation of osteoclast activity in peri-implant tissues.," *Biomaterials*, vol. 25, no. 20, pp. 4877–85, Sep. 2004.

[171] G. Lisignoli, S. Toneguzzi, A. Piacentini, L. Cattini, A. Lenti, M. Tschon, S. Cristino, F. Grassi, and A. Facchini, "Human osteoblasts express functional CXC chemokine receptors 3 and 5: activation by their ligands, CXCL10 and CXCL13, significantly induces alkaline phosphatase and beta-N-acetylhexosaminidase release.," *J. Cell. Physiol.*, vol. 194, no. 1, pp. 71–9, Jan. 2003.

[172] S. Hamlet and S. Ivanovski, "Inflammatory cytokine response to titanium chemical composition and nanoscale calcium phosphate surface modification.," *Acta Biomater.*, vol. 7, no. 5, pp. 2345–53, May 2011.

[173] Z. S. Galis, G. K. Sukhova, R. Kranzhöfer, S. Clark, and P. Libby, "Macrophage foam cells from experimental atheroma constitutively produce matrix-degrading proteinases.," *Proc. Natl. Acad. Sci. U. S. A.*, vol. 92, no. 2, pp. 402–6, Jan. 1995.

[174] S. Bord, a Horner, R. M. Hembry, and J. E. Compston, "Stromelysin-1 (MMP-3) and stromelysin-2 (MMP-10) expression in developing human bone: potential roles in skeletal development.," *Bone*, vol. 23, no. 1, pp. 7–12, Jul. 1998.

[175] K. Sasaki, M. Takagi, Y. Konttinen, A. Sasaki, Y. Tamaki, T. Ogino, S. Santavirta, and J. Salo, "Upregulation of matrix metalloproteinase (MMP)-1 and its activator MMP-3 of human osteoblast by uniaxial cyclic stimulation," *J Biomed. Mater. Part B*, vol. 80B, no. 2, pp. 491–498, 2007.

[176] K. Fuller, J. Owens, and T. Chambers, "Macrophage inflammatory protein-1 alpha and IL-8 stimulate the motility but suppress the resorption of isolated rat osteoclasts.," *J. Immunol.*, vol. 154, no. 11, pp. 6065–6072, 1995.

[177] S. Harada and G. a Rodan, "Control of osteoblast function and regulation of bone mass.," *Nature*, vol. 423, no. 6937, pp. 349–55, May 2003.

[178] J. C. Fernandes, Q. Shi, M. Benderdour, D. Lajeunesse, and P. Lavigne, "An active role for soluble and membrane intercellular adhesion molecule-1 in osteoclast activity in vitro.," *J. Bone Miner. Metab.*, vol. 26, no. 6, pp. 543–50, Jan. 2008.

[179] A. König, R. Muhlbauer, and H. Fleisch, “Tumor necrosis factor α and interleukin-1 stimulate bone resorption in vivo as measured by urinary tetracycline excretion from prelabeled mice,” *J. Bone Miner. Res.*, no. 3, pp. 621–627, 1988.

[180] T. Kukita, H. Nomiyama, and Y. Ohmoto, “Macrophage inflammatory protein-1 alpha (LD78) expressed in human bone marrow: its role in regulation of hematopoiesis and osteoclast recruitment.,” *Lab Invest*, no. 76, pp. 399–406, 1997.

[181] S. Kotake, K. Sato, and K. Kim, “Interleukin-6 and soluble interleukin-6 receptors in the synovial fluids from rheumatoid arthritis patients are responsible for osteoclast-like cell formation,” *J. Bone Miner. Res.*, no. 11, pp. 88–95, 1996.

[182] S. Wei, H. Kitaura, P. Zhou, F. P. Ross, and S. L. Teitelbaum, “IL-1 mediates TNF-induced osteoclastogenesis,” *J. Clin. Invest.*, vol. 115, no. 2, pp. 282–290, 2005.

[183] R. Kimble, A. Matayoshi, and J. Vannice, “Simultaneous block of interleukin-1 and tumor necrosis factor is required to completely prevent bone loss in the early postovariectomy period.,” *Endocrinology*, vol. 136, pp. 3054–3061, 1995.

[184] Y. Tintut, “Monocyte/Macrophage Regulation of Vascular Calcification In Vitro,” *Circulation*, vol. 105, no. 5, pp. 650–655, Feb. 2002.

[185] T. J. Martin and N. A. Sims, “Osteoclast-derived activity in the coupling of bone formation to resorption.,” *Trends Mol. Med.*, vol. 11, no. 2, pp. 76–81, Feb. 2005.

[186] K. Matsuo and N. Irie, “Osteoclast-osteoblast communication.,” *Arch. Biochem. Biophys.*, vol. 473, no. 2, pp. 201–9, May 2008.

[187] G. R. Mundy and F. Elefteriou, “Boning up on ephrin signaling.,” *Cell*, vol. 126, no. 3, pp. 441–3, Aug. 2006.

[188] a Remes and D. F. Williams, “Immune response in biocompatibility.,” *Biomaterials*, vol. 13, no. 11, pp. 731–43, Jan. 1992.

[189] T. Sato, “The biological roles of the third component of complement in osteoclast formation,” *Endocrinology*, vol. 133, no. 1, pp. 397–404, Jul. 1993.

[190] K. Nakagawa, H. Sakiyama, T. Fukazawa, M. Matsumoto, M. Takigawa, T. Toyoguchi, and H. Moriya, “Coordinated change between complement C1s production and chondrocyte differentiation in vitro.,” *Cell Tissue Res.*, vol. 289, no. 2, pp. 299–305, Aug. 1997.

[191] J. A. Andrades, M. E. Nimni, J. Becerra, R. Eisenstein, M. Davis, and N. Sorgente, “Complement proteins are present in developing endochondral bone and may mediate cartilage cell death and vascularization.,” *Exp. Cell Res.*, vol. 227, no. 2, pp. 208–13, Sep. 1996.

[192] M. Nakamura, Y. Sekijima, S. Nakamura, T. Kobayashi, K. Niwa, and K. Yamashita, "Role of blood coagulation components as intermediators of high osteoconductivity of electrically polarized hydroxyapatite.," *J. Biomed. Mater. Res. A*, vol. 79, no. 3, pp. 627–34, Dec. 2006.

[193] R. K. Andrews, J. A. López, and M. C. Berndt, "Molecular mechanisms of platelet adhesion and activation.," *Int. J. Biochem. Cell Biol.*, vol. 29, no. 1, pp. 91–105, Jan. 1997.

[194] W. E. Oprea, J. M. Karp, M. M. Hosseini, and J. E. Davies, "Effect of platelet releasate on bone cell migration and recruitment in vitro.," *J. Craniofac. Surg.*, vol. 14, no. 3, pp. 292–300, May 2003.

[195] R. E. Marx, E. R. Carlson, R. M. Eichstaedt, S. R. Schimmele, J. E. Strauss, and K. R. Georgeff, "Platelet-rich plasma: growth factor enhancement for bone grafts," *Oral Surgery, Oral Med. Oral Pathol. Oral Radiol. Endodontology*, vol. 85, no. 6, pp. 638–646, Jun. 1998.

[196] X. L. Griffin, C. M. Smith, and M. L. Costa, "The clinical use of platelet-rich plasma in the promotion of bone healing: a systematic review.," *Injury*, vol. 40, no. 2, pp. 158–62, Feb. 2009.

[197] F. Velard, D. Laurent-Maquin, C. Guillaume, S. Bouthors, E. Jallot, J.-M. Nedelec, A. Belaaouaj, and P. Laquerriere, "Polymorphonuclear neutrophil response to hydroxyapatite particles, implication in acute inflammatory reaction.," *Acta Biomater.*, vol. 5, no. 5, pp. 1708–15, Jun. 2009.

[198] W. F. Zambuzzi, K. B. S. Paiva, R. Menezes, R. C. Oliveira, R. Taga, and J. M. Granjeiro, "MMP-9 and CD68(+) cells are required for tissue remodeling in response to natural hydroxyapatite.," *J. Mol. Histol.*, vol. 40, no. 4, pp. 301–9, Aug. 2009.

[199] M. C. Matesanz, M. J. Feito, M. Oñaderra, C. Ramírez-Santillán, C. da Casa, D. Arcos, M. Vallet-Regí, J. M. Rojo, and M. T. Portolés, "Early in vitro response of macrophages and T lymphocytes to nanocrystalline hydroxyapatites.," *J. Colloid Interface Sci.*, vol. 416, pp. 59–66, Feb. 2014.

[200] M. T. Gillespie, "Impact of cytokines and T lymphocytes upon osteoclast differentiation and function.," *Arthritis Res. Ther.*, vol. 9, no. 2, p. 103, Jan. 2007.

[201] A. Marusic, D. Grcevic, V. Katavic, N. Kovacic, I. K. Lukic, I. Kalajzic, and J. A. Lorenzo, "Role of B Lymphocytes in New Bone Formation," *Lab. Investig.*, vol. 80, no. 11, pp. 1761–1774, Nov. 2000.

[202] B.-Z. Qian and J. W. Pollard, "Macrophage diversity enhances tumor progression and metastasis.," *Cell*, vol. 141, no. 1, pp. 39–51, Apr. 2010.

[203] J. G. Schneider, S. R. Amend, and K. N. Weilbaecher, “Integrins and bone metastasis: integrating tumor cell and stromal cell interactions.,” *Bone*, vol. 48, no. 1, pp. 54–65, Jan. 2011.

[204] J. Zhuang, J. Zhang, S. T. Lwin, J. R. Edwards, C. M. Edwards, G. R. Mundy, and X. Yang, “Osteoclasts in multiple myeloma are derived from Gr-1+CD11b+myeloid-derived suppressor cells.,” *PLoS One*, vol. 7, no. 11, p. e48871, Jan. 2012.

[205] S. Sundelacruz, M. Levin, and D. L. Kaplan, “Membrane potential controls adipogenic and osteogenic differentiation of mesenchymal stem cells.,” *PLoS One*, vol. 3, no. 11, p. e3737, Jan. 2008.